ADSORPTION OF COBALT ON GAMMA-Fe_2O_3

by

Martin J. Fay,,

Thesis submitted to the Graduate Faculty of the
Virginia Polytechnic Institute and State University
in partial fulfillment of the requirements for the
degree

Master of Science
in
Chemistry

Approved:

J. G. Dillard, Chairman

A. F. Clifford

L. T. Taylor

August, 1985

Table of Contents

Acknowledgments

I would like to extend sincere thanks to my research director, Professor John G. Dillard, for his thoughtful assistance and guidance during my studies and research. I would also like to thank Dr. Wayne Federer at 3M for generously providing helpful insight, and the staff at 3M for their comments and suggestions on this project. Special thanks also go to 3M for providing the financial funding for this project. I also express gratitude to Mr. Frank Cromer who aided in maintaining the Phi XPS instrument during these studies. I would like to thank my committee of Professor L. T. Taylor and Professor A. F. Clifford for their patience and guidance while I was writing my thesis. Thanks are also expressed to Alex Dillard who carried out the Fe(II) determinations. Lastly, I wish to thank my wife Karen for the understanding and moral support she provided during my studies.

List of Tables

List of Figures

CHAPTER I

INTRODUCTION

The adsorption of Co(II) on γ-Fe_2O_3 is a very important commercial process. The product, which will be called cobalt-treated γ-Fe_2O_3 or Co-γ-Fe_2O_3, is widely used as a magnetic material for magnetic recording. The treatment of γ-Fe_2O_3 with Co(II) is practiced to increase the coercivity of γ-Fe_2O_3, which itself is a magnetic material. Coercivity is a magnetic property that is a measure of the force required to demagnetize a magnetic material. It is desirable to use a magnetic material with high coercivity in magnetic recording since it allows for greater information storage densities. With the increasing demands on data storage, the availability of high coercivity materials is becoming more important.

The treatment of γ-Fe_2O_3 with Co(II) consists of interacting Co(II) with γ-Fe_2O_3 in an alkaline, aqueous suspension. The treatment process is therefore largely confined to the surface of the γ-Fe_2O_3 particles. In response to the surface nature of the treatment process, the focus of this study was to characterize the surface of Co-γ-Fe_2O_3 samples prepared under a variety of conditions. The goal of these efforts was to determine the chemical nature of the surface of Co-γ-Fe_2O_3, and to learn more about the chemical processes that occur during the reaction of Co(II) with γ-Fe_2O_3.

The surface analysis techniques used to study the Co-γ-Fe_2O_3 samples were X-ray photoelectron spectroscopy (XPS) and secondary ion

mass spectrometry (SIMS). Infrared spectroscopy (IR) was also used to aid in the characterization. Quantitative analysis of Fe(II) was accomplished to determine the Fe(II) content of the samples.

Previous studies examining cobalt treated γ-Fe_2O_3 have used Mössbauer spectroscopy and x-ray diffraction. It is hoped that the surface characterization results (XPS, SIMS, etc.) from this study will provide additional information on the chemical nature of cobalt treated γ-Fe_2O_3.

CHAPTER II

HISTORY

A) Introduction

The term "magnetic material" is used to describe materials that exhibit spontaneous magnetization at room temperature. The two main classes of magnetic materials are metals (principally iron, cobalt, nickel and their alloys) and oxides. The majority of magnetic oxides are either iron oxides (γ-Fe_2O_3, Fe_3O_4) or mixed iron oxides, commonly called ferrites (e.g., $CoFe_2O_4$, $BaFe_{12}O_{19}$) (1). Magnetic oxides are used in many practical applications, the majority of which are in electronics (e.g. inductor core material for high frequency applications) (2), but the greatest single use of magnetic oxides is for magnetic recording (3). For this thesis the discussion will focus on oxides for magnetic recording, specifically cobalt-treated γ-Fe_2O_3. The first part of this historical introduction will examine the chemical and magnetic properties of γ-Fe_2O_3; after that the discussion will consider the development of cobalt-treated γ-Fe_2O_3 for magnetic recording and studies investigating the chemical and magnetic nature of cobalt-treated γ-Fe_2O_3.

B) Chemical Composition and Magnetic Properties of γ-Fe_2O_3

History of γ-Fe_2O_3

Particulate γ-Fe_2O_3 has been used as a magnetic medium for magnetic recording since the beginning of magnetic recording in the 1930's (4). Throughout this period γ-Fe_2O_3 has been by far the most popular magnetic

material. A survey by Corradi (5) in 1978 found that over 90% of the tapes and disks produced at that time used γ-Fe_2O_3. This long standing popularity can be attributed to the low cost, stability, and reproducibility of γ-Fe_2O_3 (6).

In early applications, the γ-Fe_2O_3 used consisted of roughly spherical particles approximately 1 μm in diameter. These particles worked well, but their signal strength was low by today's standards. The γ-Fe_2O_3 particles used in magnetic recording today have an acicular shape. The average length of the particles is less than 1 μm with an axial ratio of 6-7:1 (7). Compared to the earlier spherical particles, acicular γ-F_2O_3 has vastly superior recording performance. A transmission electron micrograph of some acicular γ-Fe_2O_3 is shown in Figure 1.

Preparation of Gamma-Fe_2O_3

The general method for preparing γ-Fe_2O_3 is (4):

1) Precipitation of acicular α-FeOOH (goethite) in solution from Fe(II) (aq), usually $FeSO_4$.
2) Dehydration of α-FeOOH to α-Fe_2O_3 (hematite).
3) Reduction of α-Fe_2O_3 to Fe_3O_4 (magnetite).
4) Careful oxidation of Fe_3O_4 to γ-Fe_2O_3 (maghemtite).

In the commerical production of γ-Fe_2O_3 there are many variations of this general procedure. For example, one method of precipitating α-Fe_2O_3 uses phosphonic and carboxylic acids as growth regulating agents (8). The reduction of α-Fe_2O_3 to Fe_3O_4 can be done using a number of reducing agents. The most common reagent is hydrogen. The reduction

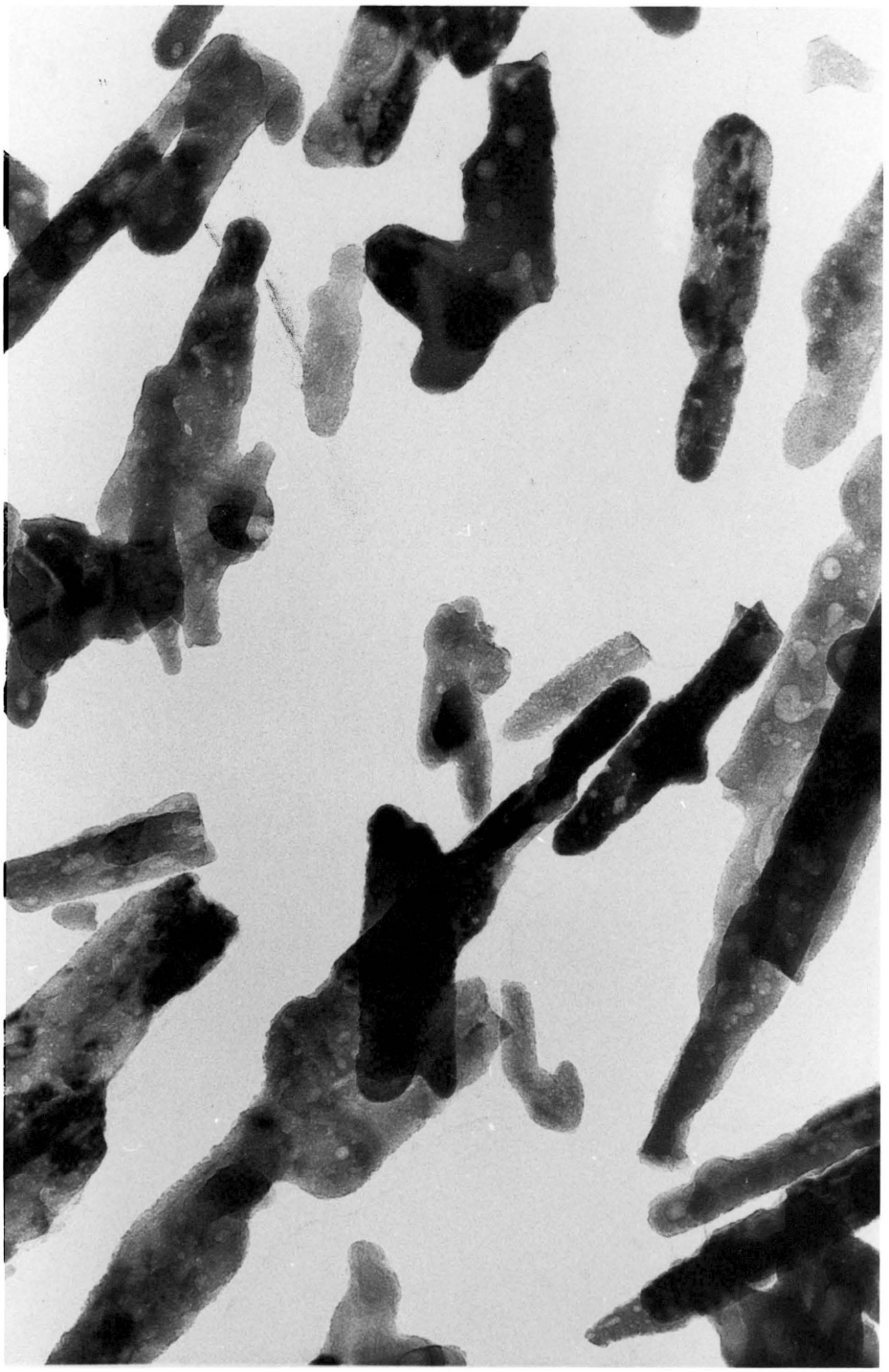

220,000X

Figure 1

Transmission Electron Micrograph of γ-Fe_2O_3

step can be entirely eliminated by precipitating γ-FeOOH (lepidocrocite) instead of α-FeOOH. The formation of γ-FeOOH instead of α-FeOOH is achieved by the presence of the Cl^- counter ion ($FeCl_2$) instead of the SO_4^{2-} counter ion ($FeSO_4$) (9). γ-Fe_2O_3 is obtained directly by dehydrating γ-FeOOH. Unfortunately, γ-Fe_2O_3 produced in this manner is not satisfactory for magnetic recording.

The primary objectives of these procedures and others are increased acicularity, better uniformity of particle size, and better dispersibility of the particles in the tape binder (4). Increasing the acicularity of the γ-Fe_2O_3 results in increased coercivity, and keeping the size distribution of the particles narrow helps reduce the noise level of the output signal (5). Another technique used to improve the signal to noise ratio is to orient the γ-Fe_2O_3 particles longitudinally along the direction of recording. This is achieved by passing the tape or disk through a strong magnetic field while the binder is still wet. This causes the γ-Fe_2O_3 particles to align themselves in a head-to-tail fashion. In order to achieve a high degree of orientation it is essential that the γ-Fe_2O_3 particles are well dispersed in the tape binder. This is not an easy task since the γ-Fe_2O_3 particles have hydrophilic surfaces and tend to agglomerate in the binder which is an organic polymer. One method of increasing dispersibility is to pre-coat the γ-Fe_2O_3 particles with binder while they are agitated in some device such as a ball-mill (10).

Crystal Structure of γ-Fe_2O_3

1) Spinel structure

Like most of the magnetic oxides, γ-Fe_2O_3 has the spinel crystal structure. The spinel structure consists of an approximate cubic close packing of oxygen atoms in which both tetrahedral and octahedral sites are present (11). The general formula of a spinel compound is AB_2O_4, where "A" denotes a metal ion in a tetrahedral site and "B" denotes a metal ion in an octahedral site. The unit cell can be represented as $[AB_2O_4]_8$, which contains a total of 64 tetrahedral sites and 32 octahedral sites. To balance the charge in the crystal lattice, a spinel compound usually has divalent and trivalent ions in its structure in a 1:2 ratio. How these ions arrange themselves in the crystal lattice determines whether a spinel compound has a normal or an inverse structure. Normal spinels have the divalent ions occupying the tetrahedral (A) sites and the trivalent ions occupying the octahedral (B) sites. Cobalt aluminate ($CoAl_2O_4$) is an example of a normal spinel. γ-Fe_2O_3, Fe_3O_4 and $CoFe_2O_4$ all have inverse spinel structures where the divalent ions occupy the octahedral (B) sites and the trivalent ions are distributed between the tetrahedral (A) and octahedral sites (B). γ-Fe_2O_3 is a special case since it contains no divalent metal ions. Its structure can be represented as $Fe^{3+}(\square_{1/3}\ Fe^{3+}_{5/3})\ O_4$, where parentheses denote an ion in an octahedral (B) site and $\square$ represents a vacancy (12).

Magnetic Properties of γ-Fe_2O_3

The presence of two different types of lattice sites in the spinel structure is responsible for the ferrimagnetic behavior of γ-Fe_2O_3. A

diagram illustrating this behavior is given in Figure 2 (13). The diagram shows how the magnetic moments of the octahedral Fe^{3+} ions are partially cancelled by anti-ferromagnetic coupling with the tetrahedral Fe^{3+} ions. The remaining uncoupled ions give γ-Fe_2O_3 its magnetic behavior (i.e. spontaneous magnetization at room temperature). Materials with this partial cancellation of opposing magnetic moments are termed ferrimagnetic.

The magnetization of acicular γ-Fe_2O_3 is anisotropic. The anisotropy is uniaxial and corresponds to the shape of the γ-Fe_2O_3 particle. To rotate the direction of magnetization away from the preferred axis requires energy. Figure 3 illustrates the anisotropic behavior of acicular γ-Fe_2O_3 (14).

An important magnetic property in magnetic recording which is related to the magnetic anisotropy of a material is its coercivity. The coercivity of a material is the magnetic force required to demagnetize it. For magnetic recording it is desirable to use a high coercivity material, since it is less susceptible to demagnetization by an external magnetic field. This increased resistance to demagnetization allows for closer packing of magnetic information since the effect of neighboring regions demagnetizing each other is reduced. This means that increased information storage is possible.

The coercivity of acicular γ-Fe_2O_3 is typically in the range of 260-320 Oe (15). By treating γ-Fe_2O_3 with cobalt the coercivity can be increased to 800 Oe and higher. The demands for greater storage density have increased the demand for high coercivity magnetic material and this

Ferrimagnetic Behavior of γ-Fe_2O_3

γ-Fe_2O_3 has the structure $Fe_3(\square_1Fe_5)O_{12}$

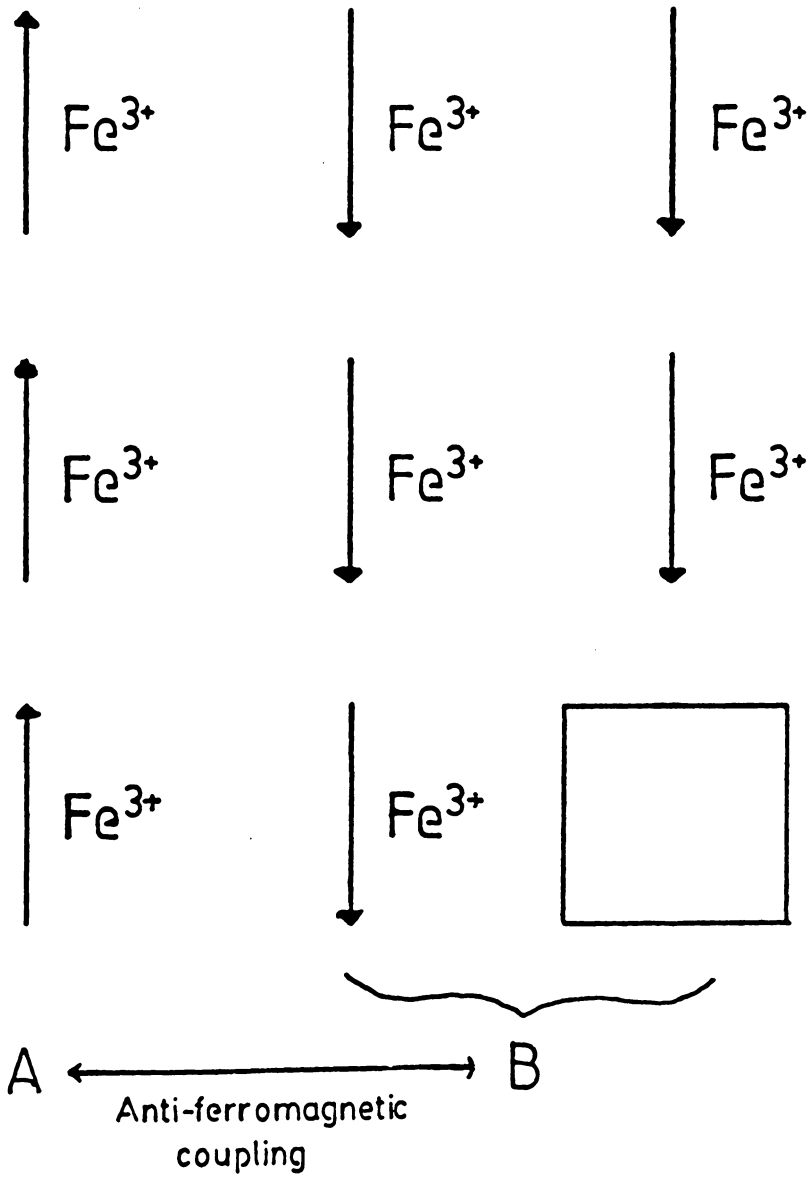

Figure 2

Ferrimagnetic Behavior of γ-Fe_2O_3

Magnetic Anisotropy of γ-Fe_2O_3 Particle

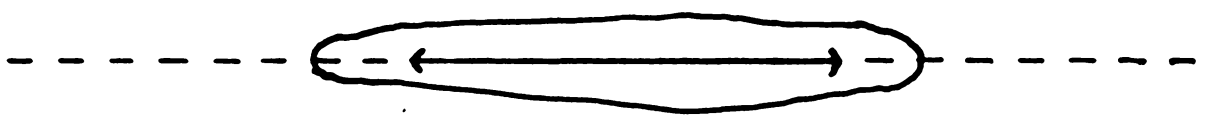

-two preferred directions of magnetization(uniaxial)

Figure 3. Magnetic Anisotropy of γ-Fe_2O_3

has been the main impetus for development of cobalt-treated γ-Fe_2O_3.

C) Development of Cobalt-Treated γ-Fe_2O_3

Bulk Treated Co-γ-Fe_2O_3

The ability of small amounts of Co(II) to increase dramatically the coercivity of γ-Fe_2O_3 has been known for many years. Two of the earliest procedures by Jeschke (1954) and Krones (1960) (16,17) consist of bulk-treating γ-Fe_2O_3 by adding cobaltous sulfate to the ferrous sulfate starting material. Krones reported that by adding 10% weight cobalt, the coercivity was increased from 100 Oe (no cobalt) to 800 Oe.

Unfortunately, bulk-treated Co-γ-Fe_2O_3 is unacceptable for magnetic recording due to the large temperature dependence of the coercivity (5-10 Oe/°C). This large temperature dependence is due to an increase in the magneto-crystalline anisotropy of the γ-Fe_2O_3 resulting from the presence of Co(II) ions in the crystal lattice (18,19). Magneto-crystalline anisotropy is the preferential orientation of magnetization of a material with respect to its crystal structure (20), and characteristically results in a large temperature dependence of the coercivity (5).

The coercivity of pure γ-Fe_2O_3 is largely due to the shape anisotropy of the γ-Fe_2O_3 particles. This "shape" anisotropy has the desirable property of being relatively insensitive to temperature, stress, and time (21). The effect Co(II) has on increasing the magneto-crystalline anisotropy of γ-Fe_2O_3 is best explained by the single ion model developed by Slonczewski (18). In this model the orbital angular

momentum of the Co(II) ion is constrained by the crystal lattice to lie on the axis of trigonal symmetry. The spin angular momentum is coupled to the orbital angular momentum by spin-orbit coupling and in this manner the 3d electron spins (magnetic moment) of the Co(II) ions are coupled to the crystal lattice (22).

The problems associated with bulk-treated Co-γ-Fe_2O_3 were eliminated for the most part by limiting the presence of Co(II) to the surface of the γ-Fe_2O_3 particles. Surface-treated Co-γ-Fe_2O_3 can have coercivities as high as bulk-treated Co-γ-Fe_2O_3 without the large temperature dependence of the coercivity.

Surface Treated Co-γ-Fe_2O_3

The first procedure for treating the surface of γ-Fe_2O_3 with Co(II) was described by Haller and Colline in 1971 (23). The procedure consisted of coating γ-Fe_2O_3 with $CoCl_2 \cdot 6H_2O$ and then decomposing the salt and diffusing the Co(II) into the γ-Fe_2O_3. This was done by heating the solids at 245°C under nitrogen. In 1978 Imaoka et al. (24) described a method of treatment wherein a cobaltous salt solution was precipitated onto γ-Fe_2O_3 in an alkaline suspension. The highest coercivity obtained using this procedure was around 550 Oe. Imaoka observed that at approximately 2% (wt.) Co(II), the increase in coercivity leveled off and relatively little coercivity enhancement was observed for higher concentrations of cobalt (up to 4% wt.). It was suggested that the leveling off of coercivity at higher concentrations was the result of non-magnetic species of cobalt being formed. The large temperature dependence that was observed with bulk treated Co-γ-

Fe_2O_3 was not characteristic of the surface treated samples. Imaoka, et al. (24) suggested that for surface treated Co-γ-Fe_2O_3 the increased magneto-crystalline anisotropy at the surface of Co-γ-Fe_2O_3 coincided with the shape anisotropy of γ-Fe_2O_3 and reinforced it.

Amemiya et al., (25) reported a method of surface treatment in which a mixture of Co(II) and Fe(II) in a 1:2 ratio was co-adsorbed on γ-Fe_2O_3. This procedure was believed to result in the formation of a cobalt ferrite ($CoFe_2O_4$) layer on the surface of the γ-Fe_2O_3. The adsorption was carried out in an aqueous suspension at high pH. Following pH adjustment, the reaction suspension was heated to facilitate the formation of $CoFe_2O_4$. By increasing the weight percent of Co to 7%, coercivities as high as 900 Oe were obtained and the leveling off behavior reported by Imaoka et al. (24) was not observed. This Co(II)/Fe(II) treated γ-Fe_2O_3 is often referred to as cobalt epitaxial-γ-Fe_2O_3 (26) reflecting the belief that cobalt ferrite is grown epitaxially on the surface of γ-Fe_2O_3. This is plausible since $CoFe_2O_4$ and γ-Fe_2O_3 both have inverse spinel crystal structures with similar lattice constants.

In an effort to further increase the coercivity of surface treated Co-γ-Fe_2O_3, the prepared samples are sometimes thermally treated (annealed) following adsorption of Co(II). The effect of heat treating the surface treated Co-γ-Fe_2O_3 was examined by Tokuoka and coworkers (27). They determined the cobalt depth profiles of treated samples by controlled acid etching. Their results indicated that samples heated in air between 250°C and 400°C experienced rapid diffusion of Co(II) into

the bulk of the γ-Fe_2O_3. The thermal treatment resulted in an increase in coercivity of the samples, but the annealed samples also showed an increase in the temperature dependence of the coercivity signaling the formation of bulk-treated Co-γ-Fe_2O_3. (Specifically, a sample annealed at 300°C for 1 hr had a temperature dependence of ~5 Oe/°C versus 1 Oe/°C for the non-annealed sample.)

D) Characterization of Cobalt-Treated γ-Fe_2O_3

Several studies have examined cobalt-treated γ-Fe_2O_3 in an effort to determine its chemical composition and structure. In an early study by Khalafalla and Morrish (28), ^{57}Fe Mössbauer spectroscopy and X-ray diffraction were used to examine bulk treated Co-γ-Fe_2O_3. Mössbauer results indicated the Co(II) ions occupied B site octahedral vacancies and also to a small extent replaced Fe(III) ions in B sites. With these results they were able to explain the large temperature dependence of the coercivity of the bulk treated Co-γ-Fe_2O_3 using the single ion model by Slonczewski (18).

Ochi and coworkers (29) examined surface-treated Co-γ-Fe_2O_3 using ^{57}Co Mössbauer spectroscopy. The samples were prepared by adsorbing $CoSO_4$ (containing ^{57}Co) on γ-Fe_2O_3 in an alkaline aqueous suspension. Based on the similarities of spectra between $CoFe_2O_4$ and the prepared samples, they suggested that the surface composition of the surface-treated samples was near $CoFe_2O_4$. They also suggested that there were small amounts of non-magnetic forms of cobalt on the surface, probably having a composition near Co_3O_4.

Surface treated Co-γ-Fe_2O_3, prepared by co-adsorbing Co(II) and Fe(II) was examined using ^{57}Fe Mössbauer spectroscopy by Li et al. (30). Based on results obtained by curve resolution of the Mössbauer spectra they found evidence that the surface of the treated samples was composed of $Co_xFe_{3-x}O_4$, a solid solution, where x is approximately one. They also mentioned that they found no evidence for other types of cobalt species.

A study examining surface treated Fe_3O_4 (magnetite) using ^{57}Co Mössbauer spectroscopy was published by Sharrock, Picone and Morrish (31). They found evidence for $CoFe_2O_4$ on the surface together with non-magnetic forms of cobalt that they suggested were oxides and hydroxides. Their results also indicated that the relative amounts of non-magnetic species were greater at higher concentrations of cobalt. This suggested that the treatment process was less efficient at higher concentrations of cobalt.

In a study using X-ray diffraction to examine surface treated Co-γ-Fe_2O_3, Sumiya and coworkers (32) determined that $CoFe_2O_4$ was grown epitaxially on the surface of the γ-Fe_2O_3 particles. Based on the lattice constants they measured, they also suggested that there was an interface between the surface $CoFe_2O_4$ and the γ-Fe_2O_3 which was similar to Fe_3O_4 in composition.

A preliminary XPS study by Witherell (33) was concerned primarily with determining the Co(II) and Fe(II) depth profiles near the surface. This interest in the depth profiles for Co(II) and Fe(II) arises from the belief that they significantly affect the magnetic properties of

surface treated Co-γ-Fe_2O_3. An effect called "aging" is commonly observed for Co-γ-Fe_2O_3 in which the coercivity increases over time along with some other undesirable properties such as increased print-through (transfer of magnetic signal between layers of tape) and broader distribution of coercivity. This aging effect is believed to be the result of Co(II) diffusion within the γ-Fe_2O_3. By curve resolving the Fe(II) component of the 2p and 3s photoelectron peaks, results were found indicating that the diffusion of Co(II) is facilitated by the presence of Fe(II) both in the bulk and at the surface. These results suggest that limiting the amount of Fe(II) in Co-γ-Fe_2O_3 would reduce the diffusion of Co(II) and possibly prevent the "aging" of Co-γ-Fe_2O_3.

Summary

This survey of the literature on Co-γ-Fe_2O_3 has shown that most authors have found evidence for $CoFe_2O_4$ on the surface of cobalt-treated γ-Fe_2O_3. There is considerable disagreement as to whether other cobalt species are present. Many believe that the lower efficiency in enhancing the coercivity at high cobalt concentrations is due to the increasing presence of "non-magnetic" cobalt species ($Co(OH)_2$, Co_3O_4, etc.).

For this thesis, characterization using XPS, SIMS, IR, and quantitative iron analysis of Co-γ-Fe_2O_3 samples prepared under a variety of conditions has been carried out. It is hoped that the characterization of these samples will provide more information on the chemical nature of the Co-γ-Fe_2O_3 surface and the chemical processes involved in the treatment.

CHAPTER III

EXPERIMENTAL

A) Preparation of Cobalt Treated γ-Fe_2O_3

The process of preparing surface treated Co-γ-Fe_2O_3 for characterization involved two basic steps. The first step was to co-adsorb a Co(II)/Fe(II) mixture (1:2 ratio, respectively) on γ-Fe_2O_3 in an aqueous suspension at pH 10. Following the adsorption of Co(II) and Fe(II), the treated solids were either dried under vacuum at room temperature, or they were thermally treated.

Adsorption of Cobalt

The first step of the adsorption procedure was to prepare a suspension of γ-Fe_2O_3 (5% by weight) in 1700 ml deionized water. This was done by shearing the γ-Fe_2O_3 suspension for 5 minutes in a blender at the highest shear rate. The γ-Fe_2O_3 used in the preparations was obtained from 3M.

Cobaltous sulfate, $CoSO_4 \cdot 7H_2O$ and ferrous sulfate, $FeSO_4 \cdot 7H_2O$ salts were added to the sheared suspension to obtain 5% cobalt(II) by weight of γ-Fe_2O_3 and 10% iron(II) by weight of γ-Fe_2O_3. After the Co(II)/Fe(II) mixture was added to the suspension the pH was adjusted using NaOH or NH_4OH. Once the pH had been adjusted, the reaction suspension was heated to 90-95°C. After the suspension had been heated for the desired period of time, the solids were washed with pH 7 deionized water. The washing procedure consisted of adding water to the solids and decanting the supernatant after the solids had settled. This

was repeated until the supernatant had a conductivity of 50 μmhos or less. The remaining water was filtered from the solids and the solid was either dried under vacuum or annealed.

The reaction vessel was a four-neck, two liter round bottom flask as shown in Figure 4. The stirring of the suspension was done mechanically with a glass stirring paddle. Two condensers were used. The larger condenser was open to the atmosphere and was used to reduce loss of water vapor when the reaction mixture was at reflux conditions. The smaller condenser was placed between the flask and the stirring rod sleeve. This was done to cool the grease used to lubricate the stirring rod and sleeve, thus preventing grease from getting into the reaction suspension. The other two necks were used for inserting the pH electrode and adding reagents. Heating was done with a hemispherical heating mantle which was controlled by a Variac.

Thermal Treatment of Co-γ-Fe_2O_3

The thermal treatment (annealing) of Co-γ-Fe_2O_3 consisted of heating the reacted solids for a specific period of time. All annealed Co-γ-Fe_2O_3 samples examined in this study were annealed under similar conditions (same temperature and time).

B) Magnetic Measurements

The coercivities for the Co-γ-Fe_2O_3 samples were measured at 3M Corporation, St. Paul, Minnesota under the direction of Dr. Wayne Federer. The measurements were made with a 60 Hz M-H meter (a.c. hysteresis loop tracer). The samples were prepared for measurement as a carbowax mull. The accuracy of the measured coercivities was ±0.5%.

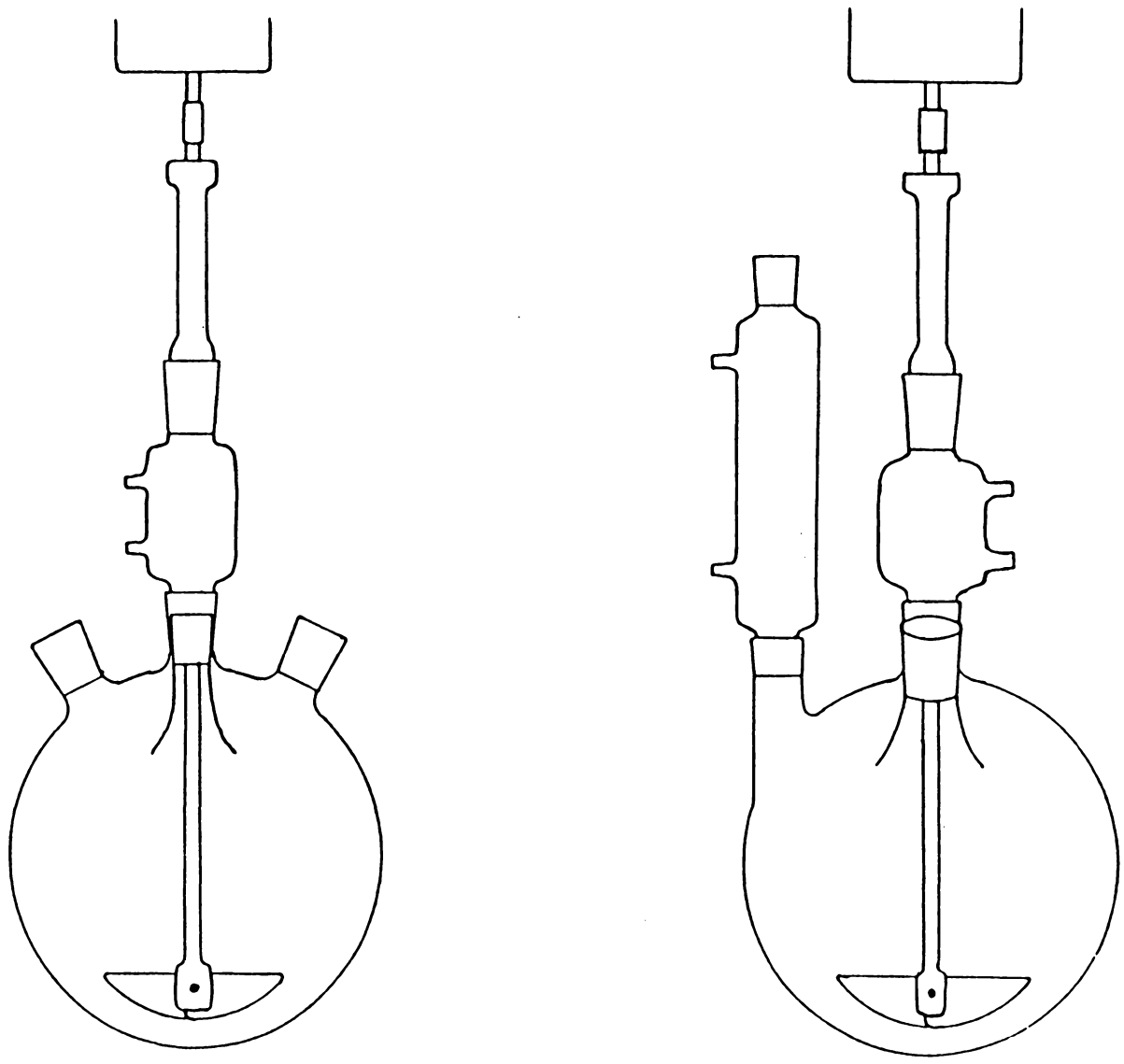

Figure 4. Adsorption Reaction Vessel

C) X-ray Photoelectron Spectroscopy (XPS)

The basis of XPS is the X-ray induced emission of electrons from atoms in a compound or substrate (34). The kinetic energy of the emitted electrons is measured by an analyzer and by knowing the energy of the incident X-rays the binding energies of the electrons are determined from the relation $h\nu$=B.E. + K.E. + ϕ which expresses the conservation of energy for the photoionization process. B.E. is the binding energy of the electron, K.E. is the kinetic energy of the photoelectron, $h\nu$ is the energy of the X-ray, and ϕ is the spectrometer work function. The work function is determined using a reference standard. For this investigation the background carbon C 1s photoelectron peak at 284.6 eV was used to calibrate the binding energy scale (35). Since the electrons cannot experience any inelastic collisions prior to being analyzed, the depth in a sample from which they originate is severely limited. This makes XPS a surface sensitive technique. Typically, the sampling depth is not more than 50 Å.

The XPS spectra were measured using a Perkin-Elmer PHI 5300 XPS instrument. This spectrometer uses a hemispherical energy analyzer and a position sensitive detector. The transmission function of the analyzer is proportional to the inverse of the kinetic energy of the photoelectrons. An analyzer pass energy of 44.74 eV was used for the wide scans and a 17.89 eV pass energy was used for the narrow scans.

Photoionization was initiated using Mg Kα radiation which has an energy of 1253.6 eV. All recorded binding energies are the average of at least two measurements. The precision of the measurements was ±0.1 eV.

The measured binding energies are used to identify the chemical nature of surface elements by comparison with reference standards. In addition to the binding energies there are often other spectral features that aid in characterization. An example of this is the intense satellite peaks associated with Co(II) compounds, but not with Co(III) compounds. Other spectral features such as peak widths, multiplet splitting, etc. can be used for characterization (33-35).

In addition to qualitative information, XPS also provides quantitative information which is obtained using the relative intensities of the photoelectron peaks. The precision is somewhat limited (±5-10%) so the information obtained is sometimes termed semi-quantitative. Still, the quantitative data from XPS is often very useful considering the surface sensitivity of the technique. For this investigation, the reported Co/Fe atomic ratios were determined from the corrected Co $2p_{1/2}$, Co $2p_{3/2}$ and Fe $2p_{1/2}$, Fe $2p_{3/2}$ peak areas. The correction factor used to convert the peak areas to atomic ratios was determined using a $CoFe_2O_4$ standard which was assumed to be stoichiometric at the surface.

The samples were mounted on 1" circular copper probes by placing an acetone dispersion of the sample on the probe and allowing the acetone to evaporate. This left a thin, smooth covering on the probe. This method was compared with other mounting methods to see if the mounting

had any effect on the spectra. The two other methods compared were water dispersion and dusting the sample on double-stick tape. There were no observable differences in the spectra of samples mounted using any of these methods. The acetone dispersion method was used since it was the simplest.

D) Secondary Ion Mass Spectrometry (SIMS)

Secondary ion mass spectrometry (SIMS) is a solid state technique of mass spectroscopy (36). The technique consists of bombarding a solid sample with an argon ion beam and measuring the mass to charge ratio of the ejected ionic species. The species ejected in this process are cations and anions. Positive SIMS measures ejected cationic species and negative SIMS measures ejected anionic species. The depth of analysis for SIMS is dependent on the duration of analysis since the surface is being continually sputtered away. A typical spectrum collected following five minutes of bombardment probes not more than 20 Å into the surface of the sample being analyzed.

There are two basic modes of SIMS analysis. They are static SIMS and dynamic SIMS. Static SIMS employs a low current density ion beam to gently erode the sample surface. The objective of static SIMS is to determine the composition of only the outermost surface species. Dynamic SIMS uses a much higher current denisty ion beam to rapidly erode the sample surface. Dynamic SIMS probes deeper into the sample and is often used to obtain depth profile information.

The SIMS spectra measured for this study were obtained using a Perkin Elmer PHI Model 3500 SIMS II. Positive SIMS spectra were

collected under dynamic conditions (high beam current). Spectra were collected using rastered and non-rastered ion beams. The use of a rastered ion beam reduced the sputter rate and made the SIMS spectra more surface sensitive. A 4 KeV ion beam was used and the ion current in the gun was 0.25 mA.

E) Infrared Spectroscopy

Infrared spectra of the Co-γ-Fe_2O_3 samples were measured at 3M, St. Paul under the direction of Dr. Wayne Federer. A Nicolet 10-DX Fourier transform infrared spectrometer was used to collect the spectra. The spectrometer has cesium iodide optics which allowed spectra to be taken to 225 cm^{-1}. The spectra were taken using KBr pellets of the samples. The pellets were prepared by mixing 0.4-0.6 mg of sample with 150 mg of KBr and then pressing the pellet with a hydraulic press at 40,000 psi.

F) Percent Fe(II) Determination

The percent Fe(II) content of the Co-γ-Fe_2O_3 samples was determined by an oxidation-reduction titration procedure using potassium dichromate as the titrating reagent. The general method of determining iron by titration with dichromate involves first reducing the iron with a reducing agent, $SnCl_2$, and then the Fe(II) is titrated with dichromate which oxidizes the Fe(II) to Fe(III). The Fe(II) content was determined by titrating a 0.2 g portion of a sample without prior reduction of the Fe(III) with $SnCl_2$. The total iron content was determined from a 0.1 g portion using the standard procedure (reducing all iron to Fe(II) with $SnCl_2$ prior to titration with dichromate).

The determination of Fe(II) was accomplished by digesting a 0.200 g sample in a 50% (by volume) hydrochloric acid solution. Gentle heating was used to aid the digestion. While the samples were being digested nitrogen was passed over the solution to help prevent oxidation of Fe(II). After the digestion, 100 ml of 25% sulfuric acid and 2.5 ml of 85% of phosphoric acid were added to the digested iron. Six to eight drops of diphenylamine sulfonate (indicator) were added and then the solution was titrated with dichromate until a purple color appeared indicating the end point .

Total Fe determination was carried out by digesting, with gentle heating, a 0.100 g sample in a 50% (by volume) hydrochloric acid solution. After digestion a sufficient volume of 0.5 M stannous chloride ($SnCl_2$) solution was added to the digested iron solution until the solution became clear or pale green indicating that Fe(III) had been reduced to Fe(II). After the reduction of iron, 15 ml of saturated mercuric chloride ($HgCl_2$) solution was added to remove any excess Sn^{2+}. One hundred milliliters (100 ml) of 25% sulfuric acid, and 2.5 ml of 85% phosphoric acid and 6-8 drops of indicator were added to the titration solution. The solution was titrated with dichromate until a purple color appeared indicating the end point.

The dichromate solution was standardized with iron wire (99.9% Fe) using the same procedure used for the total Fe determination.

CHAPTER IV

RESULTS AND DISCUSSION

A) Characterization of High Coercivity Cobalt-Treated γ-Fe_2O_3

The characterization measurements were carried out on non-annealed and annealed Co-γ-Fe_2O_3 samples prepared with reasonably high coercivities. The objectives of these measurements were to identify the surface species associated with the coercivity enhancement and to observe if there were any changes on the Co-γ-Fe_2O_3 surface as a result of the thermal treatment.

The coercivities of the non-annealed and annealed samples, were 508 Oe and 780 Oe, respectively. Both values are significantly higher than the coercivity (365 Oe) of the γ-Fe_2O_3 precursor. The Co-γ-Fe_2O_3 was prepared using concentrated NH_4OH as base and the reaction was carried out for 2 hours (after base addition). Other details on the preparation procedure are described in the experimental section. The following is a discussion of characterization measurements.

XPS Measurements

General Characteristics of XPS Spectra

XPS spectra were measured for non-annealed and annealed samples. The photoionization levels of interest were the Fe $2p_{1/2}$, Fe $2p_{3/2}$, Co $2p_{1/2}$, Co $2p_{3/2}$, O 1s, and the valence band. Before the results from these measurements are discussed, the general spectral features of the various levels will be described. This information will serve as a reference for the following discussion of the experimental data.

The Co $2p_{3/2}$ binding energies were measured to help characterize the chemical nature of surface cobalt. This is done by comparison of the Co $2p_{3/2}$ binding energies with binding energies of reference standards given in Table 1. Given the nature of the treatment process the reference standards considered were limited to oxides, hydroxides, and oxyhydroxides of cobalt and iron. The literature values (given in parentheses) agree reasonably well with the experimental values (within the ±0.1 eV precision). However, there are a few exceptions, such as the Fe $2p_{3/2}$ binding energy for α-FeOOH where there is a 0.7 eV discrepancy between the literature value and the experimental value. It is possible that the α-FeOOH could have a different surface chemistry than the material used in the literature measurements. Differences in binding energy results often occur when comparing various studies since the selection of peak maxima, etc. is subjective to some extent.

In addition to measuring the Co $2p_{3/2}$ binding energies, the splitting between the Co $2p_{1/2}$ and Co $2p_{3/2}$ peaks (Δ Co 2p) was measured to determine the chemical state of the surface cobalt. Characteristically, Co(II) compounds have a Co $2p_{1/2}$ - Co $2p_{3/2}$ splitting of approximately 16.0 eV and Co(III) compounds have a splitting of approximately 15.0 eV (35,37). Another feature that aids in determining the state of cobalt is the intensity of the satellite peaks associated with the Co 2p spectra. Generally, Co(II) compounds have intense satellite peaks, and Co(III) compounds have very weak satellite peaks. The presence of these satellite peaks is believed to

Table 1. Binding Energies (eV) for Reference Standards

Sample	Source	Fe $2p_{3/2}$	Co $2p_{3/2}$	ΔCo 2p	Δ sat.	O 1s
$CoSO_4 \cdot 7H_2O$	Alpha	---	782.1	15.8	3.7	531.9
$Co(OH)_2$	Fisher	---	780.7(780.6)[1]	15.9	5.5	530.7(530.8)[1]
CoO	Apache	---	779.9(780.0)[1]	15.6	6.0	529.7(529.6)[1]
Co_3O_4	Fisher	---	780.0(780.3)[3]	15.2	---	529.9
Co_2O_3	Baker/ Adamson	---	779.7(779.9)[1]	15.1	---	529.9(529.9)[1]
CoOOH	Apache	---	780.2(779.9)[1]	15.1	---	530.7(531.2)[1]
$CoFe_2O_4$	Alpha	710.7(710.1)[2]	779.9(780.0)[1]	15.5	6.3	529.8(529.9)[2]
γ-Fe_2O_3	3M[a]	711.0(711.0)[2]	---	---	---	530.2(530.0)[2]
α-Fe_2O_3	3M[b]	710.9(711.0)[2]	---	---	---	530.2(529.9)[2]
Fe_3O_4	3M[c]	710.4(710.6)[2]	---	---	---	530.0(530.2)[2]
α-FeOOH	3M[c],VPI[d]	711.2(711.9)[2]	---	---	---	531.3(531.4)[2]
				530.0(530.3)[2]		

- Δ 2p = Co $2p_{1/2}$ - Co $2p_{3/2}$; - Δ sat = Co $2p_{3/2}$ (satellite) - Co $2p_{3/2}$

References

1. N. S. McIntyre, M. G. Cook, Anal. Chem., 47, 2208 (1975).
2. N. S. McIntyre, D. G. Zetaruk, Anal. Chem., 49, 1521 (1977).
3. M. Oku, K. Hirokawa, J. Electron. Spectrosc. Relatd. Phenom., 8, 475 (1976).

a MTA-21152, Lot 81; b PM-2120, Lot 1.84; c undesignated lot; d VPI laboratory prep, C.V. Schenck, 1981

be the result of a charge transfer process that occurs during photoionization (38,39). The charge transfer process is a monopole transfer transition (ligand→metal 3d) and is much more prevalent in paramagnetic transition metal compounds (eg. high spin Co(II) compounds) than in diamagnetic transition metal compounds (eg. low spin Co(III) compounds).

The presence of satellite peaks in Co(II) compounds is found in the Co 2p spectra of the reference standards in Figures 5a and 5b. The cobalt(II) compounds, $CoSO_4 \cdot 7H_2O$, CoO, $Co(OH)_2$ and $CoFe_2O_4$ all have intense satellite peaks while the Co(III) compounds, Co_2O_3 and CoOOH, and the mixed oxide Co_3O_4 have very weak satellite structures. It is also evident from examination of the spectra that the Co(II) compounds tend to have broader photoelectron peaks than the Co(III) compounds. This phenomenon is believed to be the result of multiplet splitting occurring in Co(II) compounds (38-40). Multiplet splitting occurs when the unpaired electron, remaining after photoionization, couples with other unpaired electrons in the atom. Since paramagnetic transition metals have unpaired 3d electrons, the occurrence of multiplet splitting is predominantly observed in paramagnetic transition metal compounds. The Co 2p spectra for the Co-γ-Fe_2O_3 samples all have strong satellite peaks, indicating a predominance of Co(II). The splitting between the Co $2p_{3/2}$ peak and its satellite peak, Δ sat., was also measured to aid in characterization. As can be seen in Table 1 the Co $2p_{3/2}$

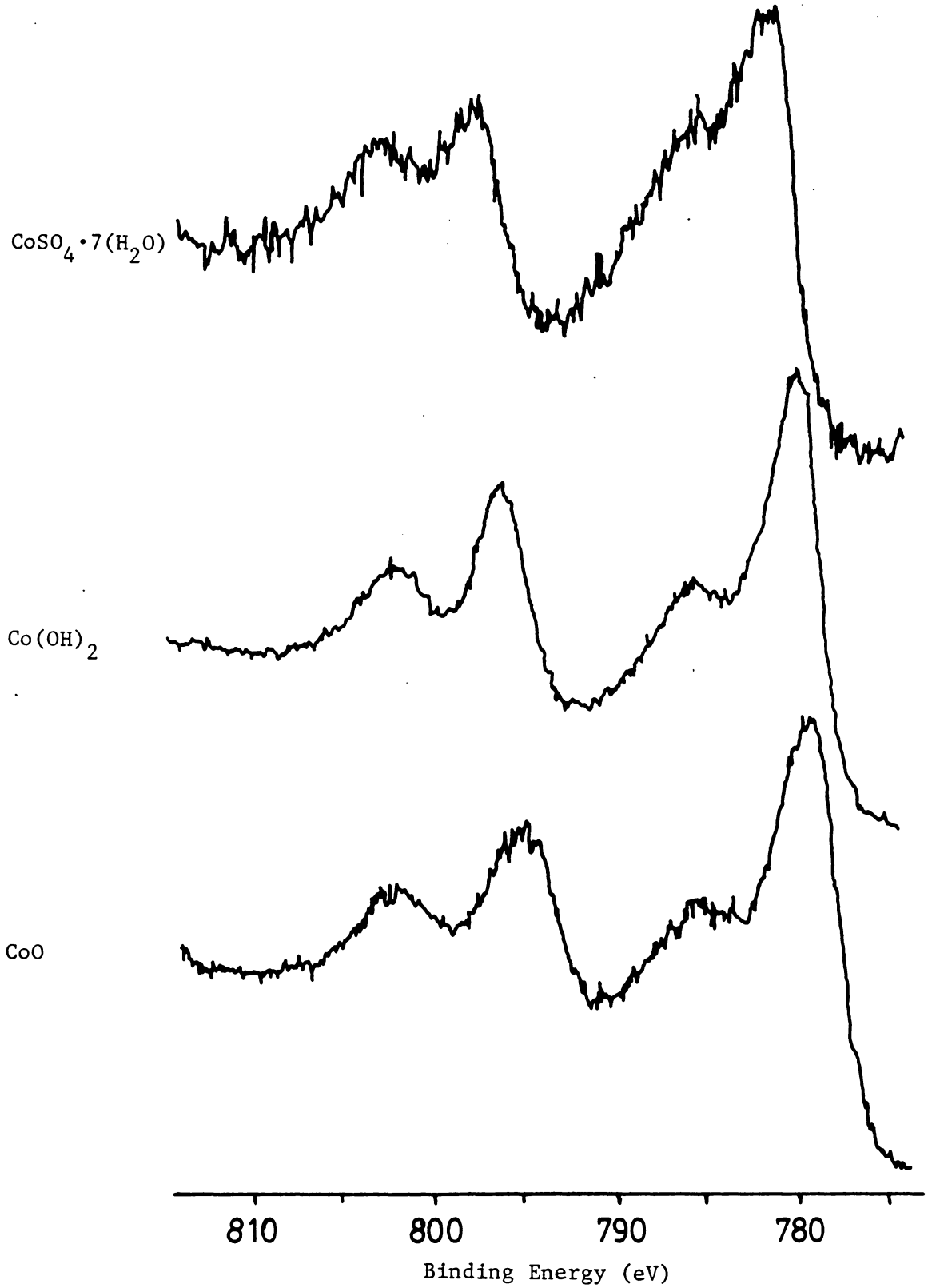

Figure 5a. XPS Co 2p Spectra of Cobalt Reference Standards

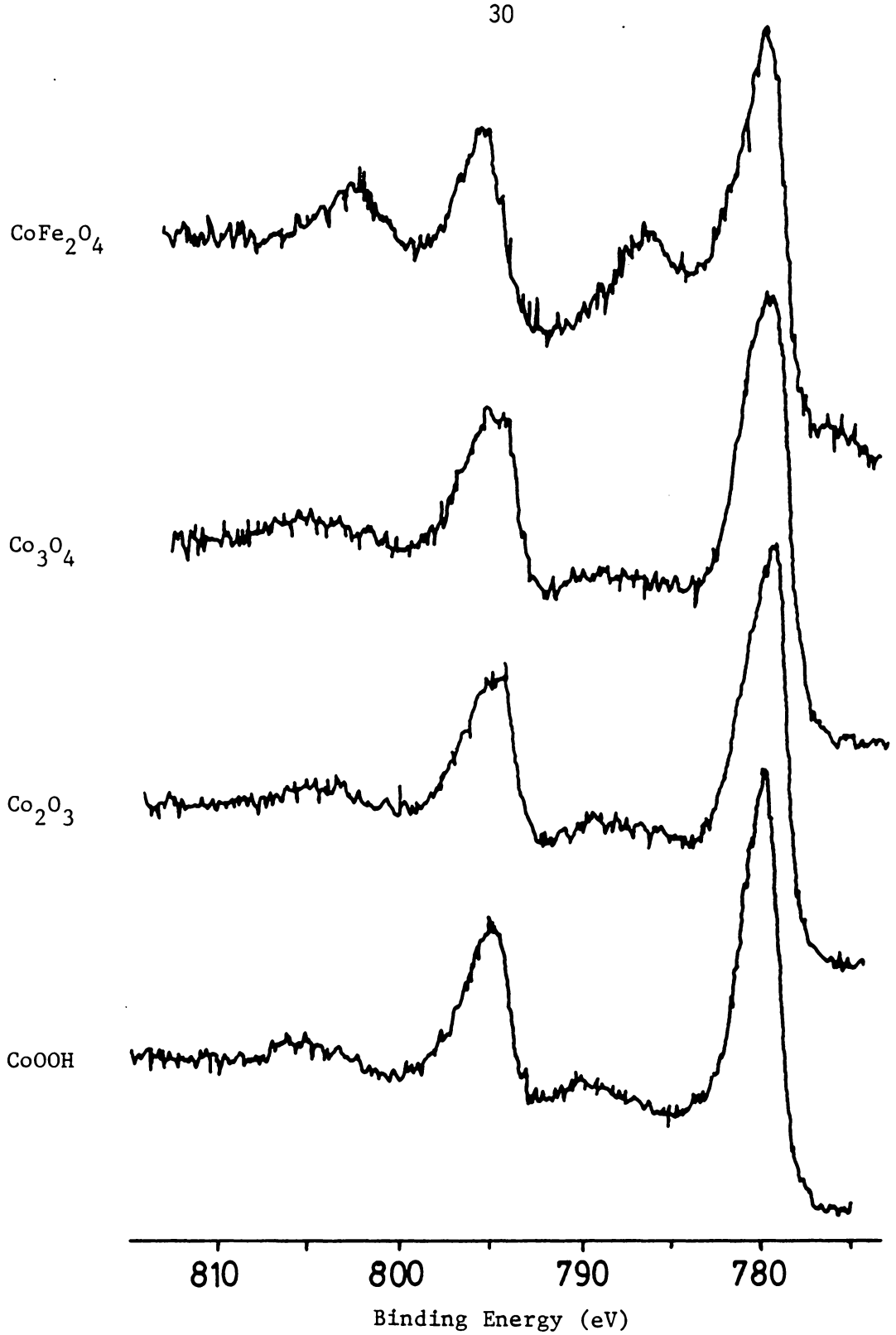

Figure 5b. XPS Co 2p Spectra of Cobalt Reference Standards

(satellite)-Co $2p_{3/2}$ splitting varies considerably among the Co(II) compounds.

The valence band spectra for the cobalt standards show a number of unique structures (Figures 6a and 6b). The Co(III) compounds, CoOOH, Co_2O_3, and Co_3O_4, show very sharp peaks at the onset of the valence band. This peak is assigned to Co 3d photoionization (41). The $Co(OH)_2$ and CoO valence bands both have peak maxima at the onset of the valence band; however, the $Co(OH)_2$ valence band has much more structure than the CoO valence band. The peak maximum of the CoO and $Co(OH)_2$ valence bands is also assigned to Co 3d photoionization. The increased breadth of these peaks compared to that for Co(III) compounds is attributed to multiplet and satellite splitting (42). The $CoFe_2O_4$ spectrum shows a broad, rounded valence band and the $CoSO_4 \cdot 7H_2O$ shows a number of small peaks. In all these spectra the O 2s peak is observed at about 22-23 eV. Based on visual comparisons of the valence band spectra, identification of the chemical form of surface cobalt in the Co-γ-Fe_2O_3 samples should be theoretically possible.

The Fe 2p spectra are unfortunately not as chemically informative as the Co 2p spectra. The Fe 2p spectra for the reference standards are given in Figure 7. The spectra shown are all similar with the exception of Fe_3O_4 which has broader peaks due to the presence of Fe(II). The extent to which the surface iron can be characterized is limited compared to the surface cobalt characterization. Besides measuring the intensity of the Fe 2p spectra for determination the Co/Fe atomic ratio, the principal measurement was the Fe $2p_{3/2}$ binding energy. The binding energies for the iron reference standards are given in Table 1.

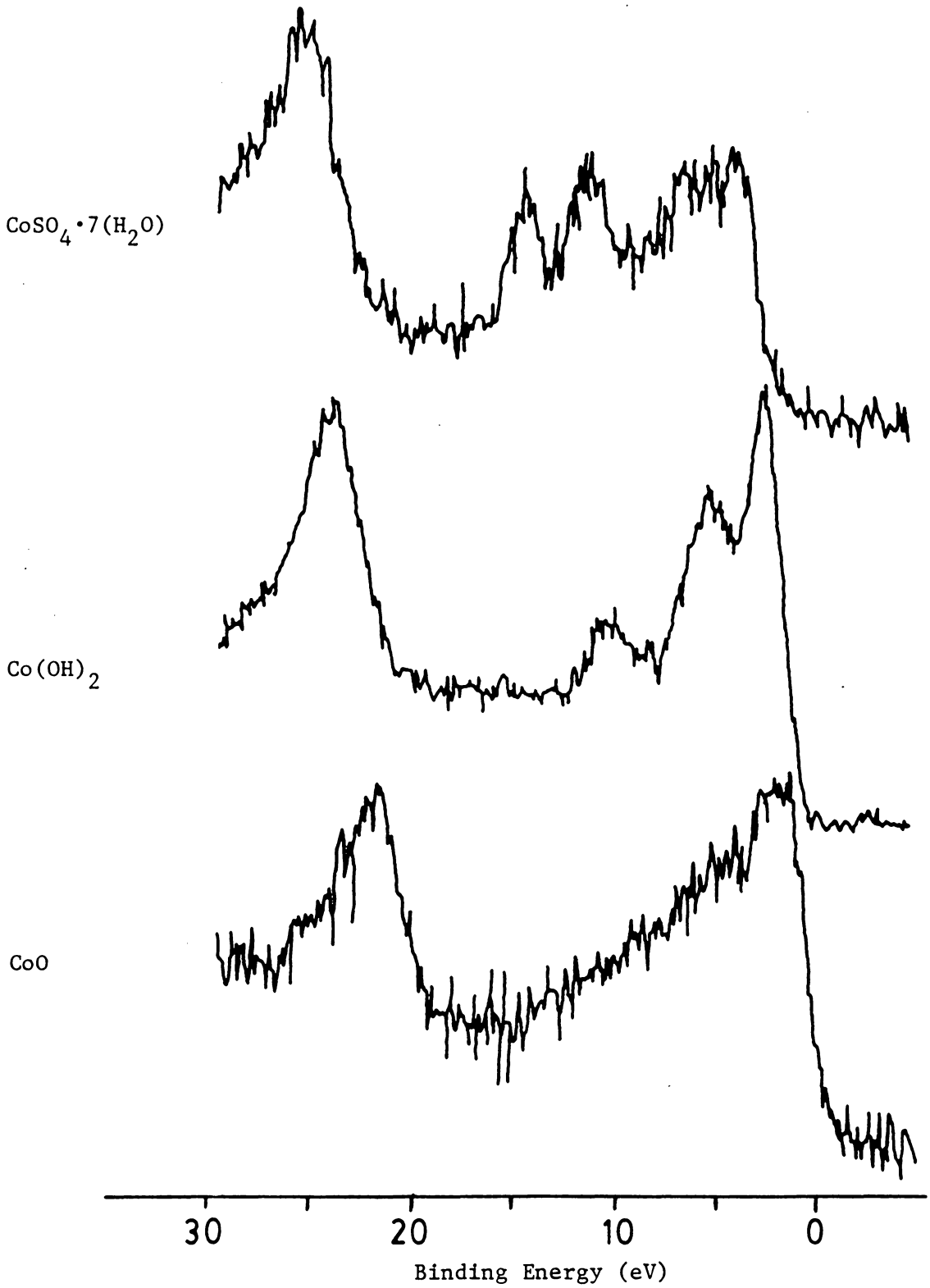

Figure 6a. XPS Valence Band Spectra of Cobalt Reference Standards

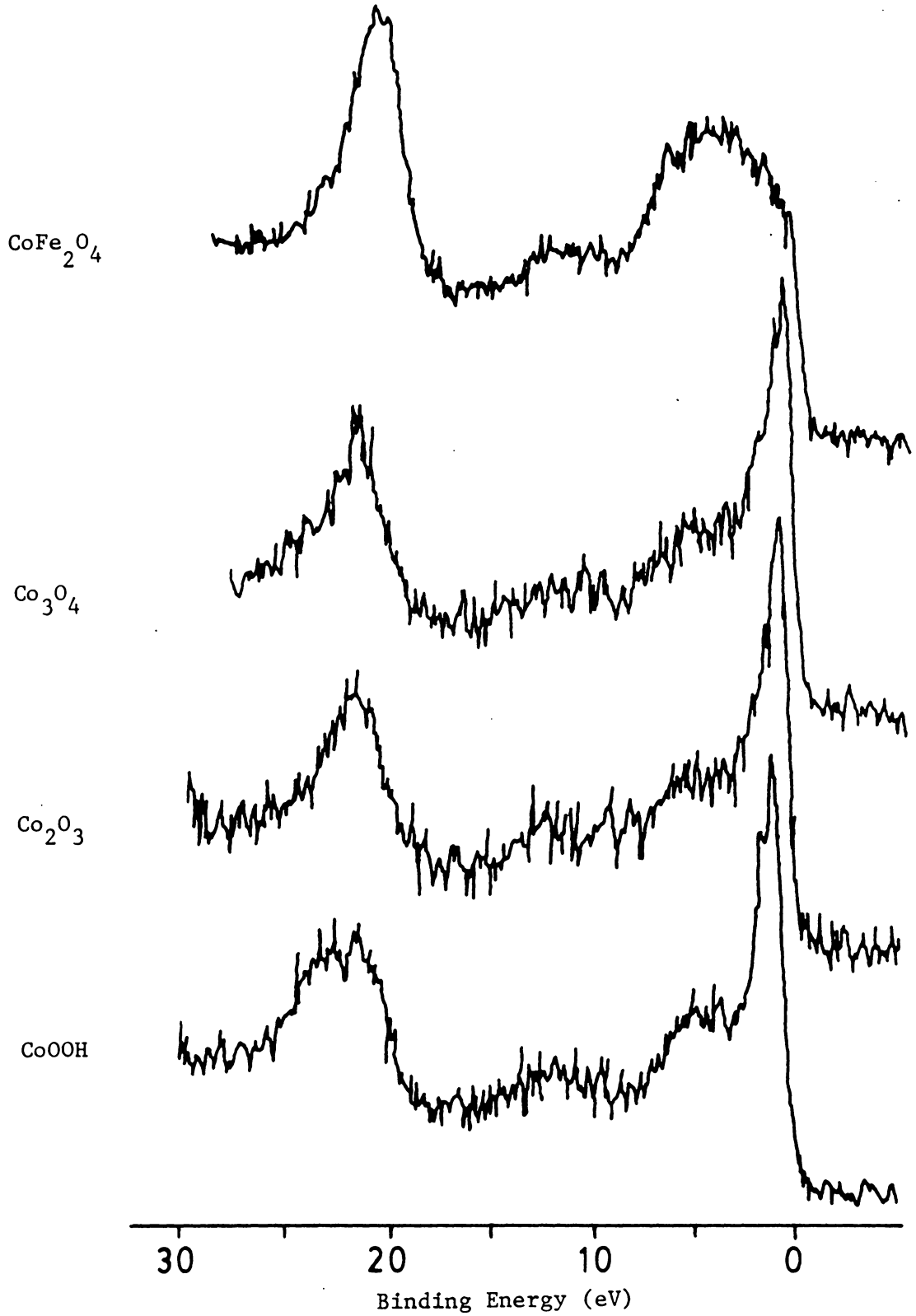

Figure 6b. XPS Valence Band Spectra of Cobalt Reference Standards

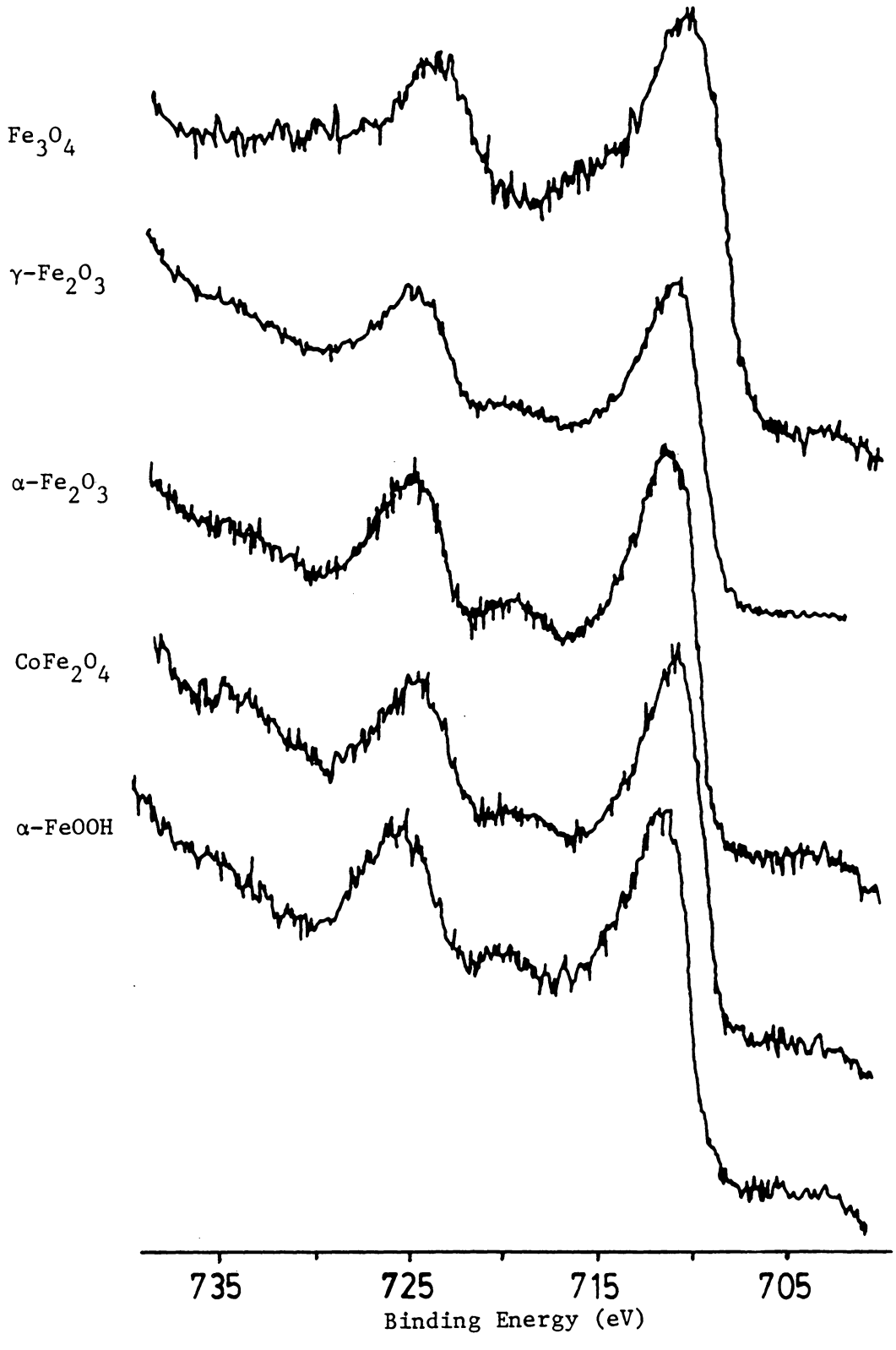

Figure 7. XPS Fe 2p Spectra of Iron Reference Standards

The valence band spectra for the iron standards are shown in Figure 8. All of the spectra show a broad, rounded valence band. The γ-Fe_2O_3 and $CoFe_2O_4$ valence bands are similar which may be a reflection of similar metal ion environments (spinel). Alpha-Fe_2O_3 has a small peak on the shoulder at the onset of the valence band. FeOOH and Fe_3O_4 show less rounded valence bands.

The O 1s spectra of the reference standards are not shown since the peaks have a simple shape. The primary information obtained from the O 1s spectrum is whether the surface oxygen is in oxide or hydroxide form. The O 1s binding energy for a hydroxyl oxygen is approximately 1 eV higher (~531.0 eV) than the oxide O 1s binding energy (~530.0 eV) (43,44). In all O 1s spectra of the oxide reference standards there is a shoulder on the high binding energy side of the main peak indicating hydroxyl groups on the surface.

XPS Results for High Coercivity Co-γ-Fe_2O_3

Cobalt 2p spectra for non-annealed and annealed samples are shown in Figure 9. Spectra for $CoFe_2O_4$ and $Co(OH)_2$ standards are included for comparison. The Co-γ-Fe_2O_3 sample spectra show intense satellites peaks indicating that surface cobalt is predominantly Co(II). The peak shapes for the non-annealed and annealed samples are very similar suggesting that the surface Co(II) species are similar in the annealed and non-annealed samples. Comparing the Co-γ-Fe_2O_3 spectra with the spectra for reference compounds, there is good agreement between the Co-γ-Fe_2O_3 spectra and the $CoFe_2O_4$ spectra. The Co-γ-Fe_2O_3 spectra have slightly broader Co 2p photoelectron peaks than those in the $CoFe_2O_4$ spectrum.

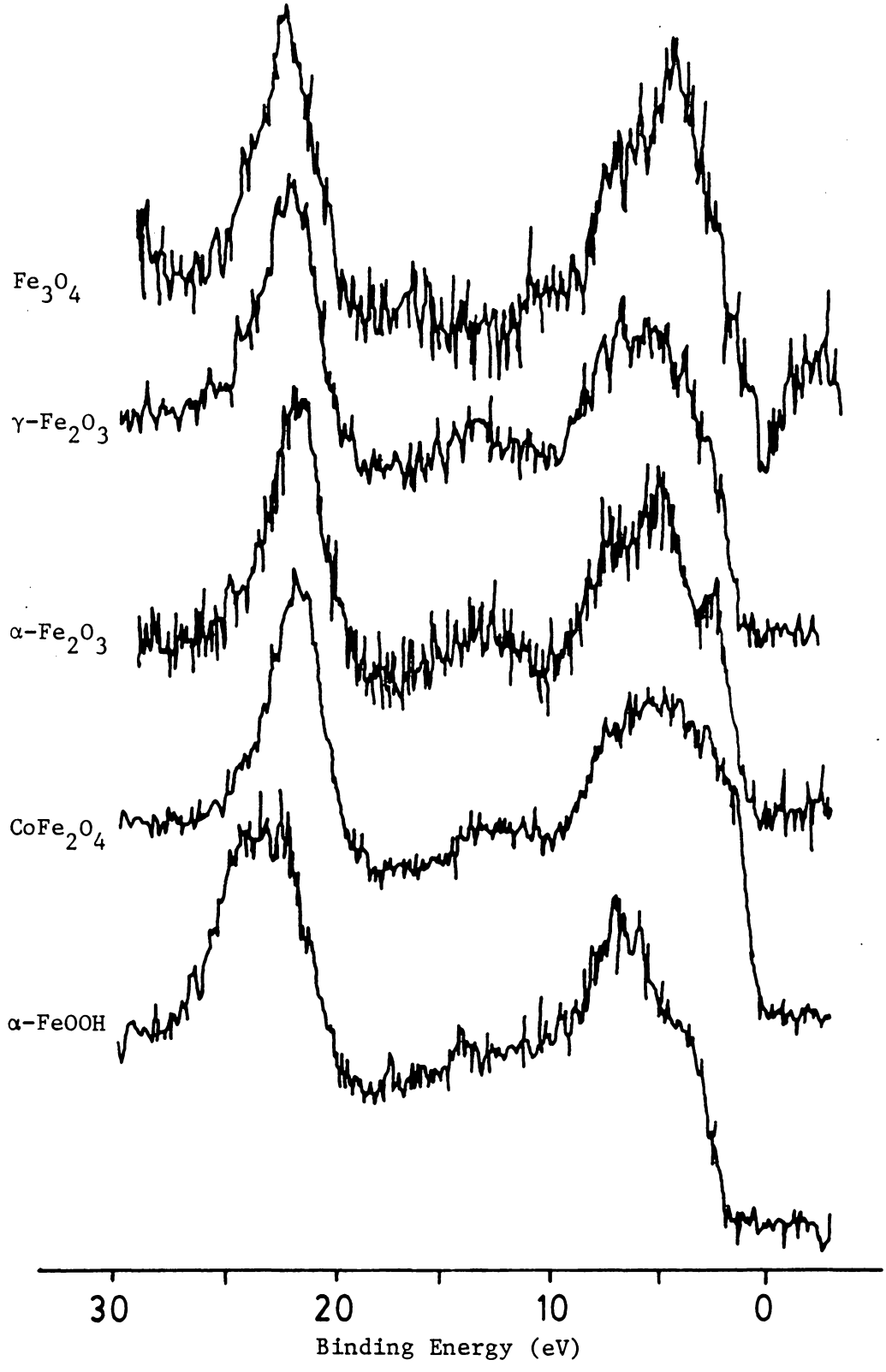

Figure 8. XPS Valence Band Spectra of Iron Reference Standards

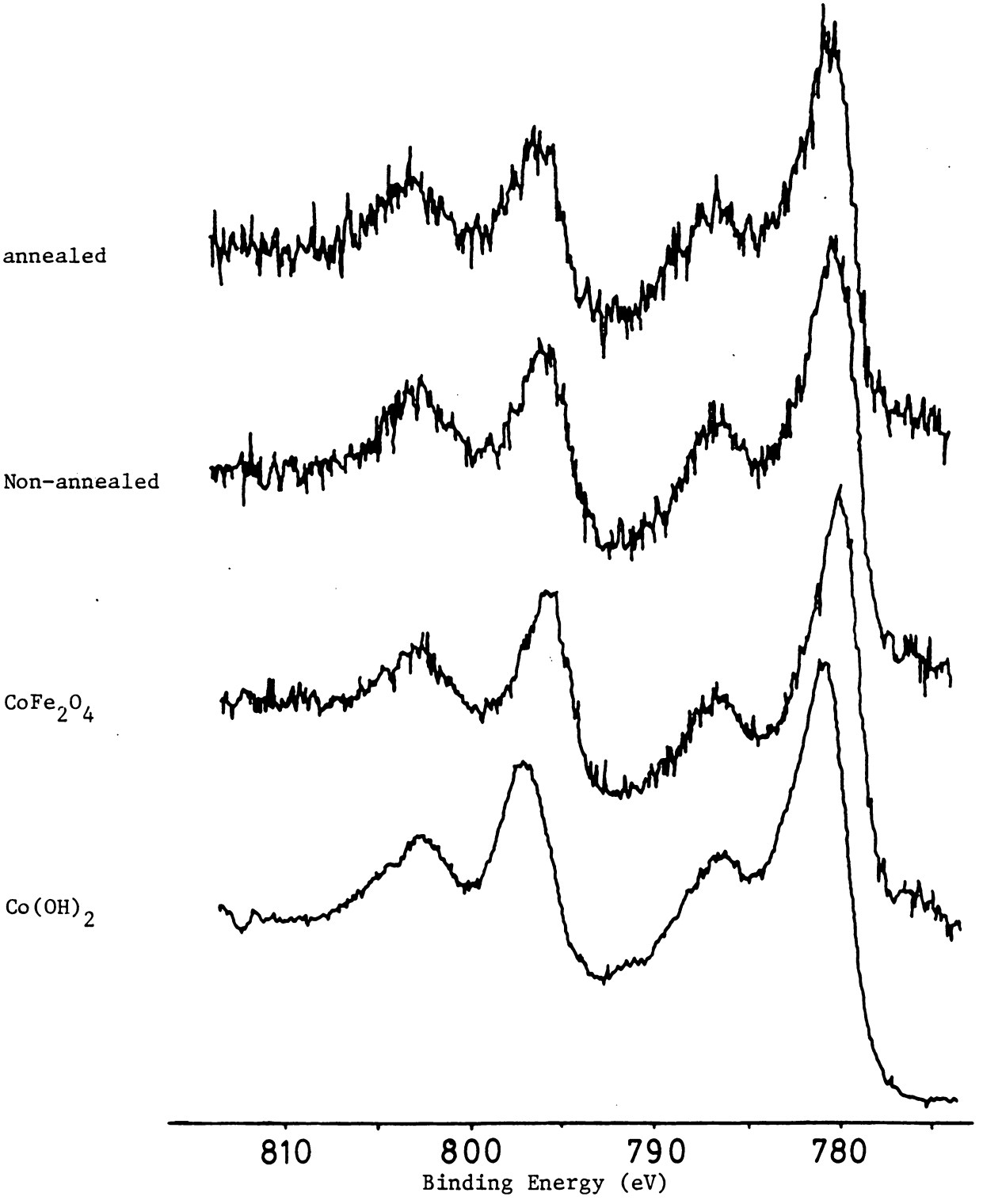

Figure 9. XPS Co 2p Spectra High Coercivity Co-γ-Fe_2O_3

This could be due to the presence of other Co(II) species on the surface such as $Co(OH)_2$ and/or CoO or a non-stoichiometric cobalt ferrite ($Co_xFe_{3-x}O_4$).

The valence band spectra for the non-annealed sample and the annealed sample are shown in Figure 10. The two spectra are very similar and show good agreement with the standard $CoFe_2O_4$ spectrum. The absence of any clear evidence for $Co(OH)_2$ peaks in the valence band spectrum of Co-γ-Fe_2O_3 samples suggests that $Co(OH)_2$ is not present in an amount greater than 10% on the surface of Co-γ-Fe_2O_3. There is also no evidence for CoO valence band features in the Co-γ-Fe_2O_3 spectrum. It must be kept in mind that the mean free path for the valence band photoelectrons is greater than the mean free path for the Co 2p photoelectrons. Using the procedure described by Penn (45) the mean free paths of the Fe 2p, Co 2p, O 1s, and valence band photoelectrons were determined. The calculated mean free path for Co 2p and Fe 2p photoelectrons is approximately 9 Å. The O 1s photoelectrons have a mean free path of 12Å and the valence band photoelectrons have a mean free path of 20 Å. If $Co(OH)_2$ were present on the outermost surface of the Co-γ-Fe_2O_3 samples, the 20 Å mean free path of the valence band electrons could cause the $Co(OH)_2$ valence band signal to be suppressed because the signals attributed to $CoFe_2O_4$ or γ-Fe_2O_3 from deeper in the particles are too great and obscure $Co(OH)_2$ features.

Based on this interpretation of the non-annealed and annealed Co-γ-Fe_2O_3 spectra, there is evidence supporting $CoFe_2O_4$ formation on the surface of γ-Fe_2O_3. The breadth of the Co $2p_{1/2}$ and Co $2p_{3/2}$

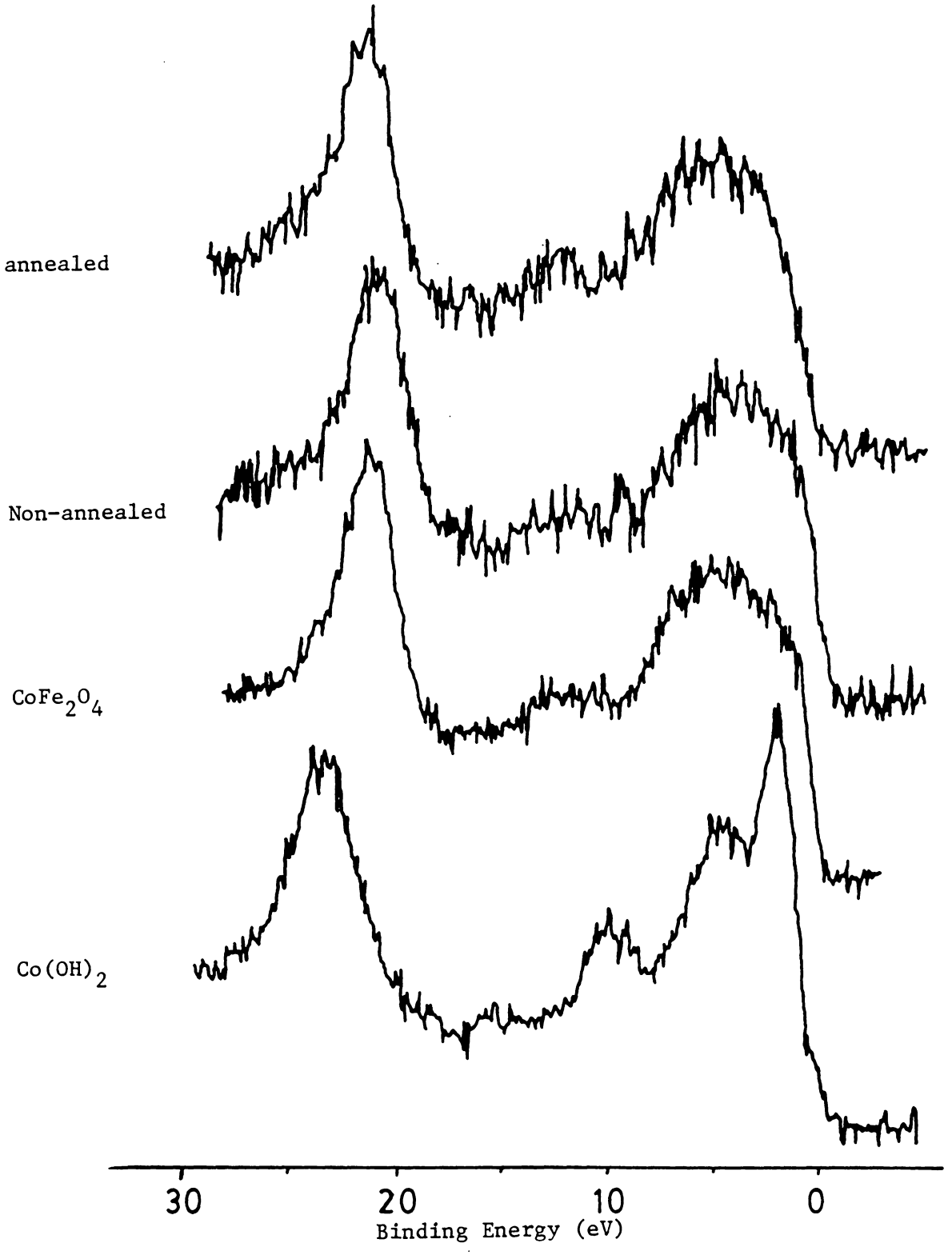

Figure 10. XPS Valence Band Spectra for High Coercivity Co-γ-Fe_2O_3

photoelectron peaks suggests that there may be other cobalt species present in small amounts on the surface. The large intensity of the satellite peaks suggests that the cobalt species present are predominantly Co(II). It should also be mentioned that it is possible that the cobalt treated γ-Fe_2O_3 samples have a cobalt ferrite surface with a different composition from that of reference $CoFe_2O_4$ (i.e., different stoichiometry).

The XPS binding energy data and Co/Fe ratios for the non-annealed and annealed samples are presented in Table 2. The binding energy results for the two Co-γ-Fe_2O_3 samples are nearly identical (within ±0.1 eV). This immediately suggests that little or no chemical change occurs on the surface of Co-γ-Fe_2O_3 as as result of the thermal treatment.

In contrast to the binding energy results, the Co/Fe ratios for the non-annealed (Co/Fe = 0.61) and annealed (Co/Fe = 0.40) samples are significantly different. The lower Co/Fe ratio observed for the annealed sample is most easily explained as the result of Co(II) diffusion into bulk γ-Fe_2O_3 during the thermal treatment. The diffusion of cobalt as a result of thermal treatment has been reported previously (27). The absence of any changes in the Co 2p binding energy and spectral results implies that the coercivity enhancement observed after annealing is due in part to Co(II) diffusion into the bulk γ-Fe_2O_3 and is not due to changes in cobalt chemistry.

The average binding energies and Co 2p splittings give somewhat conflicting results. The Co $2p_{3/2}$ binding energy and the Co $2p_{1/2}$-Co $2p_{3/2}$ splitting both compare more favorably with the values for $Co(OH)_2$, but the satellite splittings agree better with the value for $CoFe_2O_4$.

Table 2

XPS Results from High Coercivity Co-γ-Fe_2O_3 Samples

Sample	Coercivity H_c(Oe)	Binding Energy Results (eV)					Co/Fe (atomic ratio)
		Fe $2p_{3/2}$	Co $2p_{3/2}$	Δ Co 2p	Δ sat	O 1s	
Non-annealed	508	711.0	780.6	15.8	6.3	530.0	0.61
Annealed	780	711.1	780.6	15.8	6.4	530.0	0.40
γ-Fe_2O_3	365	711.1	---	---	---	530.2	---
$CoFe_2O_4$	~1300	710.7	780.2	15.5	6.4	529.7	0.50
$Co(OH)_2$	---	---	780.7	15.8	5.5	530.7	---

- Δ Co 2p = Co $2p_{1/2}$ - Co $2p_{3/2}$
- Δ sat = Co $2p_{3/2}$ (satellite) - Co $2p_{3/2}$

As was previously mentioned the Co 2p spectra for the non-annealed and annealed samples showed good agreement with the Co 2p spectrum for $CoFe_2O_4$. However, the Co-γ-Fe_2O_3 photoelectron peaks are slightly broadened. This increased peak width could be responsible for the higher measured binding energies since the increased width could systematically influence the selection of the peak maximum. This effect would also influence the measured Co $2p_{1/2}$-Co $2p_{3/2}$ splitting. Even though the measured binding energies are in better agreement with $Co(OH)_2$, its presence in appreciable amounts (> 10% atomic) can be ruled out by the absence of any indication of $Co(OH)_2$ in the valence band spectra. Furthermore, if $Co(OH)_2$ were present in significant amounts, there would be a large hydroxyl component in the O 1s spectra which was not observed in the O 1s spectra of the samples.

The Fe $2p_{3/2}$ binding energies, 711.0 and 711.1 eV, agree with the value for γ-Fe_2O_3. The Fe $2p_{3/2}$ binding energy for $CoFe_2O_4$ is 710.7. Assuming ferrite formation occurs on the surface of γ-Fe_2O_3 the Fe $2p_{3/2}$ binding energies for the Co-γ-Fe_2O_3 samples are in slight disagreement. The slightly higher binding energy could be a reflection of a ferrite-like surface which has a different stoichiometry than the $CoFe_2O_4$ standard. It could also reflect the presence of some γ-Fe_2O_3 on the surface if there are portions of the γ-Fe_2O_3 surface remaining uncovered by cobalt.

Based on the binding energy results and Co/Fe atomic ratios, it can be concluded that the coercivity enhancement observed for thermally treated Co-γ-Fe_2O_3 is largely due to the diffusion of Co(II) into bulk

γ-Fe_2O_3. The XPS analysis results indicate also that no chemical change occurs during the annealing process. This precludes a chemical transformation being responsible for the coercivity enhancement, although crystallographic changes cannot be ruled out. The XPS measurements support surface cobalt ferrite formation, possibly mixed with small amounts of other Co(II) species.

SIMS Measurements

The SIMS spectra for the non-annealed and the annealed samples are shown in Figures 11 and 12, respectively. The top spectra were collected while rastering the ion beam, and the bottom spectra were collected without rastering the ion beam. For both the annealed and non-annealed samples the spectra obtained with the rastered ion beam show relatively greater Co^+ signals, compared to Fe^+, than the spectra collected without rastering the ion beam. The spectra obtained without rastering the ion beam probe deeper into the Co-γ-Fe_2O_3 samples; therefore, the lower signals noted for both non-rastered spectra indicate that the cobalt concentration was greatest at the surface of the Co-γ-Fe_2O_3 and as sampling depth increased the cobalt concentration decreased. The same behavior was found for both the annealed and non-annealed samples. The ability to obtain a quantitative depth profile for the Co γ-Fe_2O_3 particles with an ion beam was limited, because of the multitude of particle orientations relative to the ion beam.

The non-rastered spectra for both samples exhibited some higher mass peaks. The peaks are the result of dimer cations: Fe_2^+ (m/z=112), $CoFe^+$ (m/z=115), Fe_2O^+ (m/z=128) and $CoFeO^+$ (m/z=131).

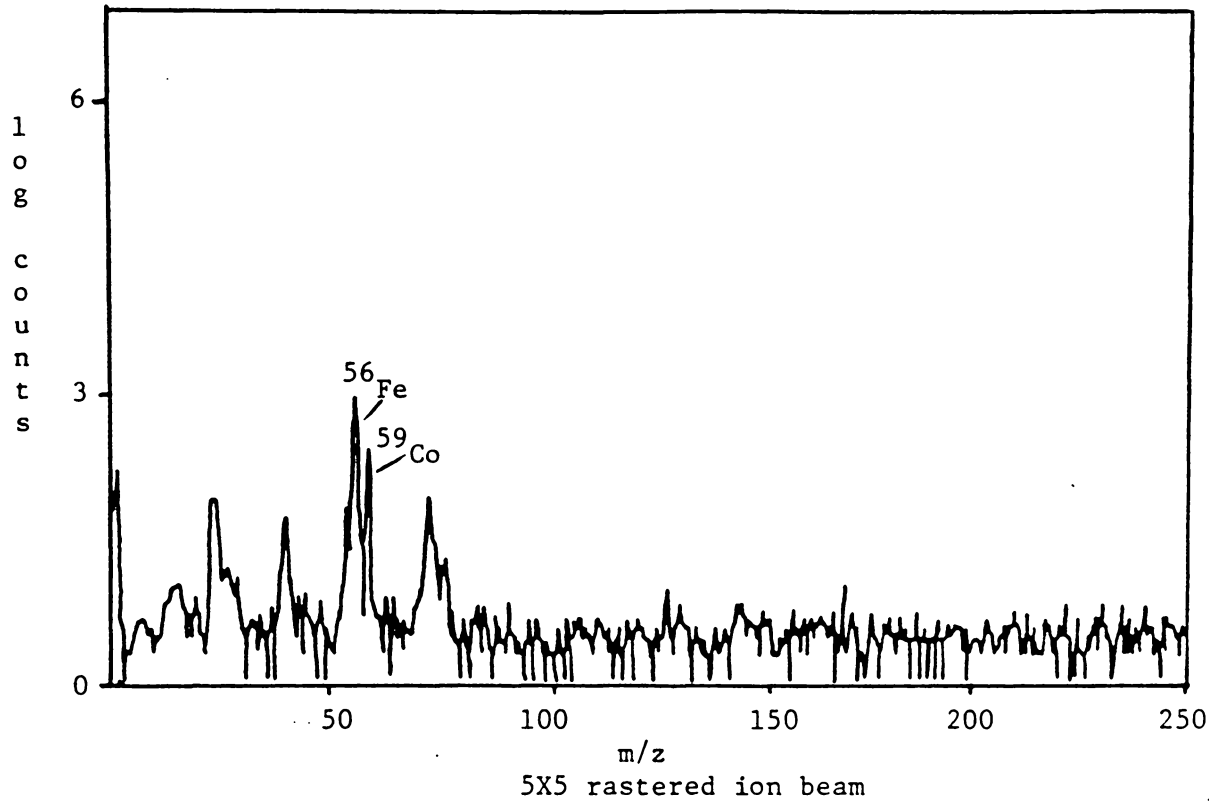

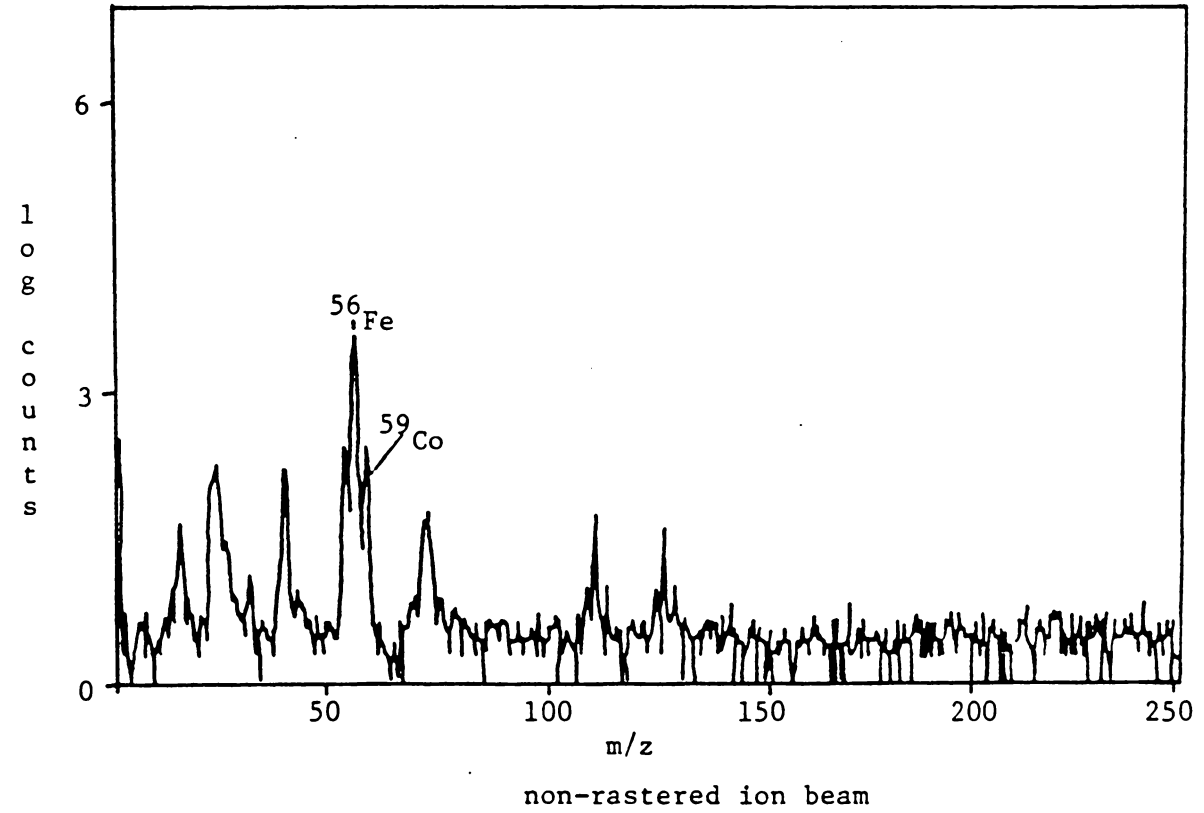

Figure 11. SIMS Spectra of Non-annealed Co-γ-Fe_2O_3 Sample

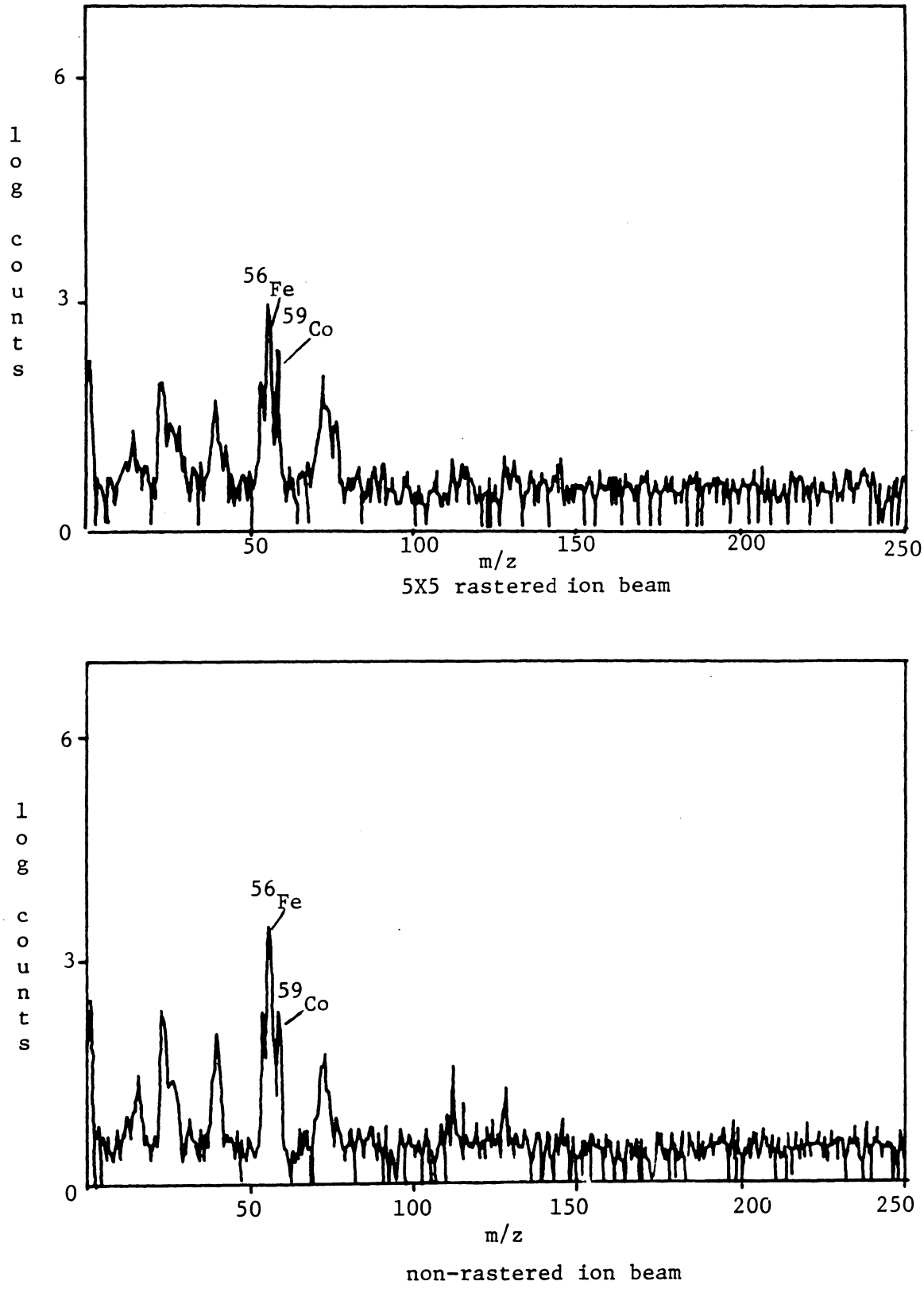

Figure 12. SIMS Spectra of Annealed Co-γ-Fe_2O_3 Sample

Infrared Measurements

The initial interest in the infrared spectra of the Co-γ-Fe_2O_3 samples was to see whether the O-H stretching band of $Co(OH)_2$ was present in the sample spectra. The infrared spectrum of $Co(OH)_2$ is shown in Figure 13. The OH band from $Co(OH)_2$ is evident at 3630 cm^{-1}. The peak is very intense and sharp. No evidence of the O-H band of $Co(OH)_2$ was contained in the infrared spectra for the non-annealed or annealed samples. This indicates either that $Co(OH)_2$ was not present in the Co-γ-Fe_2O_3 samples or that its concentration was too low to be detected in the infrared measurements

The other area of interest was in the infrared region (below ≈900 cm^{-1}). The spectra of the non-annealed and of the annealed sample are shown in Figure 14. The spectra of the two samples are essentially identical. The spectra of γ-Fe_2O_3 and $CoFe_2O_4$ are given in Figure 15. Comparing the Co-γ-Fe_2O_3 spectra with the spectra for γ-Fe_2O_3 and $CoFe_2O_4$, evidence for both γ-Fe_2O_3 and $CoFe_2O_4$ features are apparent. In an attempt to quantify the amount of $CoFe_2O_4$, individual spectra for γ-Fe_2O_3 and $CoFe_2O_4$ were added using several fractional amounts of the $CoFe_2O_4$ spectrum. An optimum combination, where the γ-Fe_2O_3 to $CoFe_2O_4$ ratio was 1:0.67, reproduces the Co-γ-Fe_2O_3 spectrum in its essential features. The combination spectrum is shown in Figure 16. The synthesized spectrum in Figure 16 is not a perfect match with the Co-γ-Fe_2O_3 sample spectrum but there are similarities in the general shape and features of the spectra. This result adds further evidence for cobalt ferrite formation on the surface of γ-Fe_2O_3.

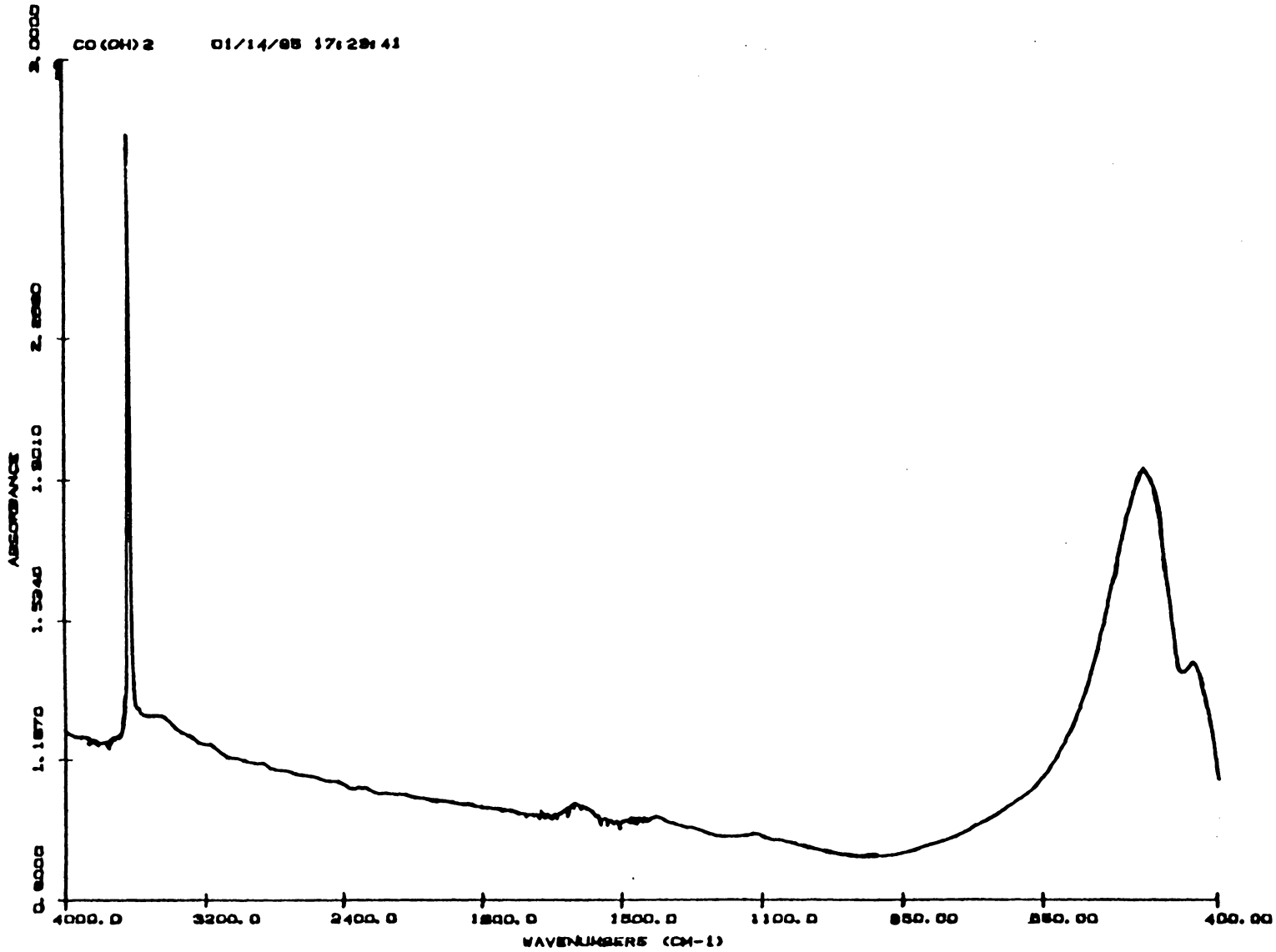

Figure 13. $Co(OH)_2$ Infrared Spectrum

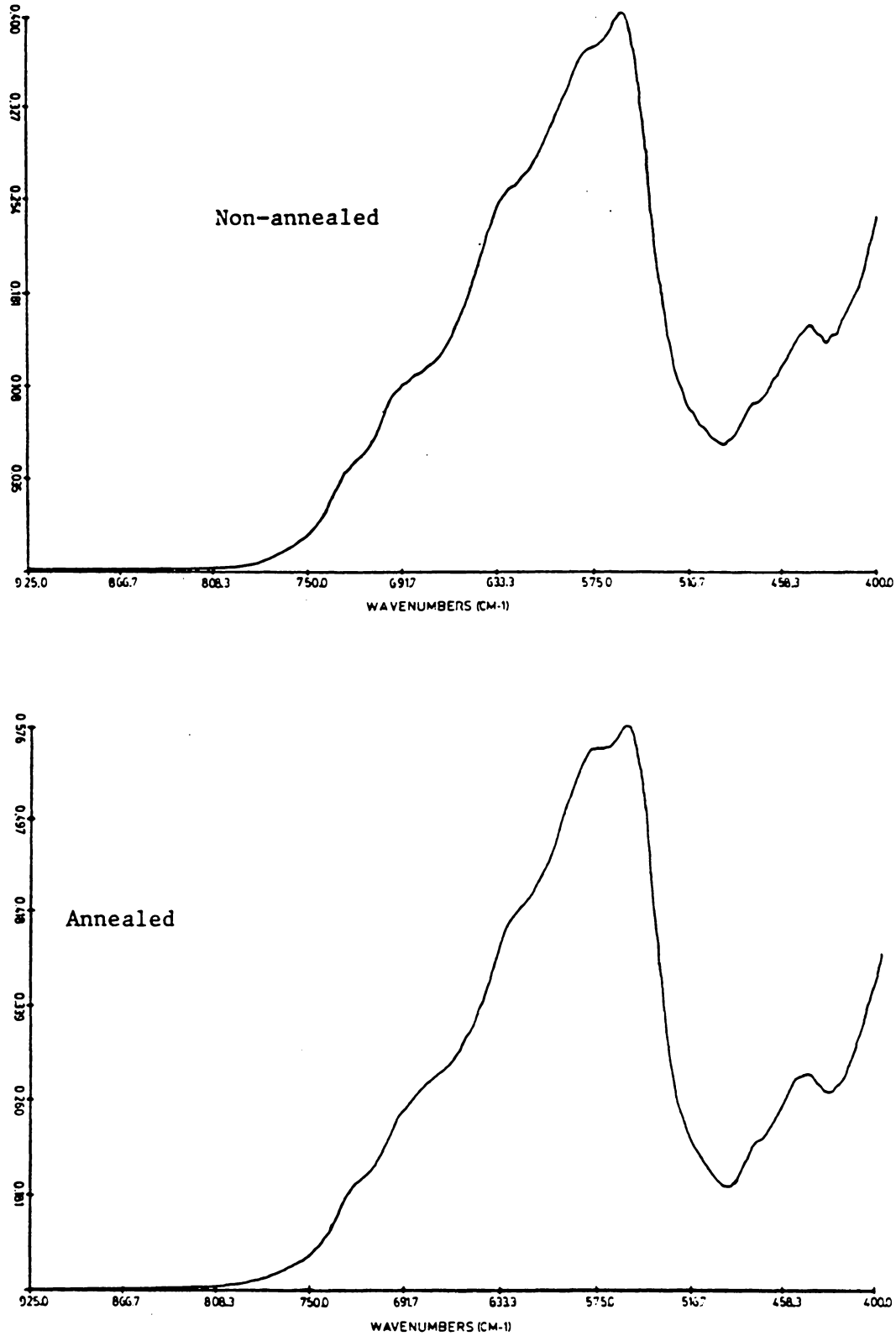

Figure 14. Infrared Spectra of Non-annealed and annealed Co-γ-Fe_2O_3 Samples

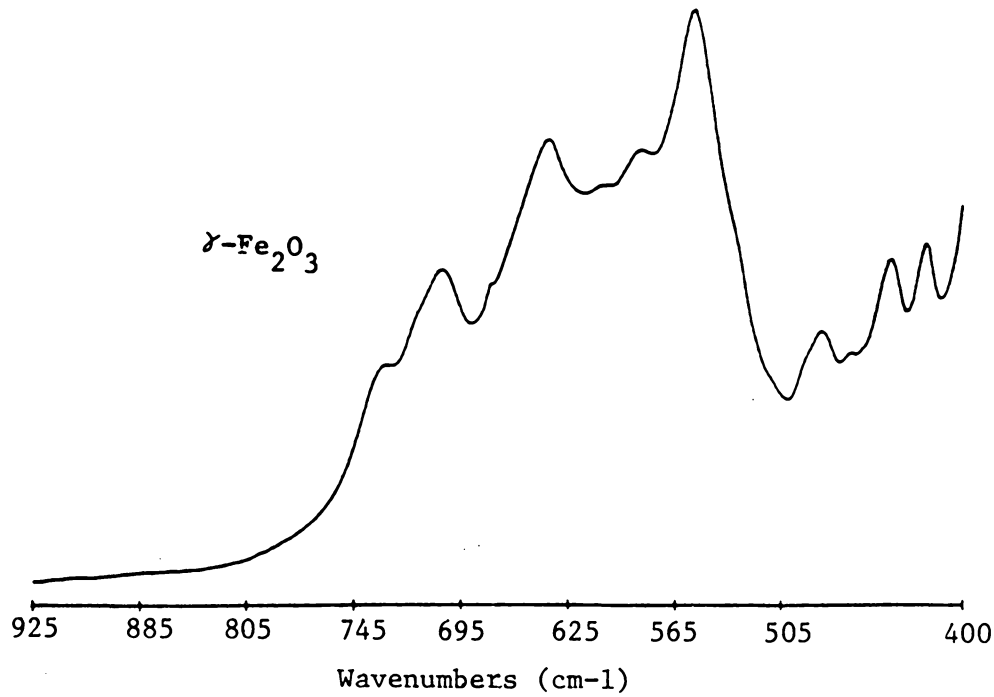

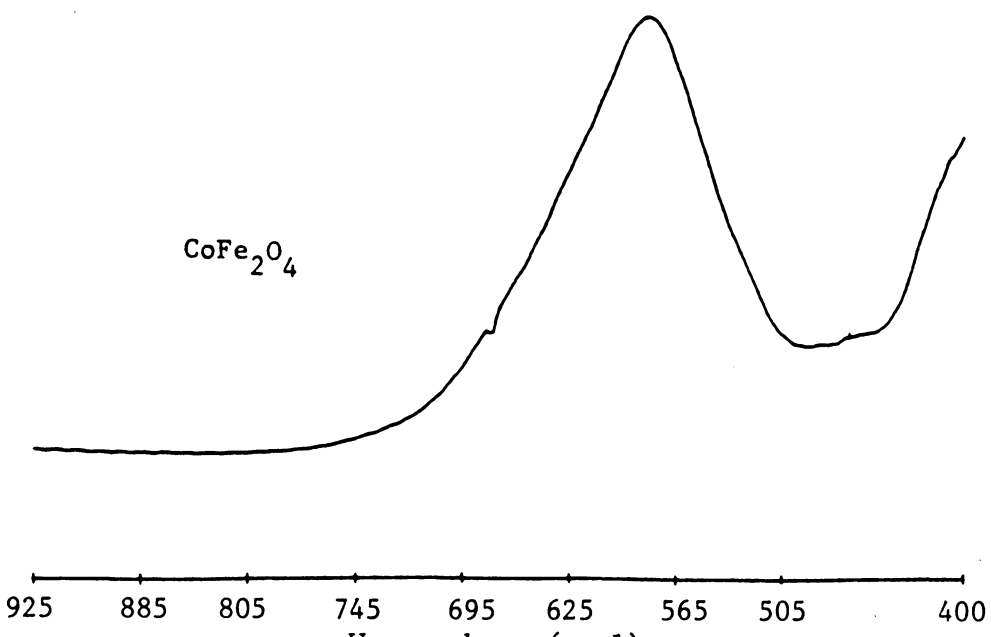

Figure 15. Infrared Spectra of γ-Fe_2O_3, $CoFe_2O_4$

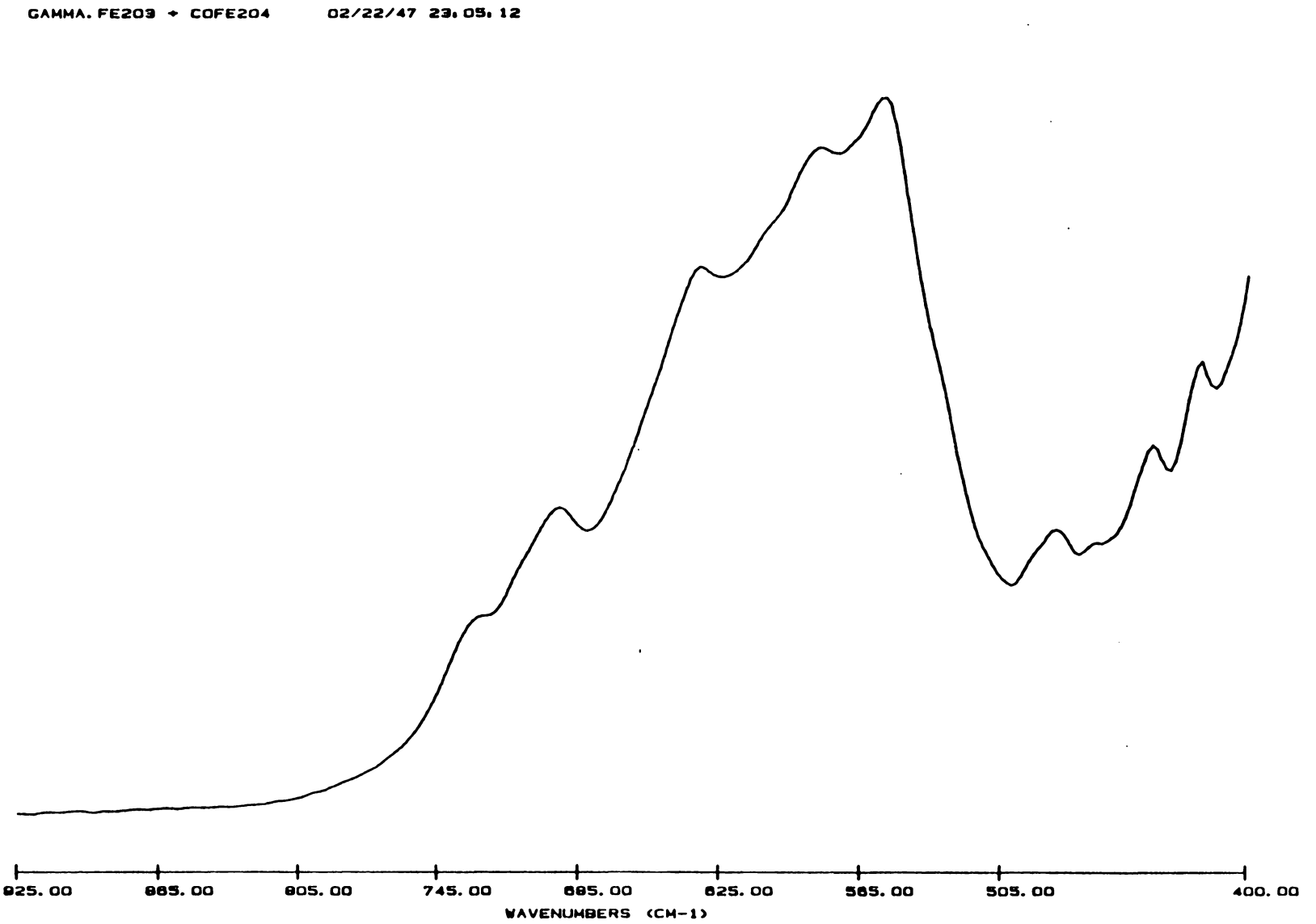

Figure 16. Infrared Spectra of γ-Fe_2O_3 and $CoFe_2O_4$ (added)

B) Kinetic Studies of the Cobalt-γ-Fe_2O_3 Reaction

Following characterization of the high coercivity Co-γ-Fe_2O_3, efforts were focused on studying how the Co(II) and Fe(II) species were adsorbed and incorporated on γ-Fe_2O_3 during the reaction. The method of study was to remove samples from the suspension during the course of the reaction, hence the term "kinetic" studies. The emphasis was on sampling the reaction suspension early in the reaction. This was due to the belief that much of the incorporation of Co(II) and Fe(II) occurred early in the reaction.

The samples taken (each ~150 ml of suspension) were "quenched" by dumping the sample suspension into approximately 1000 ml of pH 7 deionized water. After the samples were washed and the solids filtered, the solid was divided and one half was dried at room temperature under vacuum and the other half was annealed.

For the first three kinetic preparations, sampling started immediately after base addition was complete (zero time). Samples were taken at 0, 5, 10, 15, 20, 25, 30, 45, 60 and 120 minutes.

The first kinetic preparation used concentrated NH_4OH for pH adjustment and 7.4 N NaOH was used in the two subsequent preparations. Different amounts of base were used for the two NaOH preparations, corresponding to different assumed stoichiometries with respect to the Co(II) and Fe(II) mixture. After these preparations another NH_4OH preparation was carried out in which the sampling was started <u>during</u> the pH adjustment. This preparation will be described as the "early sampling" NH_4OH kinetic preparation. The following discussion will

examine the results of these kinetic preparations, and at the end of the discussion a summary of the results will be given.

NH_4OH Kinetic Preparation

Magnetic Results

The magnetic results from the NH_4OH kinetic preparation are given in Table 3, and the coercivities of the samples are plotted versus reaction time in Figure 17. The plot shows that most of the coercivity enhancement observed in the non-annealed samples occurs in the first 25 minutes of the reaction. The largest increase occurs between the 10 and 15 minute samples (320 to 397 Oe). After the first 25 minutes the rate of coercivity enhancement drops off significantly and only a modest increase takes place for the later samples. The annealed samples show the same general behavior as the non-annealed samples, where the coercivity increases rapidly in the early samples and then levels off for the later samples. Overall the annealed samples have higher coercivities.

The rapid increase in the coercivities of the non-annealed samples early in the reaction is possibly a reflection of the temperature profile for the reaction suspension, in that the large coercivity increase coincides with the time it takes the reaction suspension to reach the final reaction temperature of 94°C.

XPS Measurements

The binding energy data and Co/Fe ratios for the non-annealed and annealed samples are given in Tables 4 and 5. The Co $2p_{3/2}$ binding energies for the non-annealed samples (Table 4) show a noticeable trend

Table 3

Magnetic Results for Kinetic Preparations

Sample	Reaction Temperature Avg. (°C)	NH_4OH Prep.		NaOH Prep. Fe:OH = 1:2		NaOH Prep. Fe:OH = 1:3	
		H_c(Oe)					
		N.A.	Ann.	N.A.	Ann.	N.A.	Ann.
0 min	29	315	469	327	526	369	589
5 min	43	310	503	330	507	388	543
10 min	64	320	540	329	507	399	560
15 min	85	397	679	345	510	430	544
20 min	91	425	719	354	581	455	644
25 min	94	440	737	360	590	458	644
30 min	94	434	730	360	610	470	674
45 min	94	445	749	366	580	472	626
60 min	94	450	734	384	597	479	657
120 min	94	489	738	389	532	534	687

N.A. - non-annealed

Ann. - annealed

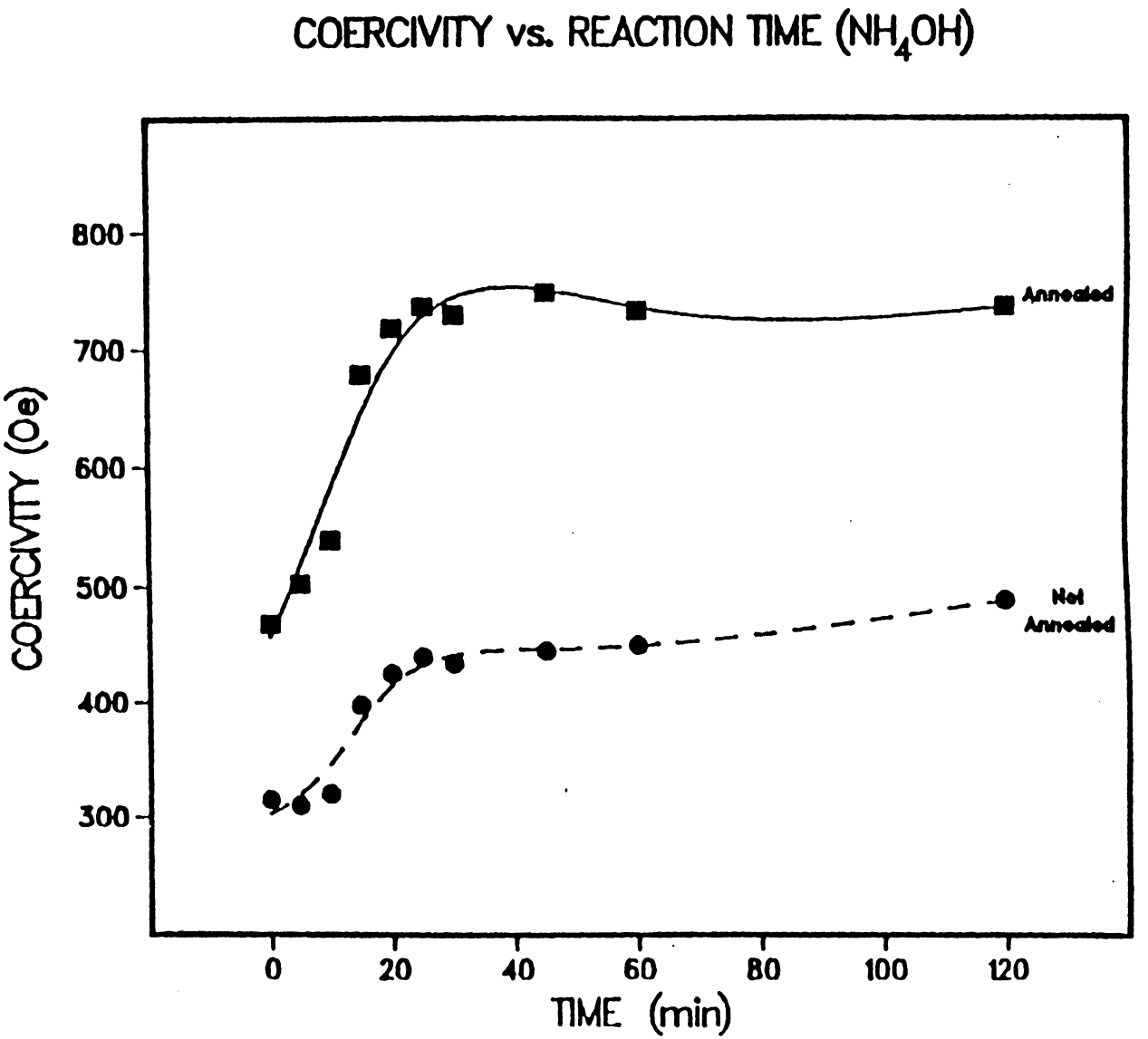

Figure 17. Coercivity Versus Reaction Time (NH_4OH Kinetic Preparation)

Table 4

XPS Results

NH_4OH Kinetic Series

Non-Annealed

Sample	Binding Energy Results (eV)					Co/Fe (atomic ratio)
	Fe $2p_{3/2}$	Co $2p_{3/2}$	Δ Co 2p	Δ sat.	O 1s	
0 min	711.2	781.0	15.7	5.8	530.3	0.56
5 min	711.1	780.9	15.7	5.9	530.2	0.59
10 min	711.1	780.8	15.7	5.9	530.1	0.60
15 min	711.0	780.6	15.8	6.2	530.0	0.79
20 min	711.0	780.6	15.8	6.2	530.1	0.78
25 min	711.0	780.5	15.8	6.2	530.2	0.78
30 min	710.9	780.6	15.8	6.3	530.2	0.72
45 min	711.1	780.5	15.8	6.4	530.1	0.76
60 min	711.0	780.6	15.7	6.3	530.2	0.74
120 min	711.1	780.6	15.6	6.2	530.2	0.73
$CoFe_2O_4$	710.7	780.2	15.5	6.3	529.8	0.50
$Co(OH)_2$	---	780.7	15.9	5.5	530.7	---

Table 5

XPS Results

NH_4OH Kinetic Series

Annealed

Sample	Binding Energy Results (eV)					Co/Fe (atomic ratio)
	Fe $2p_{3/2}$	Co $2p_{3/2}$	Δ Co 2p	Δ sat.	O 1s	
0 min	711.2	780.7	16.0	6.5	530.3	0.33
5 min	711.2	780.7	15.7	6.4	530.3	0.34
10 min	711.1	780.5	15.9	6.3	530.2	0.39
15 min	711.2	780.7	15.7	6.3	530.3	0.54
20 min	711.2	780.5	15.9	6.5	530.2	0.49
25 min	711.0	780.5	15.9	6.5	530.2	0.47
30 min (annealed ~24 hrs)	711.0	780.4	15.9	6.6	530.1	0.26
45 min	711.1	780.6	15.6	6.4	530.2	0.50
60 min	711.2	780.6	15.8	6.2	530.2	0.48
120 min	711.2	780.6	15.8	6.2	530.2	0.48
$CoFe_2O_4$	710.7	780.2	15.5	6.3	529.8	0.50
$Co(OH)_2$	---	780.7	15.9	5.5	530.7	---

of decreasing binding energy with increasing reaction time. The binding energy for the 0 min. sample has a value of 781.0 eV and as the reaction time increases the Co $2p_{3/2}$ binding energies decrease to a value of ~780.6 eV. This decrease in binding energy takes place in approximately the first 20 minutes of the reaction. Another trend is observed for the satellite splitting. The 0 min. sample has a low value of 5.8 eV and as the reaction time increases the satellite splitting increases to a value of ~6.3 eV. The Fe $2p_{3/2}$ and O 1s binding energies and the Co $2p_{1/2}$-Co $2p_{3/2}$ splitting show no significant trends.

Comparing the Co-γ-Fe_2O_3 Co $2p_{3/2}$ binding energies with the Co $2p_{3/2}$ binding energy values for $Co(OH)_2$ (780.7 eV) and $CoFe_2O_4$ (780.2 eV), the values suggest a hydrous form of cobalt is on the surface initially, and as the reaction time and temperature increase there is a conversion to a ferrite-like surface. The trend of increasing satellite splitting follows a pattern where the early samples have splittings closer to the $Co(OH)_2$ satellite splitting (5.5 eV), and as the reaction time increases the satellite splitting for the Co-γ-Fe_2O_3 samples increases to an average value very similar to the $CoFe_2O_4$ splitting (6.3 eV). The average Co $2p_{3/2}$ binding energy (780.6 eV) and satellite splitting (6.3 eV) of the latter samples (20-120 min) are similar to the values for the "high coercivity" samples. As was previously discussed, the average Co $2p_{3/2}$ binding energy of 780.6 eV compares more favorably with the Co $2p_{3/2}$ binding energy for $Co(OH)_2$ (780.7 eV) than $CoFe_2O_4$ (780.2 eV). However, for the same reasons described in the previous section, the XPS results generally support ferrite formation. The Co

$2p_{3/2}$ binding energies for the early samples are sightly higher than the 780.7 eV value for $Co(OH)_2$. This is possibly the result of $Co^{2+}(aq)$ species adsorbed on the surface. The Co $2p_{3/2}$ binding energy of $CoSO_4 \cdot 7H_2O$ is 782.1 eV (Table 1) so the presence of small amounts of $Co^{2+}(ads)$ could be responsible for the high Co $2p_{3/2}$ binding energies in the early samples.

The Co 2p spectra for the early non-annealed samples are shown in Figure 18. There is a noticeable decrease of the Co $2p_{3/2}$ peak width and an increase in satellite splitting with increasing reaction time. Comparing the sample spectra with $Co(OH)_2$ and $CoFe_2O_4$ spectra one can see how these trends reflect a pattern of decreasing hydrous cobalt content to a more $CoFe_2O_4$-like Co 2p spectrum. Possibly in the early samples there is a mixture of cobalt species in hydrous and ferrite forms and as the reaction continues ferrite formation progresses to completion.

The O 1s spectra of these early samples are shown in Figure 19. The early samples (0, 10 min) have large shoulders on the high binding energy side of the O 1s photoelectron peak. This is undoubtedly due to a large number of hydroxyl groups on the surface. As can be seen this shoulder decreases significantly with increasing reaction time indicating dehydration of the surface. These results support the trends observed for the Co $2p_{3/2}$ binding energies and satellite splitting.

The valence band spectra for these samples are shown in Figure 20. Surprisingly, there is no evidence for $Co(OH)_2$ in the Co-γ-Fe_2O_3 valence band spectrum at early sampling times. This apparent contradiction to

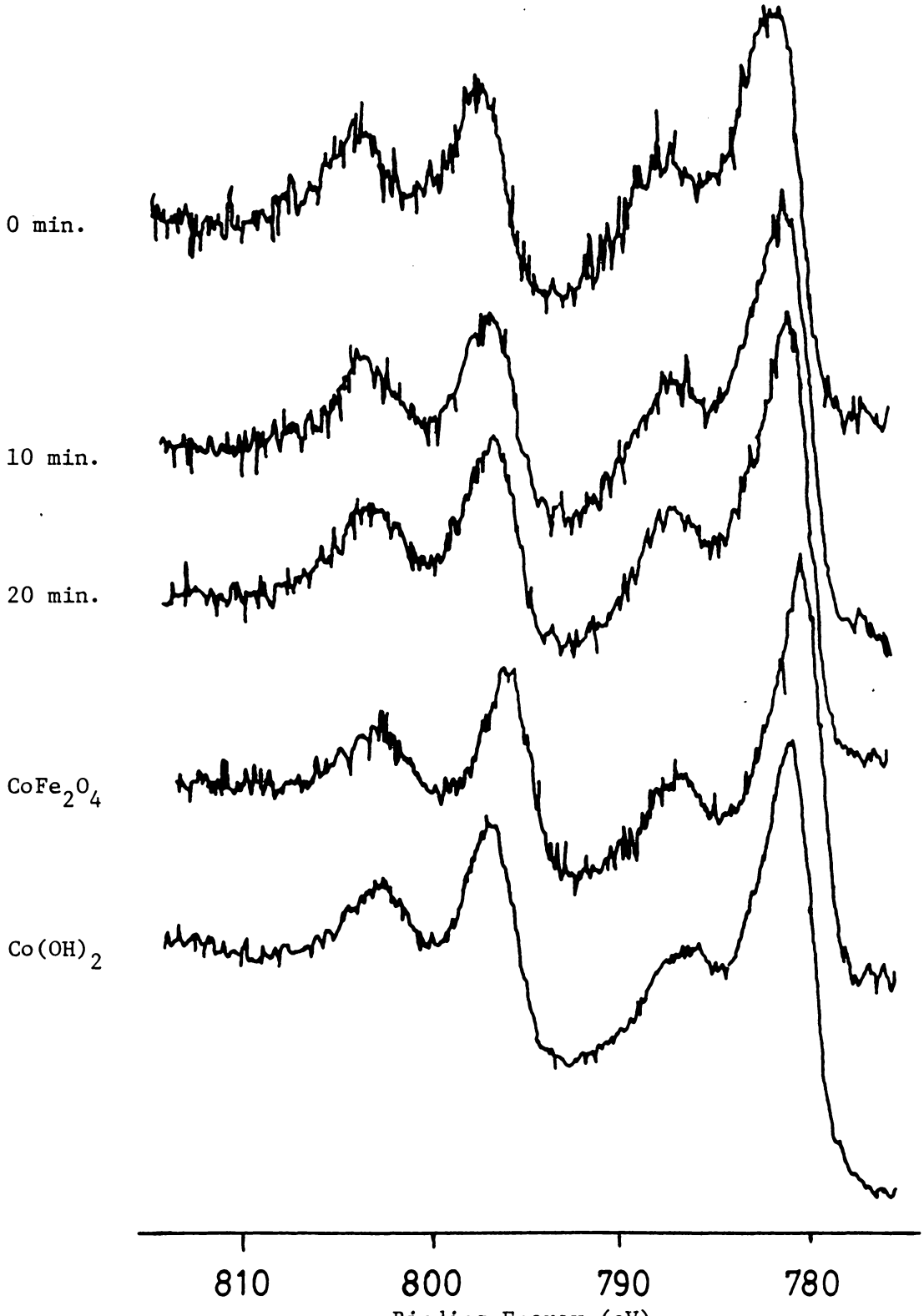

Figure 18. XPS Co 2p Spectra (NH_4OH Kinetic Preparation)

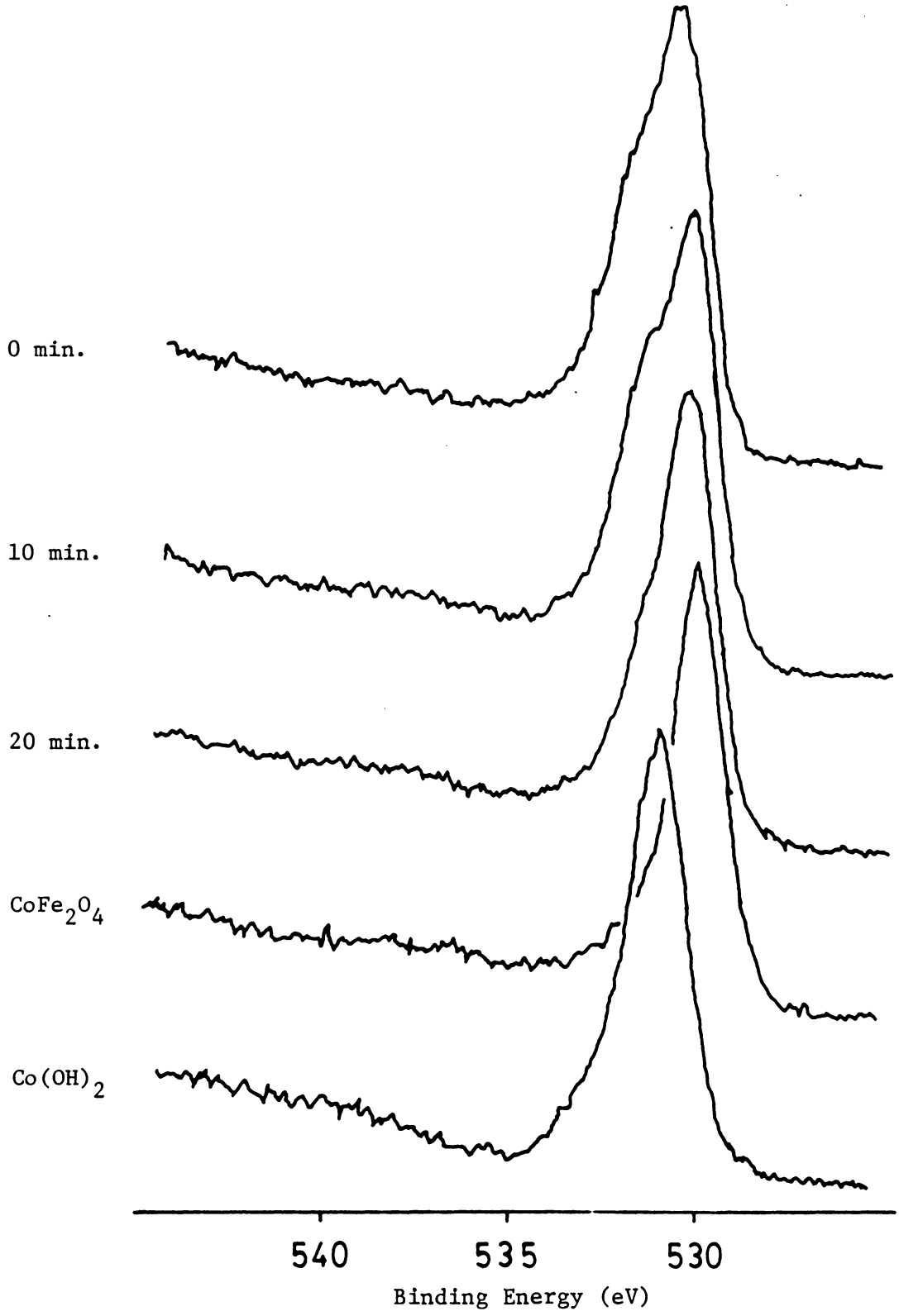

Figure 19. XPS O 1s Spectra (NH_4OH Kinetic Preparation)

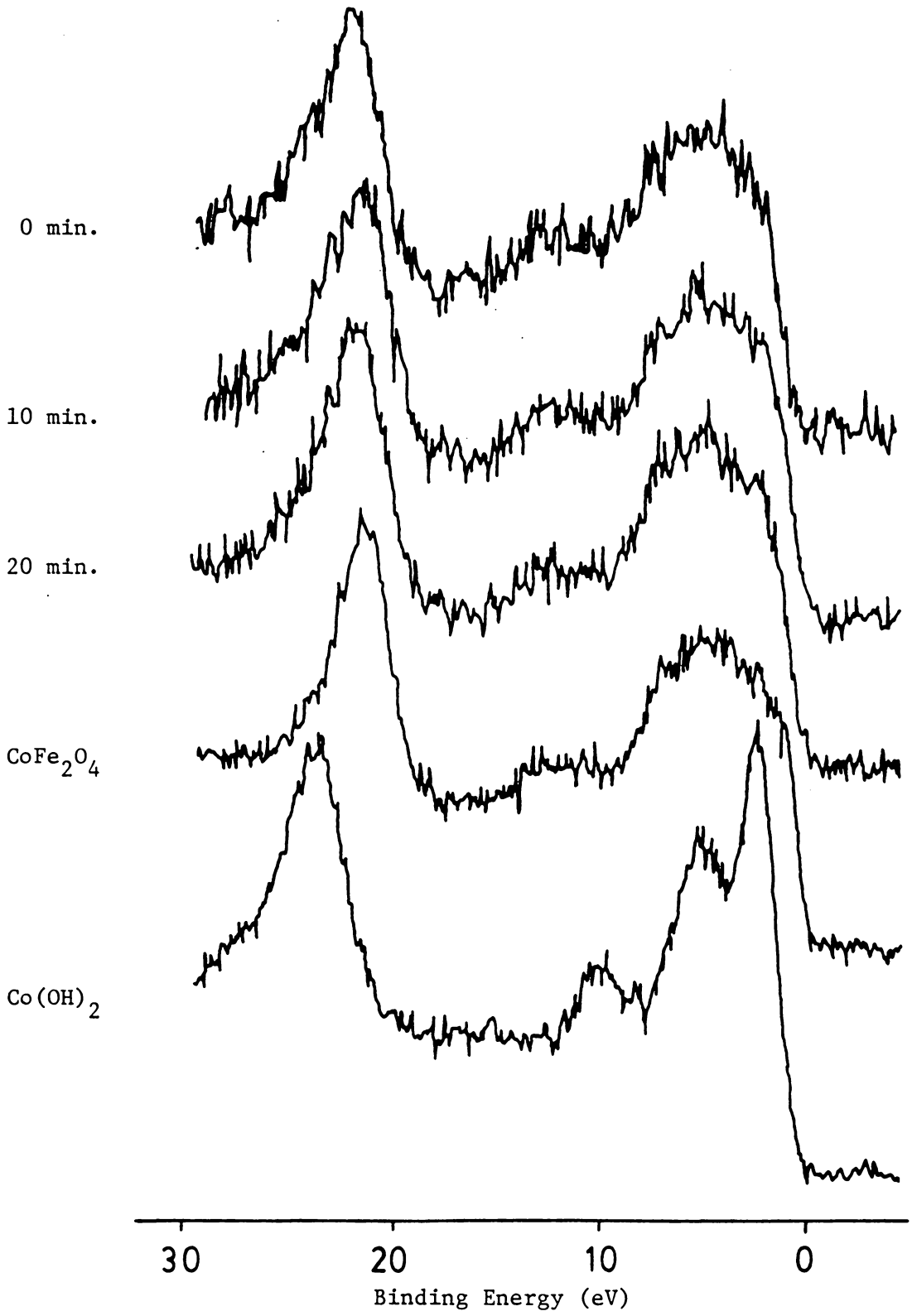

Figure 20. XPS Valence Band Spectra (NH_4OH Kinetic Preparation)

the Co 2p and O 1s spectra could be due to the large mean free path of the valence band electrons. If the hydrous species suggested by the Co 2p and O 1s spectra are on the very surface of the Co-γ-Fe_2O_3 samples, then the large mean free path (~20Å) of the valence band versus ~10Å for Co 2p and O 1s photoelectrons could result in supression of the $Co(OH)_2$ valence band features.

In summary, the XPS results for the non-annealed samples suggest that the surface of Co-γ-Fe_2O_3 in the early stages of the reaction is composed of a hydrous precipitate, containing hydrous Co(II) species and possibly Co^{2+}(ads) species. As the reaction suspension heats up a trend is observed suggesting the formation of a ferrite-like surface.

The binding energy data for the annealed samples (Table 5) show similar results for all samples. It appears that the hydrous surfaces, which are characteristic of the early samples, may be converted to ferrite-like surfaces during annealing. The binding energies are similar to the values measured for the high coercivity Co-γ-Fe_2O_3 samples.

The XPS Co/Fe atomic ratios are plotted versus reaction time in Figure 21. The non-annealed and annealed samples both show increasing Co/Fe atomic ratios with increasing time of reaction with the greatest increases occurring in the first 20 minutes of the reaction. The Co/Fe ratios are lower for the annealed samples. The increasing Co/Fe ratio with increasing reaction time may be due to increased absorption of Co(II). Another possibility is that some of the Co(II) was removed during washing of the early Co-γ-Fe_2O_3 samples. This possibility is

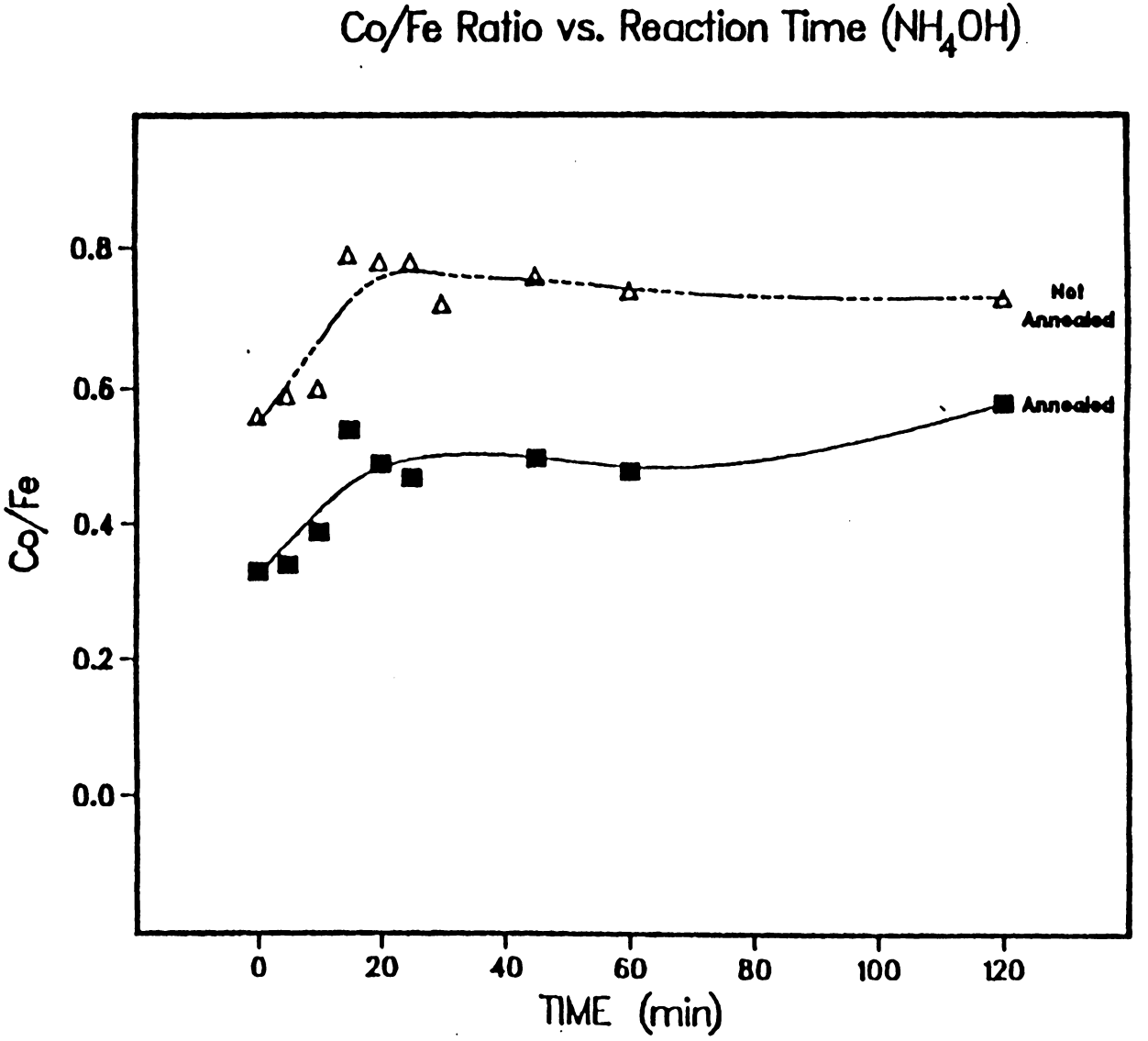

Figure 21. XPS Co/Fe Ratio Versus Reaction Time (NH_4OH Kinetic Preparation)

supported by the fact that during the washing of the samples it was noted that the earlier samples required several more washing steps than the later samples in order to attain the desired conductivity level. If the surface was composed of a hydrous precipitate, then it is reasonable to expect that some of the surface species would be washed off even in pH 7 water. Assuming the later samples have a more ferrite-like surface, there should be less probability of Co(II) removal by washing.

Comparing the Co/Fe atomic ratio versus reaction time curve (Figure 21) with coercivity versus reaction time curve (Figure 17), there is a noticeable correlation between the two. This suggests that the observed increase in coercivity with increasing reaction time is related to the amount of Co(II) on the sample surface.

Infrared Measurements

None of the infrared spectra measured for the samples from the NH_4OH kinetic preparation (non-annealed and annealed) showed evidence for the O-H stretching band at 3630 cm^{-1} as in $Co(OH)_2$. Since the XPS spectra showed strong evidence for hydrous forms of cobalt on the surface, it was anticipated that the O-H peak for $Co(OH)_2$ would appear. A possible reason that the OH band did not appear is that the surface concentration of cobalt species was too low compared to the bulk for it to be detected in the infrared spectra.

The IR spectra of selected non-annealed and annealed samples are shown in Figures 22 and 23, respectively. The spectra of the early non-

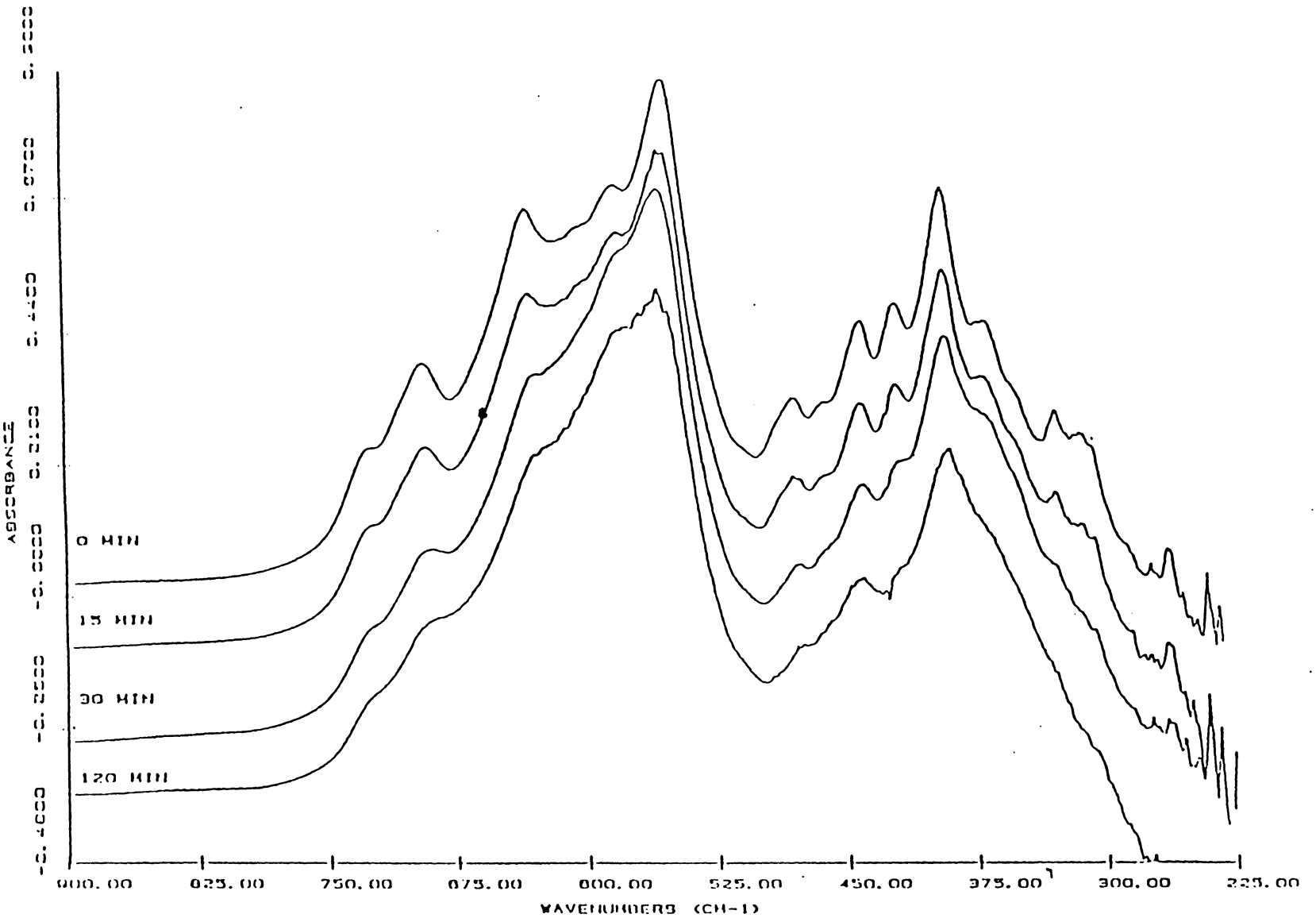

Figure 22. Infrared Spectra of Non-annealed Co-γ-Fe_2O_3 Samples (NH_4OH Kinetic Preparation)

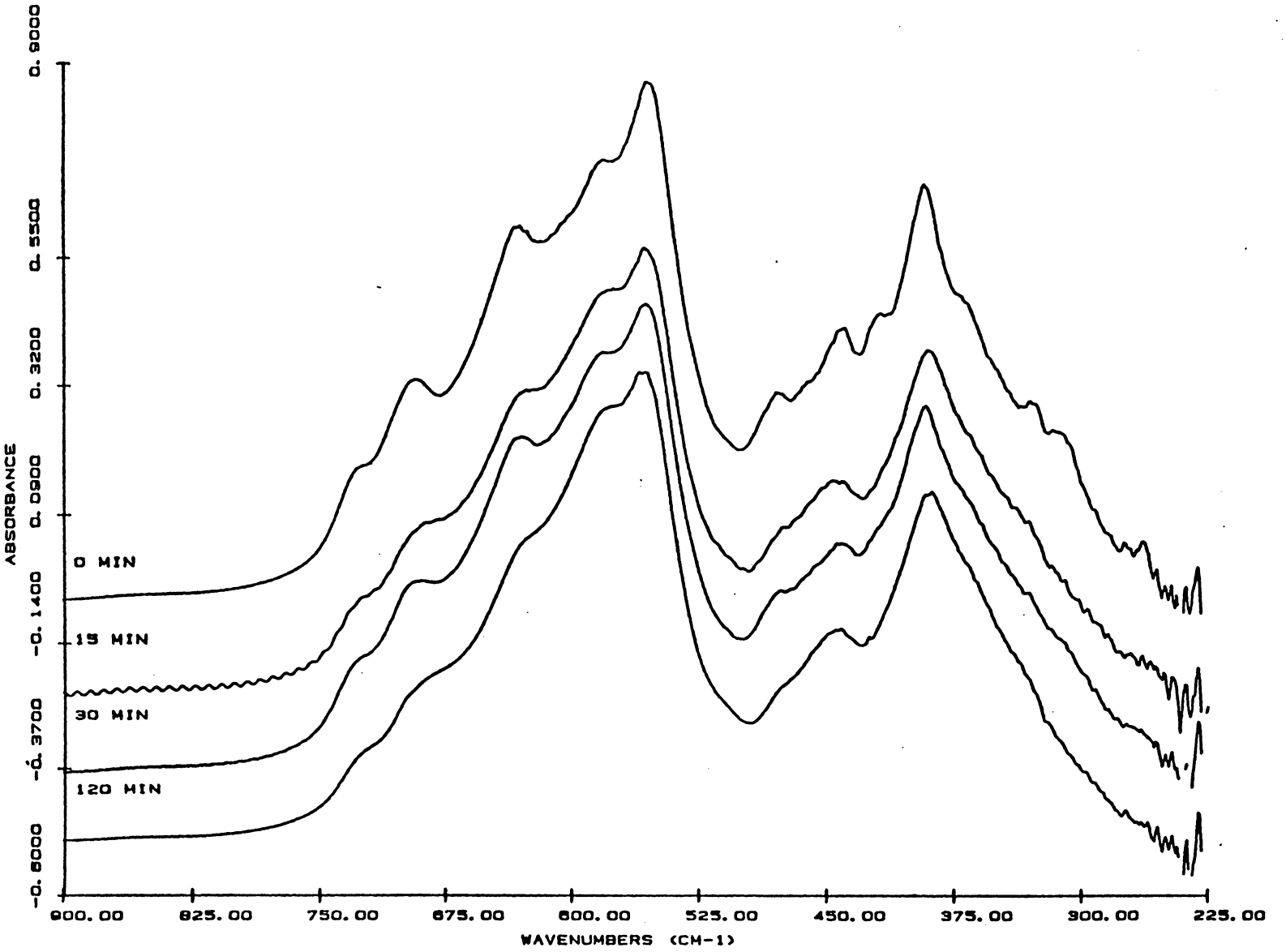

Figure 23. Infrared Spectra of Annealed Co-γ-Fe_2O_3 Samples (NH_4OH Kinetic Preparation)

annealed samples (0, 15 min) show spectra similar to γ-Fe_2O_3 (Figure 15). As the reaction time increases, the sample spectra (30, 120 min) lose the fine structure associated with γ-Fe_2O_3 and the spectra become more like the spectra from the high coercivity Co-γ-Fe_2O_3 (Figure 14). This characteristic Co-γ-Fe_2O_3 spectrum was shown to be similar to a spectrum synthesized by adding γ-Fe_2O_3 and $CoFe_2O_4$ spectra (Figure 16). The trend of the early non-annealed samples exhibiting spectra similar to γ-Fe_2O_3, and then changing to characteristic Co-γ-Fe_2O_3 spectra supports ferrite formation during the course of the kinetic NH_4OH reaction.

The spectra for the annealed samples (Figure 23) are similar to the spectra for the non-annealed samples but the annealed sample spectra show greater overall similarity to the characteristic Co-γ-Fe_2O_3 spectra. This suggests that ferrite formation has been enhanced by annealing the samples.

Fe(II)- Content

The percent Fe(II) versus total iron is shown in Table 6. The results show two trends. One is that the Fe(II) content increases in the non-annealed samples with increasing reaction time. The other trend is that the early annealed samples have greater amounts of Fe(II) than the corresponding non-annealed samples. The results for the non-annealed samples suggest increasing Fe(II) adsorption/incorporation with increasing reaction time. The higher Fe(II) percentages for the annealed samples suggest that Fe(III) is reduced during annealing.

Table 6

Percent Fe(II) for NH_4OH Kinetic Series

Sample	Non-annealed	Annealed
0 min	1.3%	2.3%
5 min	1.3%	4.7%
10 min	2.0%	3.5%
20 min	4.6%	6.7%
30 min	6.3%	6.4%
60 min	6.6%	5.9%
120 min	6.6%	6.8%

It is not likely that Co(II) is reducing Fe(III) since no evidence for Co(III) has been obtained in any of the Co-γ-Fe_2O_3 XPS spectra. One possibility is that residual hydrocarbon material on the γ-Fe_2O_3 reduces some Fe(III). XPS analysis of undigested material from the digested Co-γ-Fe_2O_3 samples indicates that the undigested material is primarily composed of carbon. It is unclear, however, what form of carbon is on the samples. The reduction of Fe(III) by residual organics could also explain the increasing Fe(II) content of the non-annealed samples, since the increase in Fe(II) content in the non-annealed materials follows the temperature profile for the reaction suspension.

NaOH Kinetic Preparation (Fe(II):OH = 1:2)

To explore the effect of added base on the Co-γ-Fe_2O_3 preparation, a kinetic preparation using 7.4 N NaOH was carried out using a stoichiometric amount of base assuming that $Co(OH)_2$ and $Fe(OH)_2$ were the initial species formed in the reaction. The pH after the addition of base was 11.1. This NaOH kinetic preparation is identified as: Fe:OH = 1:2.

Magnetic Results

The coercivities for the non-annealed and annealed samples from the NaOH kinetic preparation (Fe:OH = 1:2) are given in Table 3, and the coercivities are plotted versus reaction time in Figure 24. The coercivities obtained in this preparation are considerably lower than the coercivities for the NH_4OH preparation. The plots of the non-annealed and annealed coercivities versus reaction time (Figure 24) show

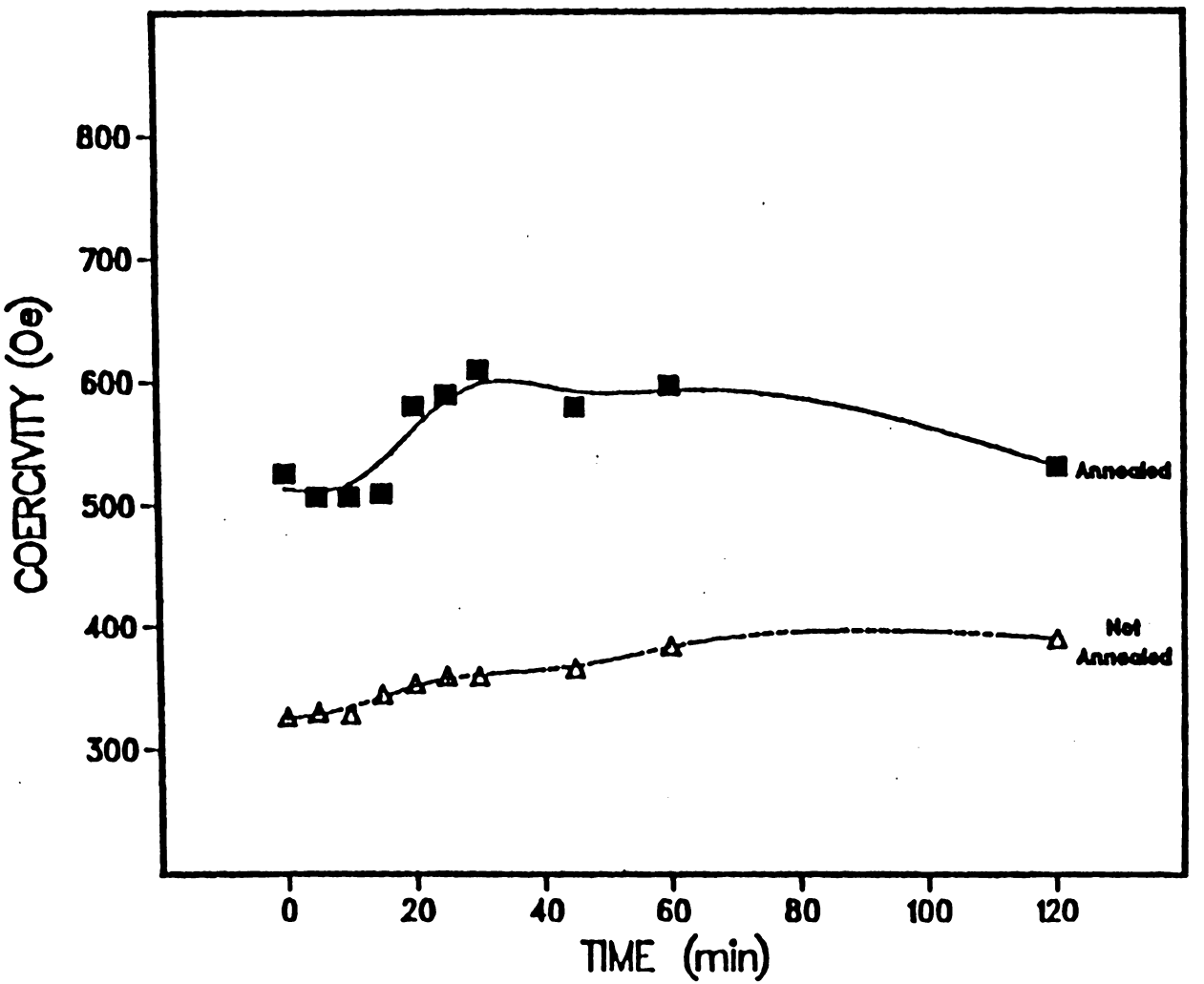

Figure 24. Coercivity Versus Reaction Time (NaOH-Kinetic Preparation, Fe:OH = 1:2)

different behavior from that of the NH_4OH preparation (Figure 17). The non-annealed samples show a gradual increase in coercivity which is in contrast to the initial large increase and leveling off of coercivity noted for the non-annealed NH_4OH samples. For the annealed samples the coercivity increases gradually in the first thirty minutes, then peaks, and decreases in the later stages. This is in contrast to the large initial increase in coercivity and leveling off that was found for the annealed NH_4OH samples.

XPS Measurements

The binding energy results and the Co/Fe atomic ratios for the non-annealed and annealed NaOH (Fe:OH = 1:2) samples are given in Tables 7 and 8, respectively. The non-annealed samples show the same trends of decreasing Co $2p_{3/2}$ binding energy and increasing satellite splitting with reaction time that were observed in the NH_4OH preparation. There are differences, though, between the results for the two preparations. One of these differences is that the Co $2p_{3/2}$ binding energies are shifted about 0.2 eV lower in the NaOH (Fe:OH = 1:2) preparation. The highest binding energy for the NaOH (Fe:OH = 1:2) non-annealed sample is 780.8 eV (0, 5 min) compared to 781.0 eV (0 min) for the NH_4OH non-annealed sample. The Co $2p_{3/2}$ binding energies for the non-annealed NaOH (Fe:OH = 1:2) samples decrease to an average value of approximately 780.4 eV while the Co $2p_{3/2}$ binding energies for the non-annealed NH_4OH samples decrease to an average of ~780.6 eV. It should be noted that the 0.2 eV shift to lower binding energies is within the precision of the measurement (±0.1 eV), but the shift is consistent for all the non-

Table 7

XPS Results

NaOH (Fe:OH = 1:2) Kinetic Series

Non-Annealed

Sample	Binding Energy Results (eV)					Co/Fe (atomic ratio)
	Fe $2p_{3/2}$	Co $2p_{3/2}$	Δ Co 2p	Δ sat.	O 1s	
0 min	711.0	780.8	15.7	6.0	530.2	0.64
5 min	711.0	780.8	15.9	6.1	530.2	0.59
10 min	711.0	780.5	15.9	6.3	530.2	0.53
15 min	710.9	780.4	15.7	6.1	530.1	0.47
20 min	710.8	780.3	15.8	6.2	530.0	0.46
30 min	710.8	780.2	15.9	6.3	530.0	0.44
45 min	710.9	780.4	15.7	6.2	530.1	0.44
60 min	710.9	780.4	15.8	6.2	530.2	0.44
120 min	710.8	780.4	15.7	6.2	530.1	0.45
$CoFe_2O_4$	710.7	780.2	15.5	6.3	529.8	0.50
$Co(OH)_2$	---	780.7	15.9	5.5	530.7	---

Table 8

XPS Results

NaOH (Fe:OH = 1:2) Kinetic Series

Annealed

Sample	Binding Energy Results (eV)					Co/Fe (atomic ratio)
	Fe $2p_{3/2}$	Co $2p_{3/2}$	Δ Co 2p	Δ sat.	O 1s	
0 min	711.0	780.5	15.8	6.2	530.2	0.37
5 min	711.0	780.5	15.8	6.4	530.2	0.35
10 min	711.0	780.5	15.8	6.4	530.2	0.32
15 min	710.9	780.4	15.8	6.4	530.2	0.34
20 min	710.9	780.3	15.7	6.4	530.0	0.34
25 min	710.9	780.4	15.8	6.2	530.1	0.30
30 min	710.8	780.4	15.8	6.4	530.1	0.31
45 min	710.0	780.5	15.6	6.3	530.2	0.28
60 min	710.9	780.4	15.8	6.4	530.2	0.31
120 min	710.9	780.3	15.8	6.4	530.0	0.32
$CoFe_2O_4$	710.7	780.2	15.5	6.3	529.8	0.50
$Co(OH)_2$	---	780.7	15.9	5.5	530.7	---

annealed NaOH (Fe:OH = 1:2) samples. Additionally, if the 0.2 eV shift was the result of an incorrect calibration, etc., the effect should also be seen in the O 1s binding energies. A 0.2 eV shift between the O 1s binding energies of the two preparations is not observed, suggesting that a calibration error is not involved. The increase in satellite splitting observed in the NaOH (Fe:OH = 1:2) preparation is less dramatic (6.0 eV - ~6.3 eV) than the trend observed in the NH_4OH preparation (5.8 eV - ~6.3 eV).

The lower Co $2p_{3/2}$ binding energies and larger satellite splittings are in better agreement with the values for $CoFe_2O_4$. This suggests that the surface of Co-γ-Fe_2O_3 samples in the NaOH (Fe:OH = 1:2) preparations have a composition closer to the reference $CoFe_2O_4$ than do the NH_4OH preparations.

The Co 2p spectra for the 0, 10, and 20 minute non-annealed samples are shown in Figure 25. There is a slight trend of decreasing Co $2p_{3/2}$ peak width and increasing satellite splitting with increasing time, but to a much lesser extent than was observed for the NH_4OH preparation. The narrower Co 2p spectra are in better agreement (visually) with the $CoFe_2O_4$ spectrum.

The O 1s spectra of the 0, 10, and 20 minute non-annealed samples are shown in Figure 26. A large hydroxyl component is observed in the 0 min sample and the intensity of the hydroxyl component decreases with increasing reaction time. The intensity of the hydroxyl component appears to be greater than for the NH_4OH samples. The valence band spectra are shown in Figure 27. No evidence for $Co(OH)_2$ is observed in these valence band spectra.

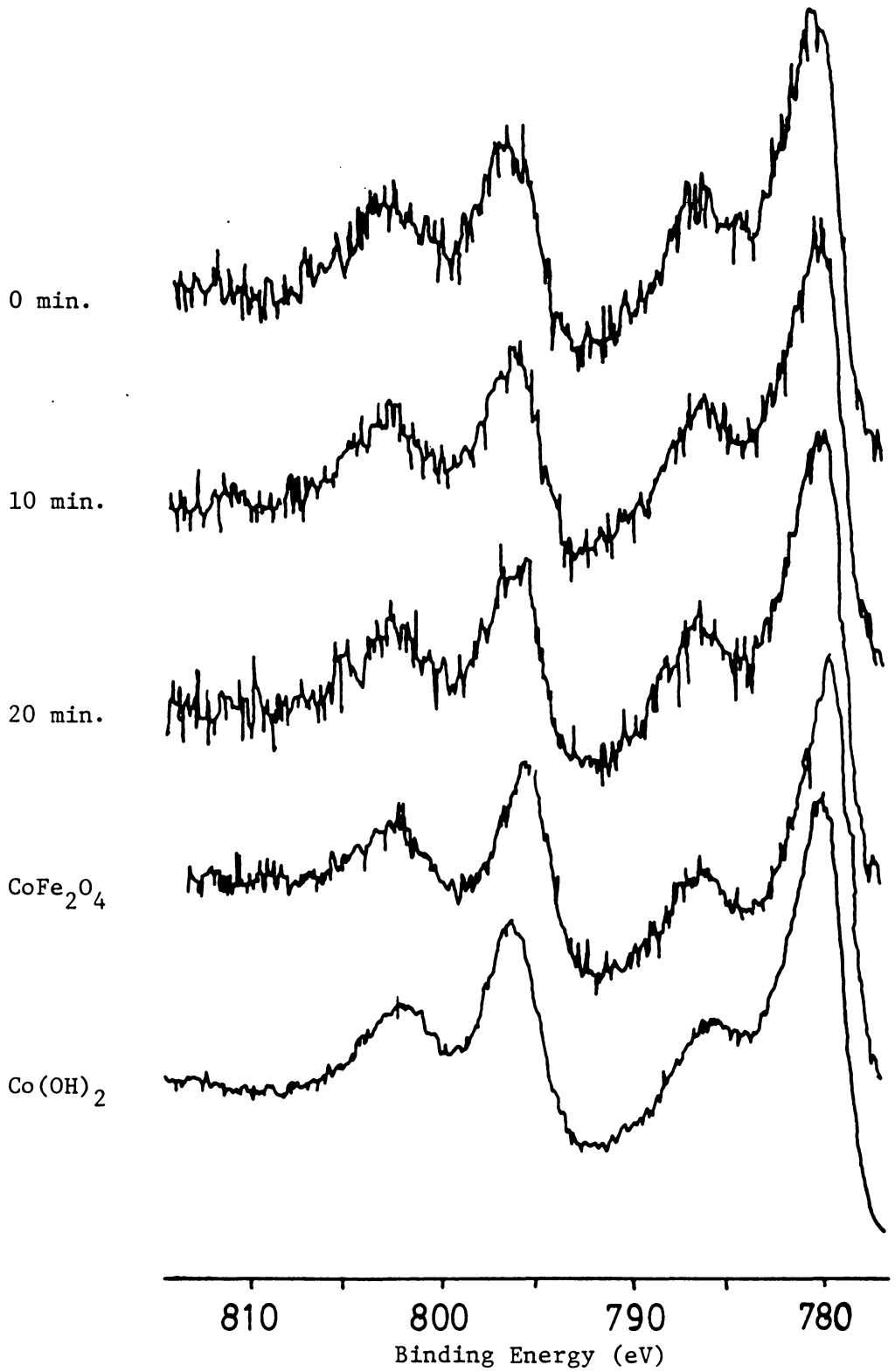

Figure 25. XPS Co 2p Spectra (NaOH Kinetic Preparation, Fe:OH = 1:2)

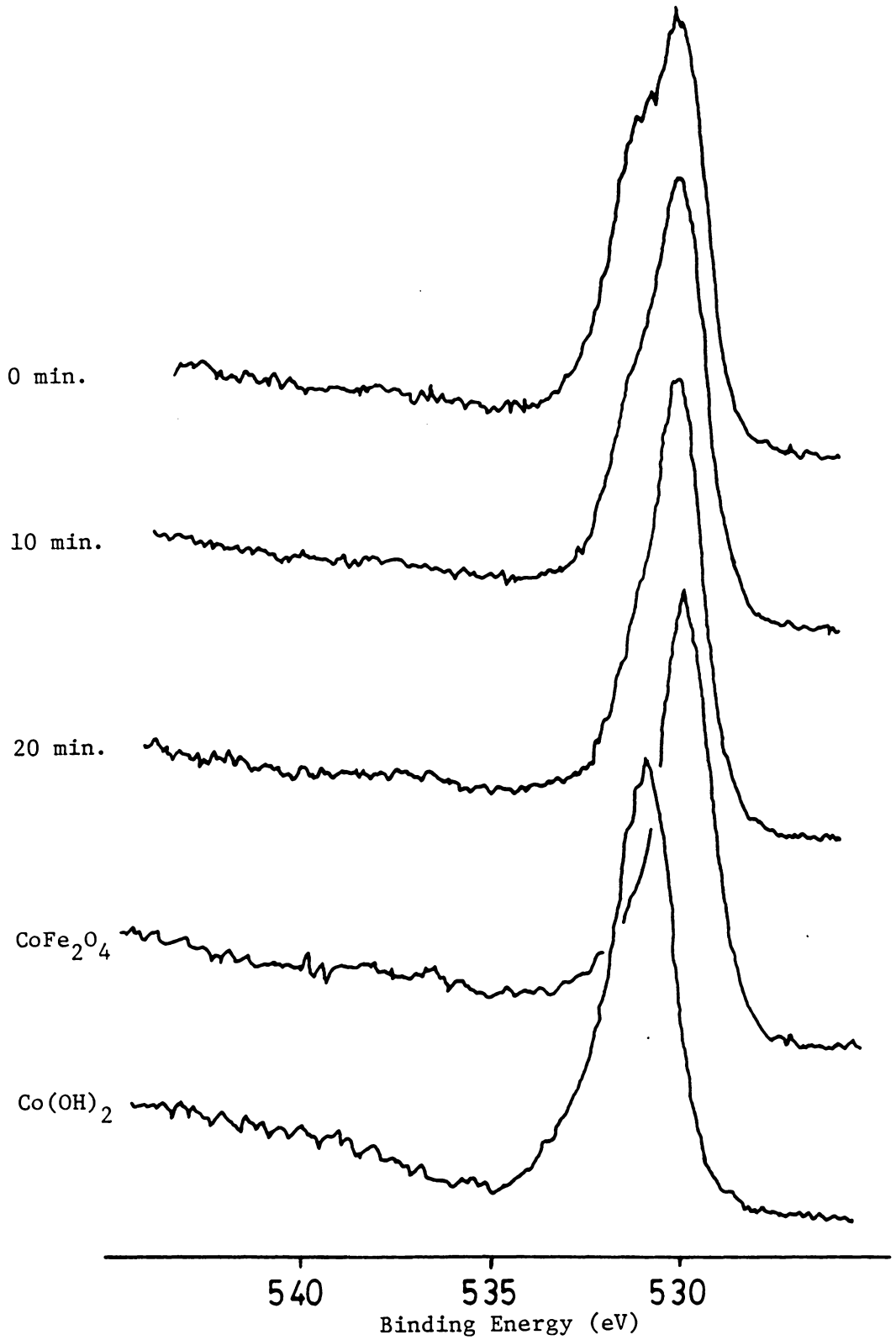

Figure 26. XPS O 1s Spectra (NaOH Kinetic Preparation, Fe:OH = 1:2)

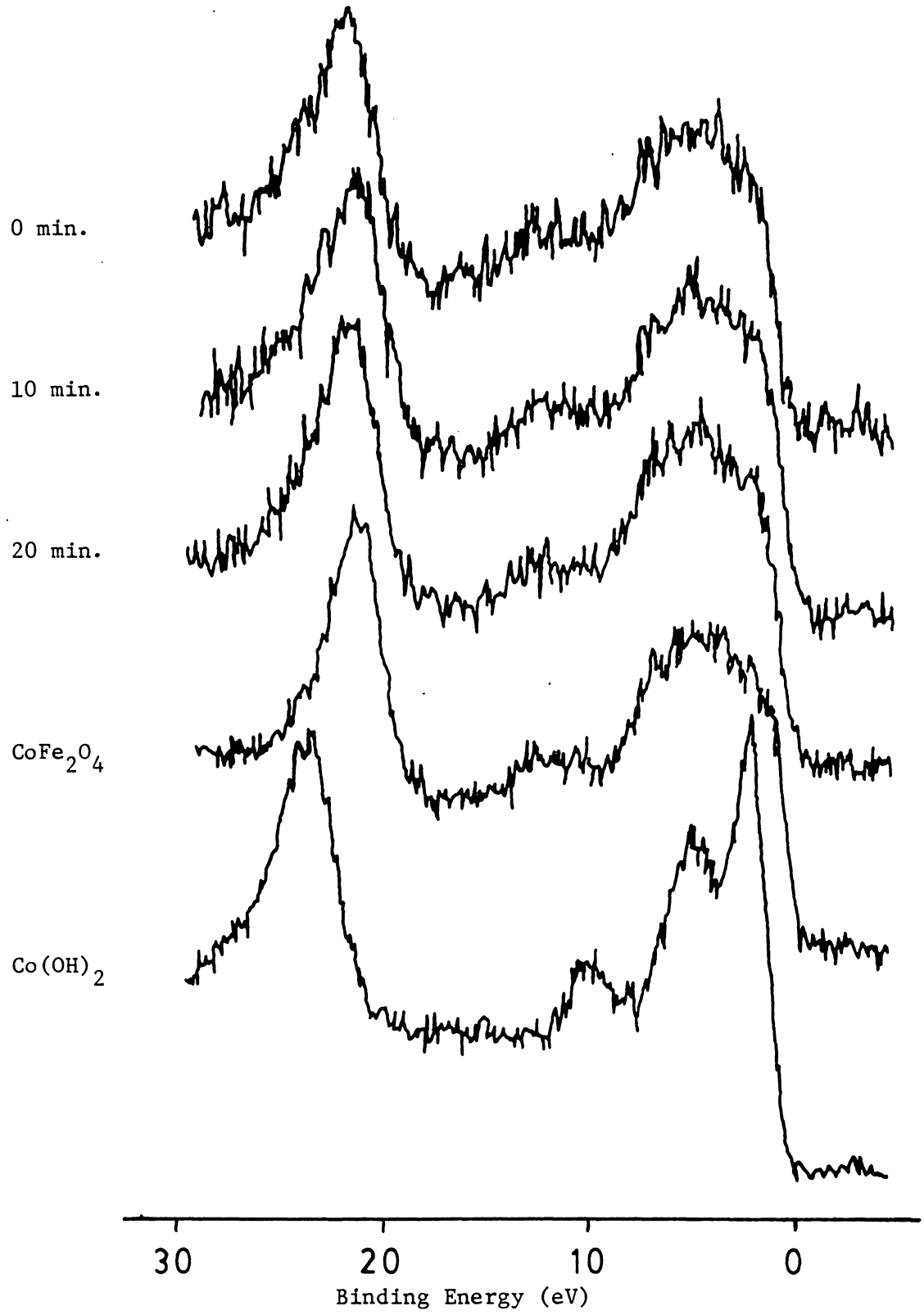

Figure 27. XPS Valence Band Spectra (NaOH Kinetic Preparation, Fe:OH = 1:2)

The binding energies for the annealed samples (Table 8) exhibit a similar uniformity in values; a behavior noted previously for annealed NH_4OH samples (Table 5). The Fe $2p_{3/2}$ and Co $2p_{3/2}$ binding energies show slightly lower average values, 710.9 and 780.4 eV, respectively, than the annealed samples from the NH_4OH preparation, 711.1 eV and 780.6 eV, respectively. These lower binding energies are in better agreement with values for $CoFe_2O_4$.

The binding energy results and the spectral features suggest that the Co-γ-Fe_2O_3 samples from the NaOH (Fe:OH = 1:2) preparation have a different surface chemistry compared to that for the NH_4OH samples. The lower binding energies (Co $2p_{3/2}$, Fe $2p_{3/2}$) observed for the NaOH (Fe:OH = 1:2) preparation are in better agreement with the $CoFe_2O_4$ standard binding energies, and the Co 2p spectra for the NaOH (Fe:OH = 1:2) samples more closely resemble those for the $CoFe_2O_4$ spectra. This suggests that the surfaces of the Co-γ-Fe_2O_3 samples prepared with NaOH are closer in composition to $CoFe_2O_4$ than Co-γ-Fe_2O_3 samples prepared with NH_4OH.

These results would appear to contradict the lower coercivities obtained for the NaOH (Fe:OH = 1:2) prepared samples relative to the NH_4OH preparations. The lower coercivities for the NaOH (Fe:OH = 1:2) preparation are probably best explained by an observation made during the washing of the samples. This observation was a noticeable pink color to the wash water, indicating that soluble Co^{2+} species were still present and that the adsorption of Co(II) was incomplete. As remarked

in the historical section, greater Co(II) content usually results in higher coercivity.

The Co/Fe atomic ratios are plotted versus reaction time in Figure 28. The behavior for the Co/Fe atomic ratios for the non-annealed samples and annealed samples is significantly different from the behavior observed for the NH_4OH preparation. Instead of an increasing Co/Fe atomic ratio with increasing reaction time (NH_4OH preparation) the NaOH (Fe:OH = 1:2) samples show a decrease in the ratios with increasing reaction time. This behavior is especially pronounced for the NaOH (Fe:OH = 1:2) non-annealed samples. This behavior of decreasing Co/Fe atomic ratio with increasing reaction time could be the result of a limited amount of Co(II) being adsorbed, and as the reaction proceeds, the smaller concentration of Co(II) diffuses into bulk γ-Fe_2O_3 leading to a decrease in the Co/Fe ratio. The annealed samples show a slight decrease in the Co/Fe atomic ratios with increasing reaction time, but the values are all essentially the same. This could be a reflection of an initial, limited amount of Co(II) being adsorbed and as the samples are annealed the Co(II) surface concentration reaches an equilibrium value reflected by the similar Co/Fe atomic ratios.

Fe(II) Content

The percent Fe(II) contents are given in Table 9. As was found for the NH_4OH kinetic preparation the percent Fe(II) content for the non-annealed samples increases with increasing time of reaction, and the annealed samples have higher Fe(II) concentrations than the non-annealed samples. As was mentioned in the discussion on the Fe(II) content of

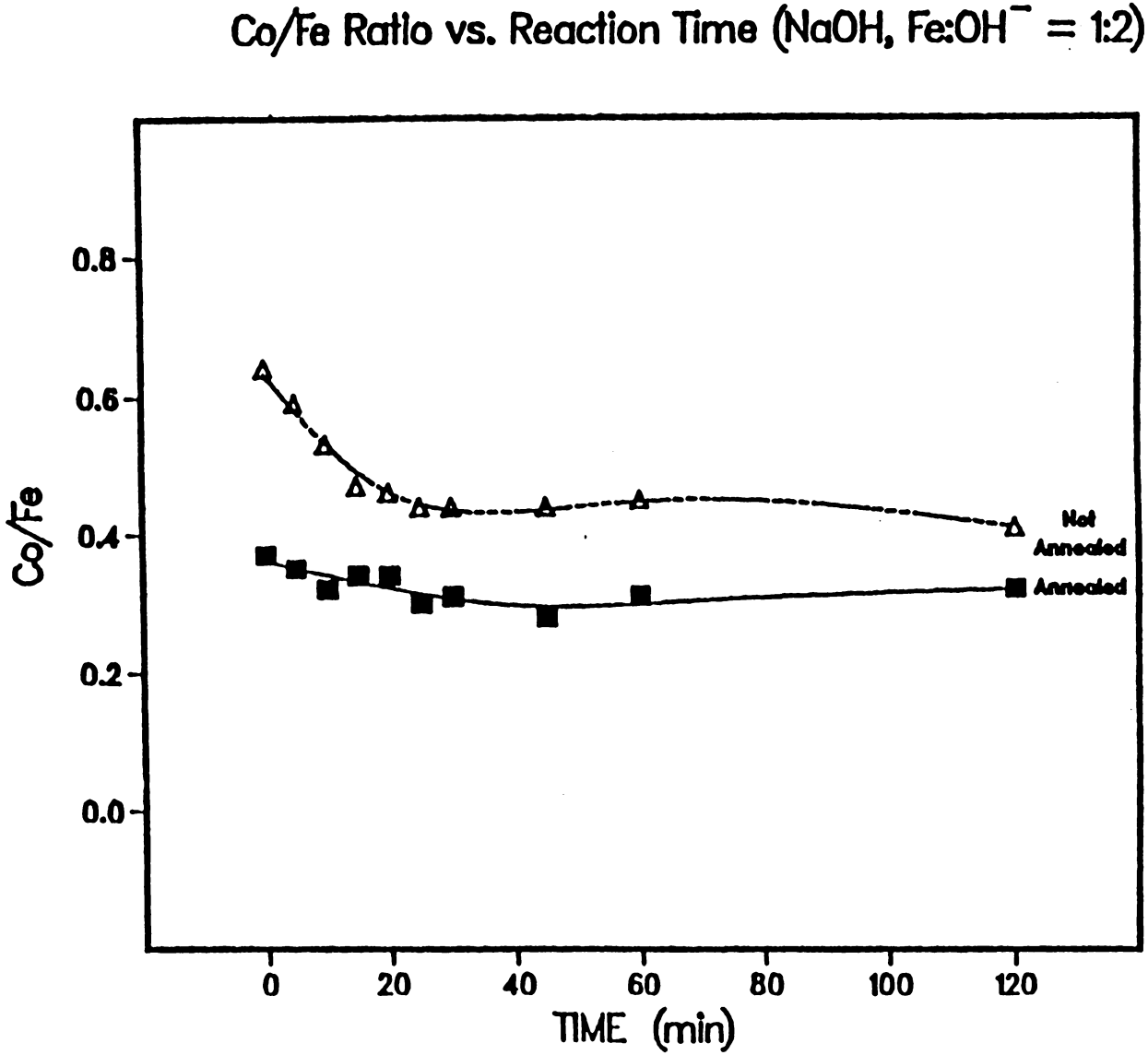

Figure 28. XPS Co/Fe Ratio Versus Reaction Time (NaOH Kinetic Preparation, Fe:OH = 1:2)

Table 9

Percent Fe(II) for NaOH (Fe:OH = 1:2) Kinetic Series

Sample	Non-annealed	Annealed
0 min	3.4%	4.1%
10 min	3.3%	2.7%
20 min	4.3%	4.6%
30 min	4.3%	8.1%
120 min	4.7%	5.9%

the NH_4OH samples, there is an indication that something is reducing the Fe(III) in the samples, possibly residual hydrocarbons.

NaOH Kinetic (Fe(II):OH = 1:3) Preparation

The low coercivities obtained in the kinetic NaOH (Fe:OH = 1:2) preparation and the pink color of the wash water suggested that an insufficent amount of base (NaOH) was added to the reaction suspension. To explore this phenomena another kinetic NaOH preparation was completed assuming a higher stoichiometry for iron. The amount of base added to this preparation was based on $Co(OH)_2$ and $Fe(OH)_3^-$ being the inital species formed during the reaction. The pH of the suspension after the addition of base was 12.3. The absence of pink color in the wash water suggested that complete deposition of Co(II) had occurred.

Magnetic Results

The coercivities for the non-annealed and annealed NaOH (Fe:OH = 1:3) samples are given in Table 3, and a plot of the coercivities versus reaction time is shown in Figure 29. There is a noticeable increase in the coercivities of both the non-annealed and annealed samples relative to the NaOH (Fe:OH = 1:2) preparation. The coercivities for the non-annealed NaOH (Fe:OH = 1:3) samples are also higher than values for the non-annealed NH_4OH samples, but the annealed NH_4OH samples (except 0, 5, 10 min samples) have higher coercivities than the annealed NaOH (Fe:OH = 1:3) samples. The plots of coercivity versus reaction time (Figure 29) show similar behavior to the NH_4OH preparation (Figure 17). The greatest increase in coercivity occurs in the first 30 minutes of reaction for both the non-annealed and annealed samples. After 30

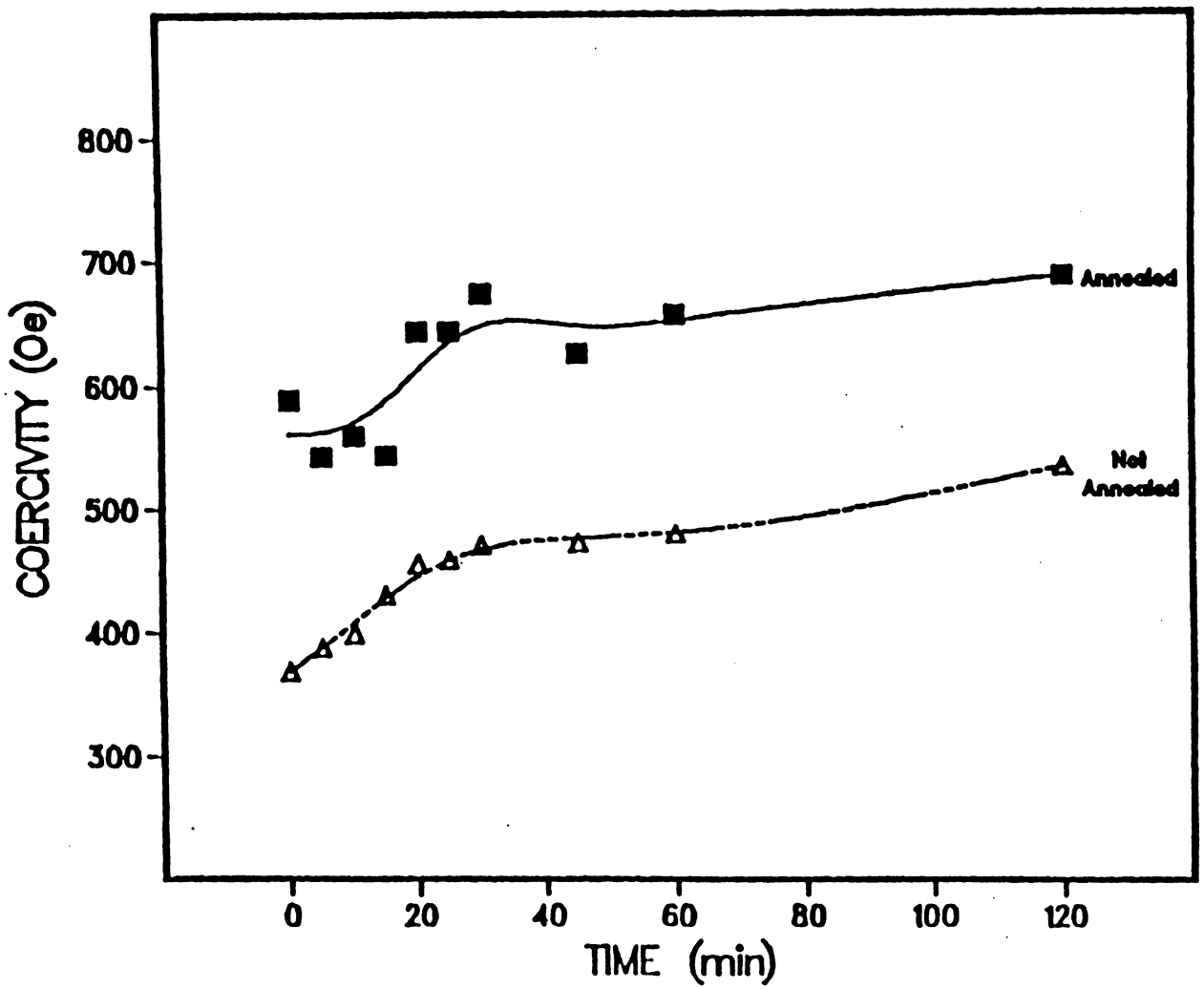

Figure 29. Coercivity Versus Reaction Time (NaOH Kinetic Preparation, Fe:OH = 1:3)

minutes of reaction the rate of coercivity enhancement decreases. The increase in coercivity in the early stages of the reaction is not as dramatic as was discovered for the NH_4OH preparation.

XPS Measurements

The binding energy results and Co/Fe atomic ratios for the non-annealed and annealed samples are given in Tables 10 and 11, respectively. The two previously discussed trends of decreasing Co $2p_{3/2}$ binding energy and increasing satellite splitting are also observed in the binding energy results for the non-annealed NaOH (Fe:OH = 1:3) samples. The phenomenon of lower overall Co $2p_{3/2}$ binding energies measured in the previous NaOH (Fe:OH = 1:2) preparation is also found.

The Co $2p_{3/2}$ binding energies for the non-annealed samples begin at 780.6 eV (0 min.) and decrease to an average of ~780.3 eV for the later samples. As has been discussed, the NH_4OH preparation showed a decrease from 781.0 eV to 780.6 eV and the NaOH (Fe:OH = 1:2) preparation had a decrease from 780.8 eV to 780.4 eV. It is evident that the trend observed in the NaOH (Fe:OH = 1:2) preparation of lower overall Co $2p_{3/2}$ binding energy compared to the NH_4OH samples has been carried further by the use of additional NaOH. The increase in satellite splitting is slight (6.1 eV to 6.3 eV). The Fe $2p_{3/2}$ binding energies of the NaOH (Fe:OH = 1:3) also appear to be slightly lower than for the NH_4OH preparation (710.9 and 711.1 eV, respectively).

The lower binding energies and increased satellite splitting both show better agreement with the $CoFe_2O_4$ standard values, suggesting a

Table 10

XPS Results

NaOH (Fe:OH = 1:3) Kinetic Series

Non-Annealed

Sample	Binding Energy Results (eV)					Co/Fe (atomic ratio)
	Fe $2p_{3/2}$	Co $2p_{3/2}$	Δ Co 2p	Δ sat.	O 1s	
0 min	711.0	780.6	15.8	6.1	530.2	0.70
5 min	711.0	780.5	15.7	6.1	530.2	0.70
10 min	710.9	780.4	15.7	6.2	530.1	0.68
15 min	710.8	780.3	15.7	6.2	530.1	0.65
20 min	710.9	780.3	15.8	6.2	530.1	0.66
25 min	710.8	780.1	15.9	6.4	530.0	0.66
30 min	711.0	780.3	15.8	6.4	530.1	0.70
45 min	710.9	780.3	15.8	6.3	530.0	0.61
60 min	710.8	780.3	15.7	6.2	530.0	0.65
120 min	711.0	780.3	15.8	6.5	530.1	0.60
$CoFe_2O_4$	710.7	780.2	15.5	6.3	529.8	0.50
$Co(OH)_2$	---	780.7	15.9	5.5	530.7	---

Table 11

XPS Results

NaOH (Fe:OH = 1:3) Kinetic Series

Annealed

Sample	Binding Energy Results (eV)					Co/Fe (atomic ratio)
	Fe $2p_{3/2}$	Co $2p_{3/2}$	Δ Co 2p	Δ sat	O 1s	
0 min	710.8	780.4	15.7	6.2	530.0	0.52
5 min	710.8	780.3	15.8	6.2	530.1	0.51
10 min	710.9	780.2	15.9	6.4	530.1	0.52
15 min	710.8	780.3	15.7	6.3	530.0	0.48
20 min	710.8	780.3	15.7	6.3	530.1	0.52
25 min	710.9	780.2	15.7	6.5	530.0	0.48
30 min	710.8	780.3	15.7	6.3	530.0	0.46
45 min	710.9	780.2	15.8	6.2	530.1	0.41
60 min	710.9	780.2	15.8	6.3	530.0	0.51
120 min	710.8	780.2	15.7	6.3	530.1	0.53
$CoFe_2O_4$	710.7	780.2	15.5	6.3	529.8	0.50
$Co(OH)_2$	---	780.7	15.9	5.5	530.7	---

more stoichiometric ferrite-like surface than for the samples from the NH_4OH and NaOH (Fe:OH = 1:2) preparations.

The Co 2p spectra for the 0, 10 and 20 min. non-annealed samples are shown in Figure 30. The spectra for the 0, 10, 20 min samples are essentially identical and show good agreement with the $CoFe_2O_4$ spectrum. The O 1s spectra shown in Figure 31 display a noticeable hydroxyl component in the early samples, but the hydroxyl component is smaller than in the previous preparations and decreases rapidly with increasing reaction time.

The valence band spectra are shown in Figure 32. There is the usual similarity in the Co-γ-Fe_2O_3 spectra with the $CoFe_2O_4$ valence band spectrum. The 0 min. sample shows a slight skew of the valence band toward the valence band onset. This could be an indication of $Co(OH)_2$ (or CoO) or a result of the counting statistics.

There is an overall agreement among the binding energies for the annealed NaOH (Fe:OH = 1:3) samples as has been observed in all groups of annealed samples. The average Fe $2p_{3/2}$ binding energy is 710.8 eV and the average Co $2p_{3/2}$ binding energy is 780.3 eV. Both of these values show very good agreement with the value for $CoFe_2O_4$. The average satellite splitting (6.3 eV) also agrees well with the splitting for $CoFe_2O_4$. The binding energy results from this preparation appear to confirm the deduction made in the NaOH (Fe:OH 1:2) preparation, which is that Co-γ-Fe_2O_3 samples from NaOH preparations have surfaces nearer to $CoFe_2O_4$ in composition than Co-γ-Fe_2O_3 from NH_4OH preparations.

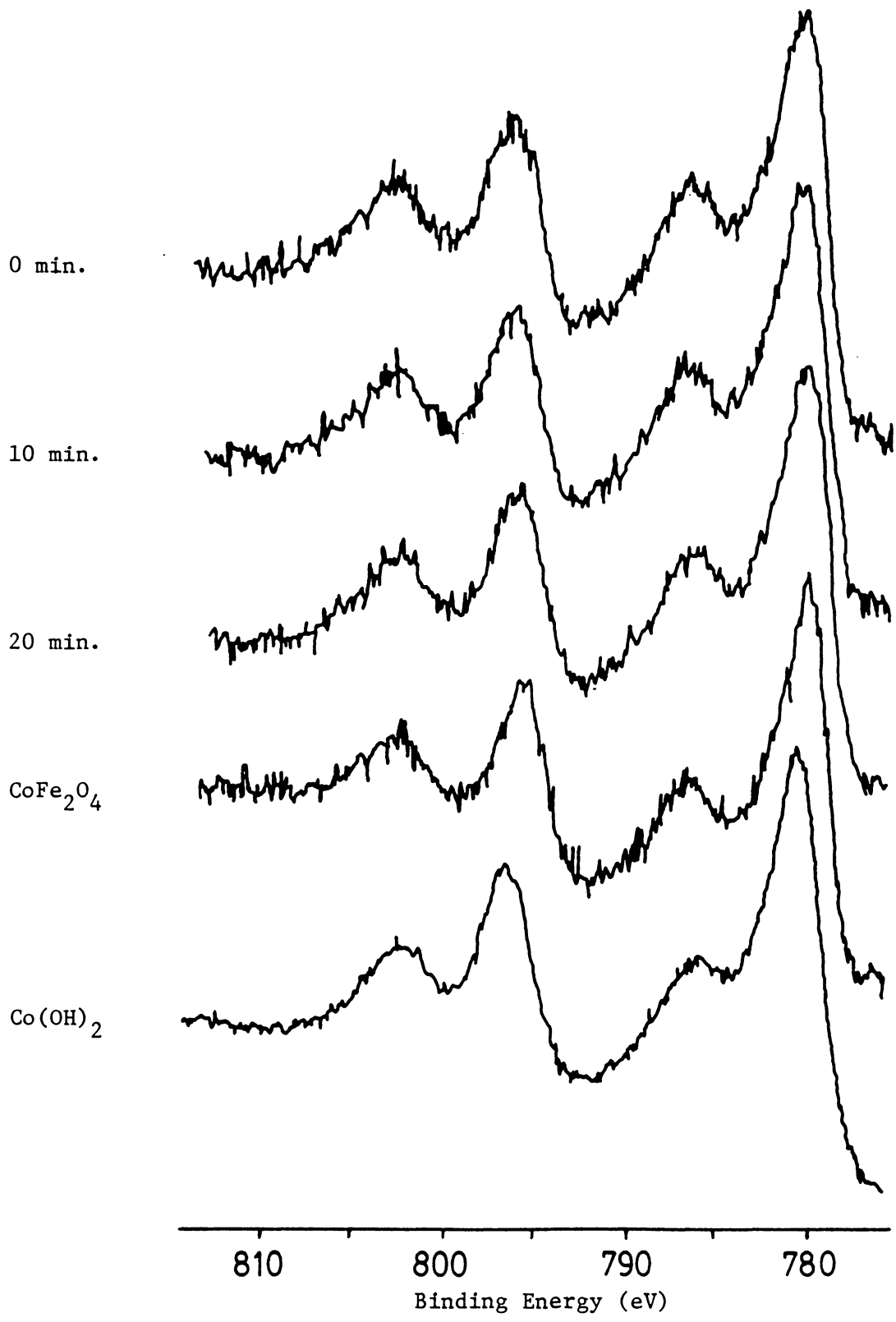

Figure 30. XPS Co 2p Spectra (NaOH Kinetic Preparation, Fe:OH = 1:3)

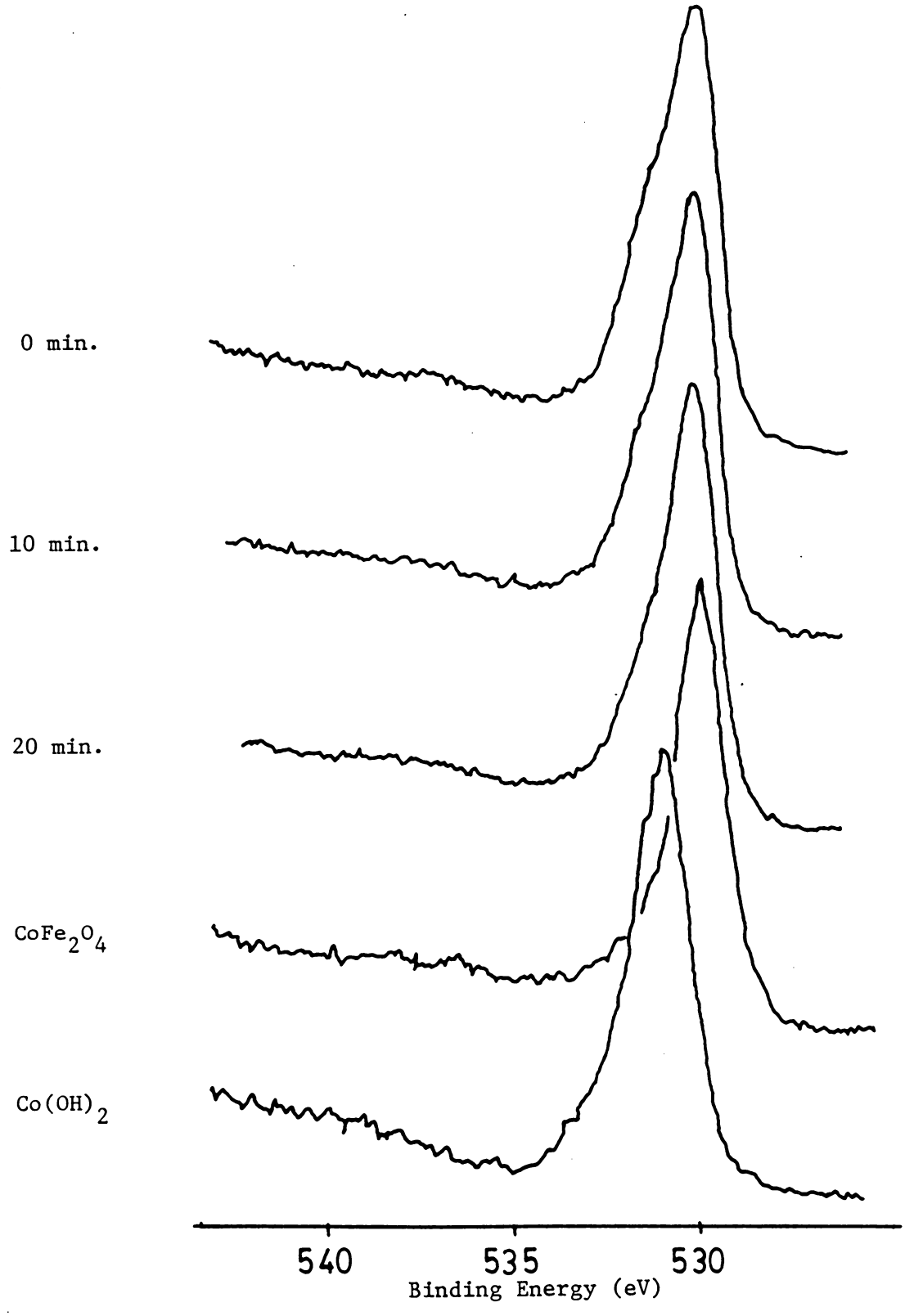

Figure 31. XPS O 1s Spectra (NaOH Kinetic Preparation, Fe:OH = 1:3)

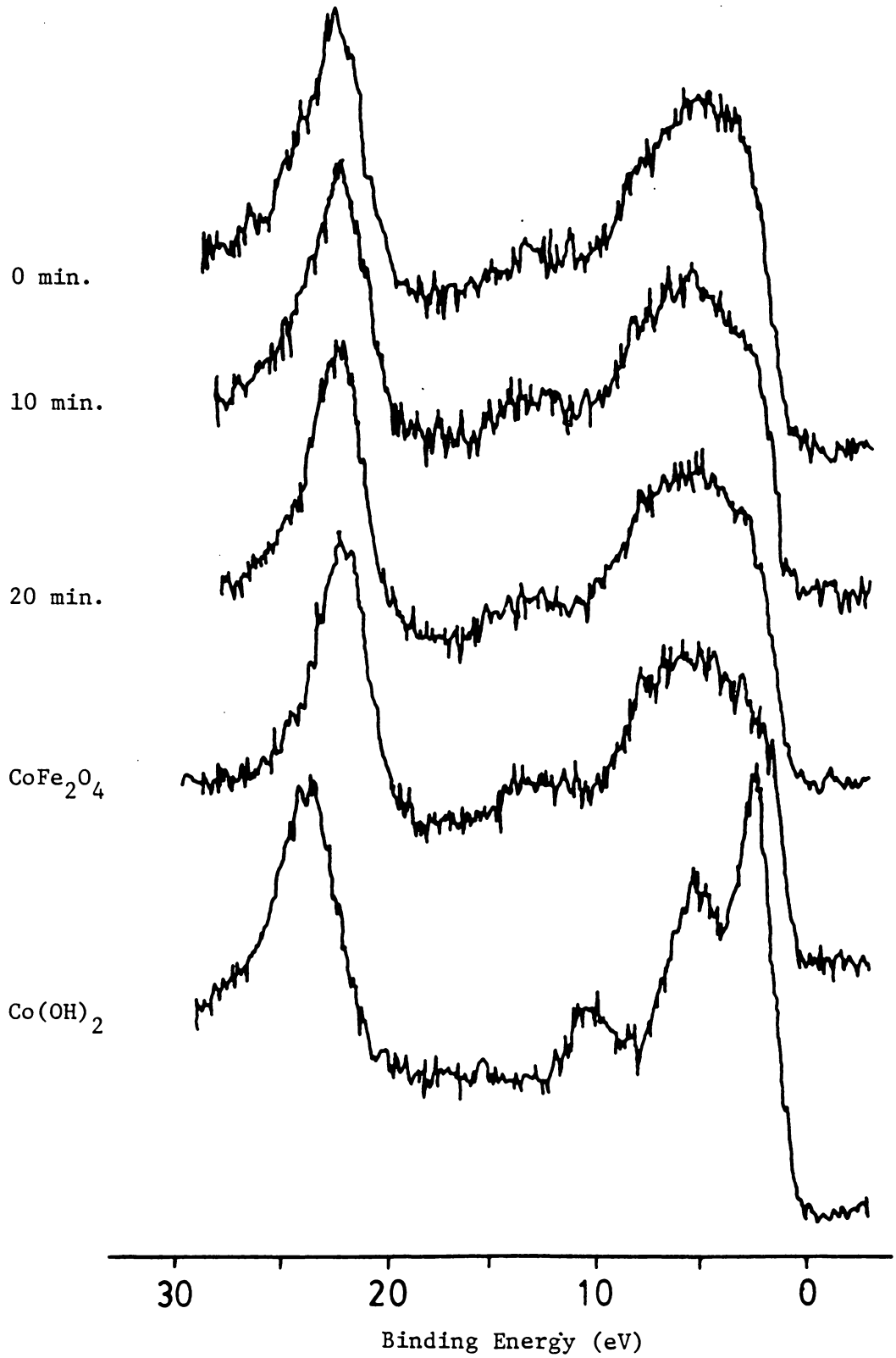

Figure 32. XPS Valence Band Spectra (NaOH Kinetic Preparation, Fe:OH = 1:3)

Ammonium hydroxide preparations show higher Co $2p_{3/2}$ and Fe $2p_{3/2}$ binding energies, suggesting a greater concentration of hydrous oxide species such as $Co(OH)_2$ and FeOOH. The reason for this behavior is not clear. Possibly these results are due to a complexation effect in preparations using NH_4OH. Another possibility is that NaOH, a stronger base than NH_4OH, facilitates the formation of $CoFe_2O_4$ to a greater extent than NH_4OH.

The Co/Fe atomic ratios for the non-annealed and annealed NaOH (Fe:OH = 1:3) samples show different behavior than for NaOH (Fe:OH = 1:2) and NH_4OH preparations. The plot of Co/Fe atomic ratio versus reaction time (Figure 33) shows that the Co/Fe ratio for the non-annealed samples decreases slightly with time while values for the annealed samples remain essentially constant with reaction time. As was recorded for the NaOH (Fe:OH = 1:2) preparation the Co/Fe ratio for the non-annealed samples decreased early in the reaction suggesting that an initial adsorption of Co(II) occurs very early in the reaction and as the Co-γ-Fe_2O_3 is heated some diffusion takes place.

The Co/Fe atomic ratios for the NaOH (Fe:OH = 1:3) preparation decrease by 0.1 - 0.2 following annealing and the Co/Fe atomic ratios from the NH_4OH preparation decrease to a greater extent (0.2-0.3). This difference in the extent of Co(II) diffusion suggests that the surface of the NaOH (Fe:OH = 1:3) samples is less prone to Co(II) diffusion than surface Co(II) in the NH_4OH samples. Perhaps a more well defined, crystalline $CoFe_2O_4$ surface formed in the NaOH preparations inhibits the diffusion of Co(II).

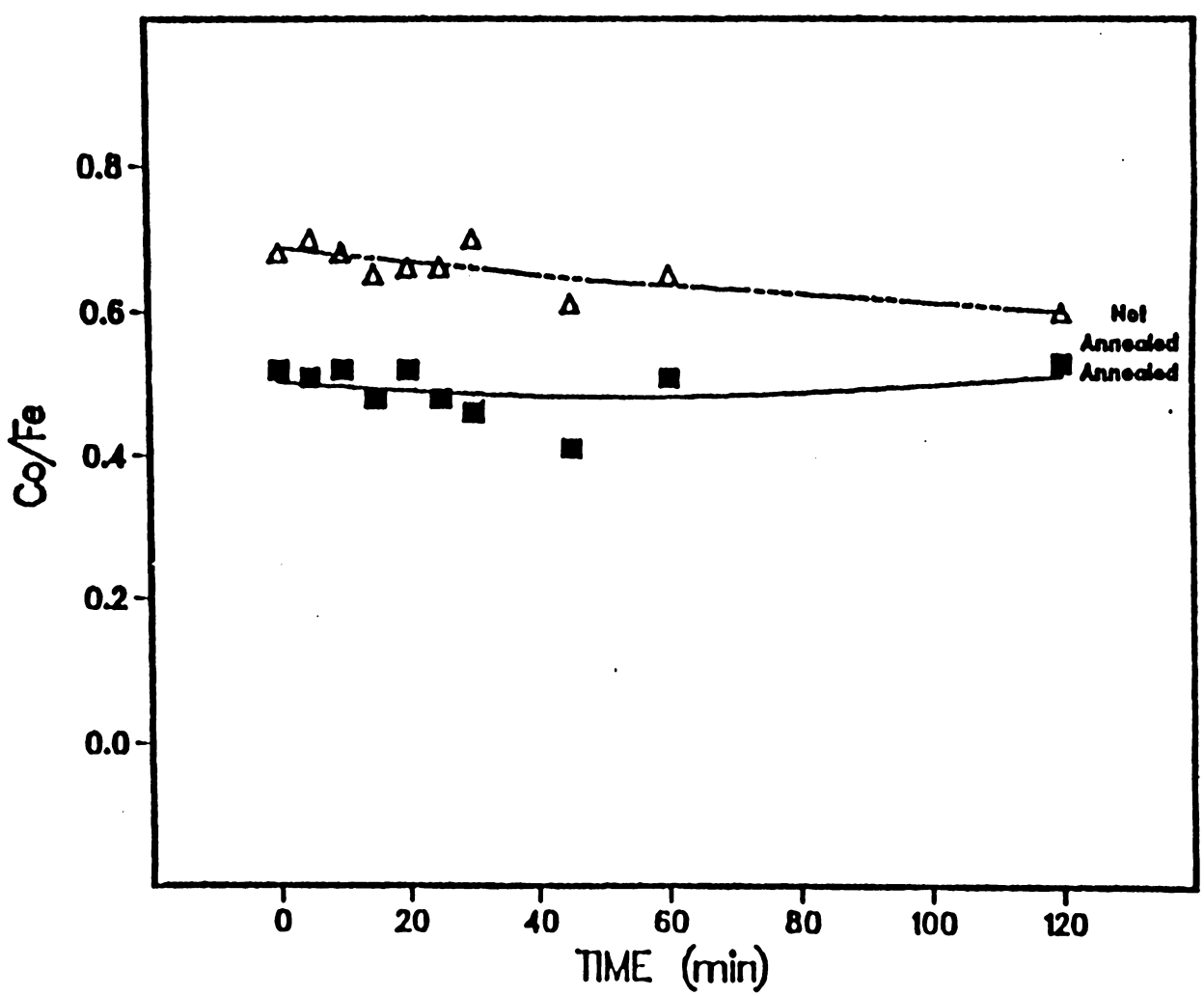

Figure 33. XPS Co/Fe Ratio Versus Reaction Time (NaOH Kinetic Preparation, Fe:OH = 1:3)

Infrared Measurements

The infrared spectra (900-225 cm^{-1}) for the non-annealed and annealed samples are shown in Figures 34 and 35. No evidence for the O-H band of $Co(OH)_2$ was noted in the sample spectra. The far infrared spectra show the same basic trends as noted in the NH_4OH kinetic preparation. The non-annealed samples show a trend of going from a spectrum similar to γ-Fe_2O_3 to the characteristic Co-γ-Fe_2O_3 spectrum with increasing reaction time. The annealed samples all show spectra similar to the characteristic Co-γ-Fe_2O_3 spectrum.

Fe(II) Content

The same trends found in the previous two kinetic preparations are evident in the Fe(II) results for the NaOH (Fe:OH = 1:3) preparation shown in Table 12. These trends are increasing Fe(II) content with longer reaction time and higher Fe(II) content in the annealed samples.

Early Sampling NH_4OH Kinetic Preparation

To investigate further the adsorption process, a kinetic study was carried out in which the sampling was initiated when base addition was started (zero time). Concentrated NH_4OH was used to adjust the suspension pH and the reaction conditions were kept as similar as possible to the previous kinetic NH_4OH preparations, with one exception, which was that the samples were not washed. The decision not to wash the samples was due to observations made in the previous kinetic NH_4OH preparation that suggested that the Co(II) species on the surface of the early samples were being washed away.

Magnetic Results

The coercivities for the non-annealed and annealed samples along

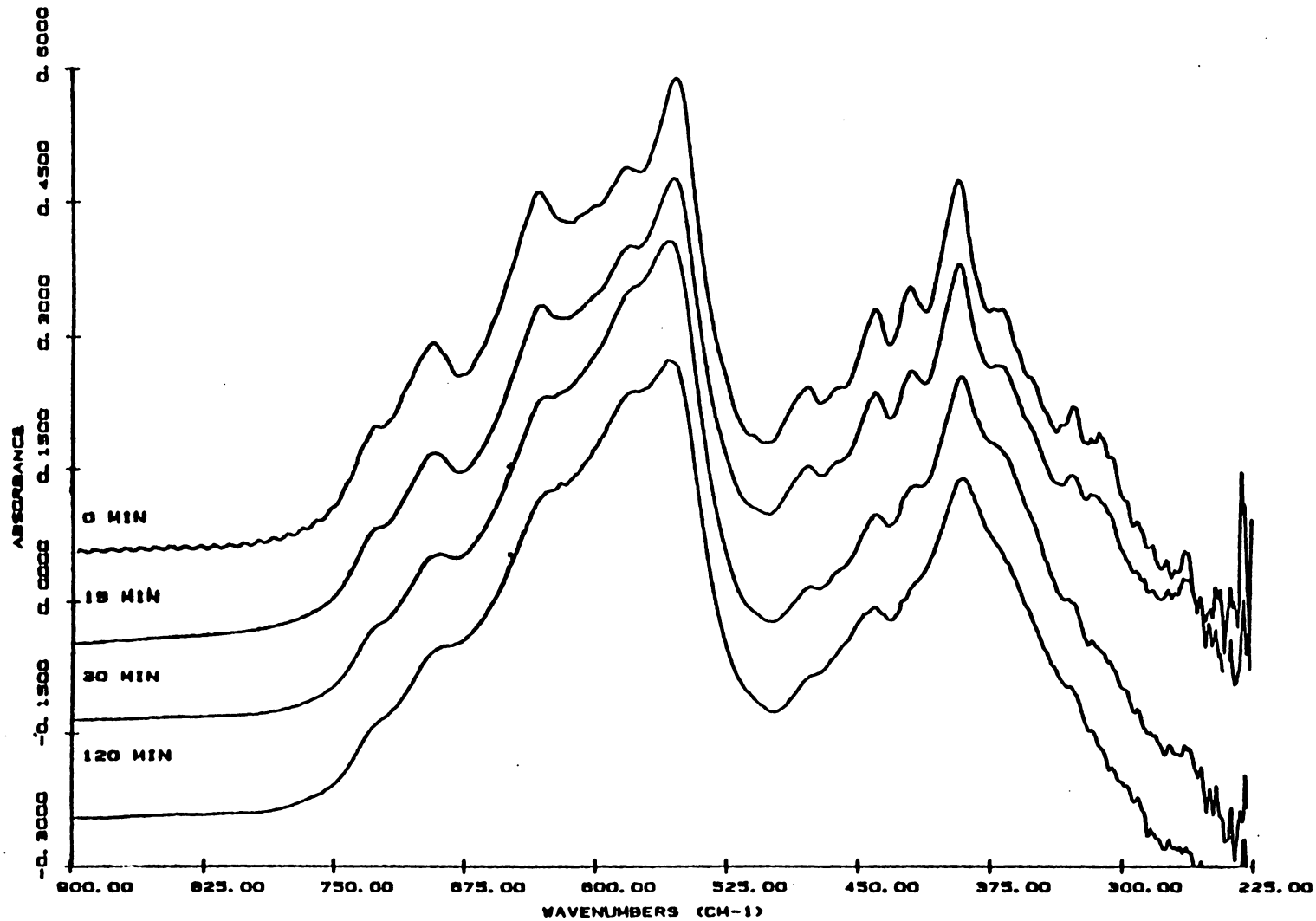

Figure 34. Infrared Spectra of Non-annealed Co-γ-Fe_2O_3 Samples (NaOH Kinetic Preparation, Fe:OH = 1:3)

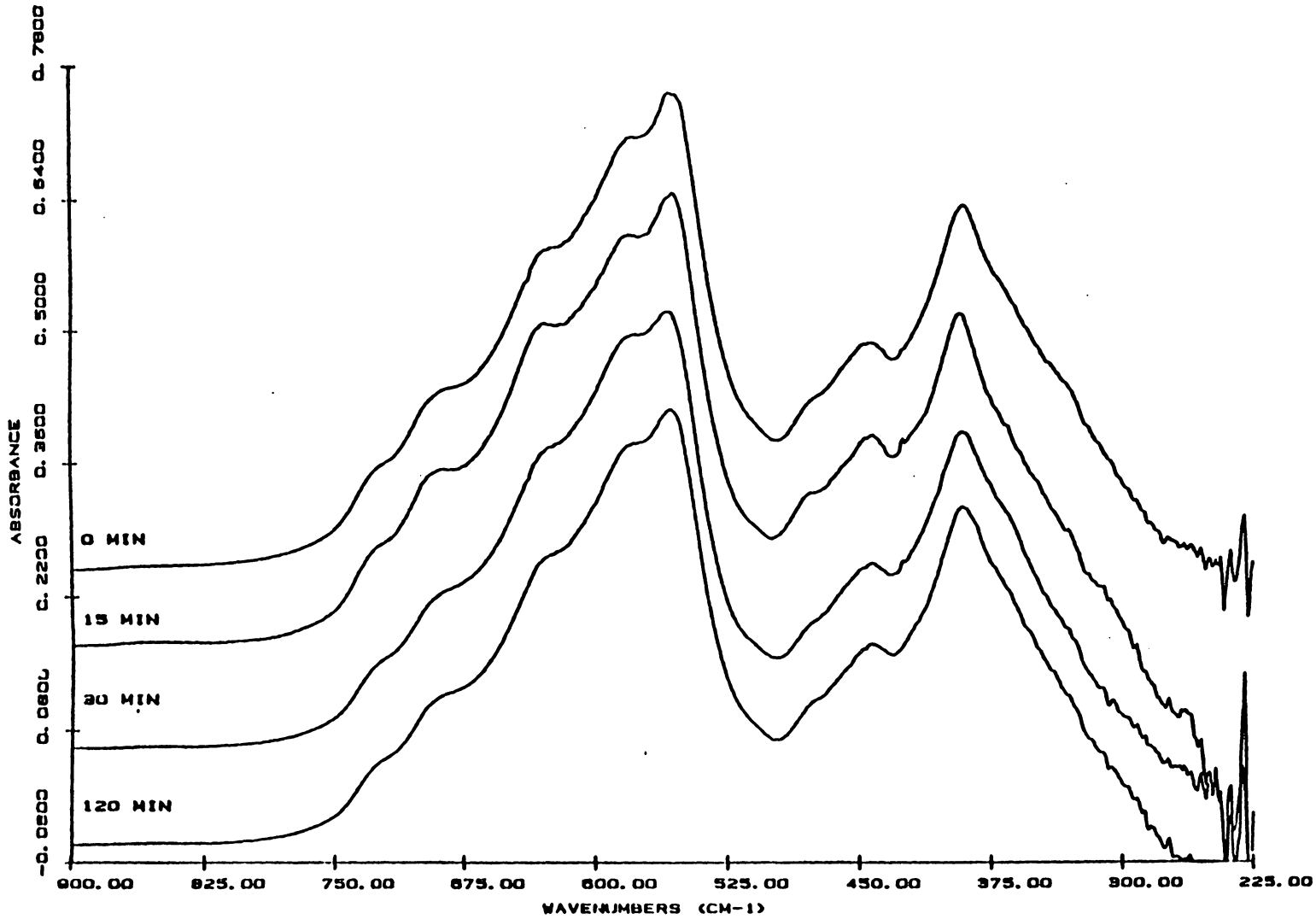

Figure 35. Infrared Spectra of Annealed Co-δ-Fe_2O_3 Samples (NaOH Kinetic Preparation, Fe:OH = 1:3)

Table 12

Percent Fe(II) for NaOH (Fe:OH = 1:3) Kinetic Series

Sample	Non-annealed	Annealed
0 min	1.4%	5.9%
10 min	1.3%	3.8%
20 min	6.1%	4.9%
30 min	5.4%	6.8%
120 min	6.8%	7.6%

with the reaction suspension pH and temperature are given in Table 13. The coercivities are graphed versus reaction time in Figure 36. The plots show the coercivity for the non-annealed samples decreasing slightly early in the reaction and then increasing during the 20 to 40 minute time interval before leveling off. The annealed samples show a large increase early in the reaction and then a small plateau is observed before further coercivity enhancement occurs.

XPS Measurements

The XPS binding energy data and Co/Fe ratios for the non-annealed and annealed samples are given in Tables 14 and 15, respectively. The XPS spectra for the 1 minute non-annealed sample (pH = 5.7) showed no evidence of Co on the surface. The samples taken after this show Co $2p_{3/2}$ binding energies and satellite splittings similar to those observed in the previous NH_4OH kinetic preparation. The same trend of the Co $2p_{3/2}$ binding energies decreasing from ~781.0 eV to ~780.6 eV with increasing reaction time is noted. The trend of increasing satellite splitting from 5.6 to ~6.2 eV is also present. The Fe $2p_{3/2}$ and O 1s binding energies, and the Co $2p_{1/2}$- Co $2p_{3/2}$ splitting values also show general agreement with the XPS results for the original non-annealed NH_4OH samples (Table 4).

The Co 2p spectra for the 3, 5, and 10 minutes samples are shown in Figure 37. These samples were all taken during pH adjustment (base addition). The spectra all have similar broad photoionization peaks suggesting a mixture of Co(II) species on the surface.

Table 13

Magnetic Results for Early Sampling NH_4OH Kinetic Series

Sample	Temperature (°C)	pH	Non-annealed	Annealed
1 min	30	5.7	337	345
3 min	30	7.4	315	355
5 min	30	8.7	300	501
10 min	30	9.6	304	595
20 min	44	9.6	316	577
25 min	68	9.0	325	596
30 min	92	8.3	390	613
35 min	95	8.1	397	672
75 min	95	8.0	466	763
135 min	96	7.6	440	698

- pH of suspension reached 10 at 15 min.

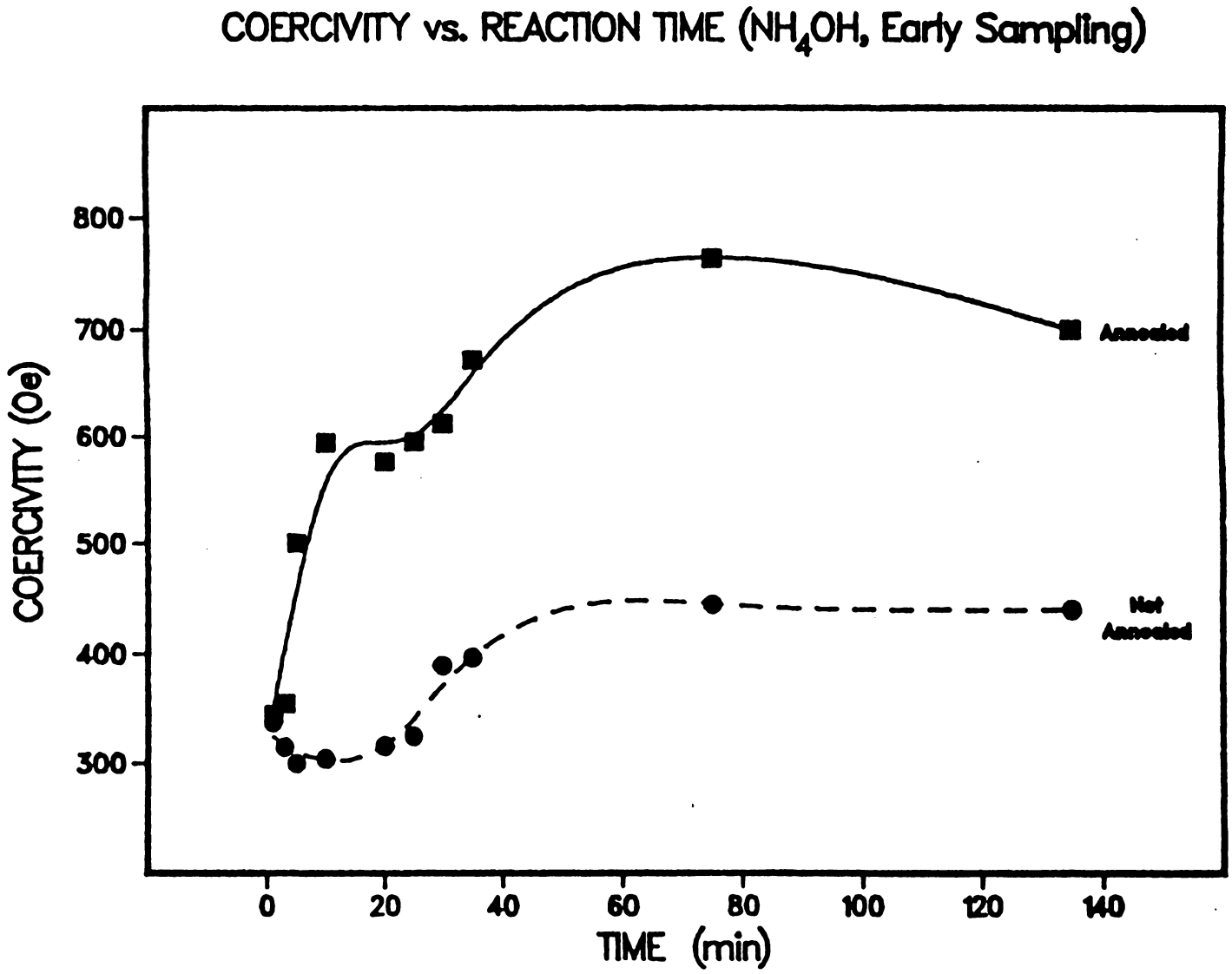

Figure 36. Coercivity Versus Reaction Time (Early Sampling NH_4OH Kinetic Preparation)

Table 14

XPS Results

Early Sampling NH_4OH Kinetic Series

Non-Annealed

Sample	Temp. (°C)	pH	Binding Energy Results (eV)					Co/Fe (atomic ratio)
			Fe $2p_{3/2}$	Co $2p_{3/2}$	Δ Co 2p	Δ sat.	O 1s	
1 min	30	5.7	710.9	---	---	---	530.1	<0.05
3 min	30	7.4	711.0	780.9	15.9	5.7	530.3	0.32
5 min	30	8.7	711.0	780.1	15.8	5.8	530.3	0.52
10 min	30	9.6	711.1	780.9	15.8	5.7	530.2	0.63
20 min	44	9.6	711.0	780.8	15.8	5.6	530.2	0.66
25 min	68	9.0	711.1	780.7	15.9	6.0	530.2	0.72
30 min	92	8.3	711.0	780.4	15.8	6.3	530.1	0.85
35 min	95	8.1	710.8	780.5	15.7	6.2	530.1	0.82
75 min	95	8.0	710.9	780.6	15.8	6.0	530.1	0.76
135 min	96	7.6	711.0	780.5	15.7	6.2	530.1	0.75

Table 15

XPS Results

Early Sampling NH_4OH Kinetic Series

Annealed

Sample	Binding Energy Results (eV)					Co/Fe (atomic ratio)
	Fe $2p_{3/2}$	Co $2p_{3/2}$	Δ Co 2p	Δ sat.	O 1s	
1 min	710.9	---	---	---	530.1	<0.05
3 min	710.9	780.8	16.0	---	530.2	<0.05
5 min	711.0	780.7	15.8	5.6	530.2	0.37
10 min	710.9	780.3	15.8	5.4	530.1	0.55
20 min	710.9	780.2	15.9	5.3	530.0	0.53
25 min	710.9	780.3	15.8	6.2	530.0	0.53
30 min	710.7	780.2	15.8	6.2	529.9	0.59
35 min	710.7	780.3	15.8	6.4	530.0	0.53
75 min	710.8	780.3	15.8	6.3	529.9	0.49
135 min	710.9	780.4	15.8	6.2	530.1	0.44

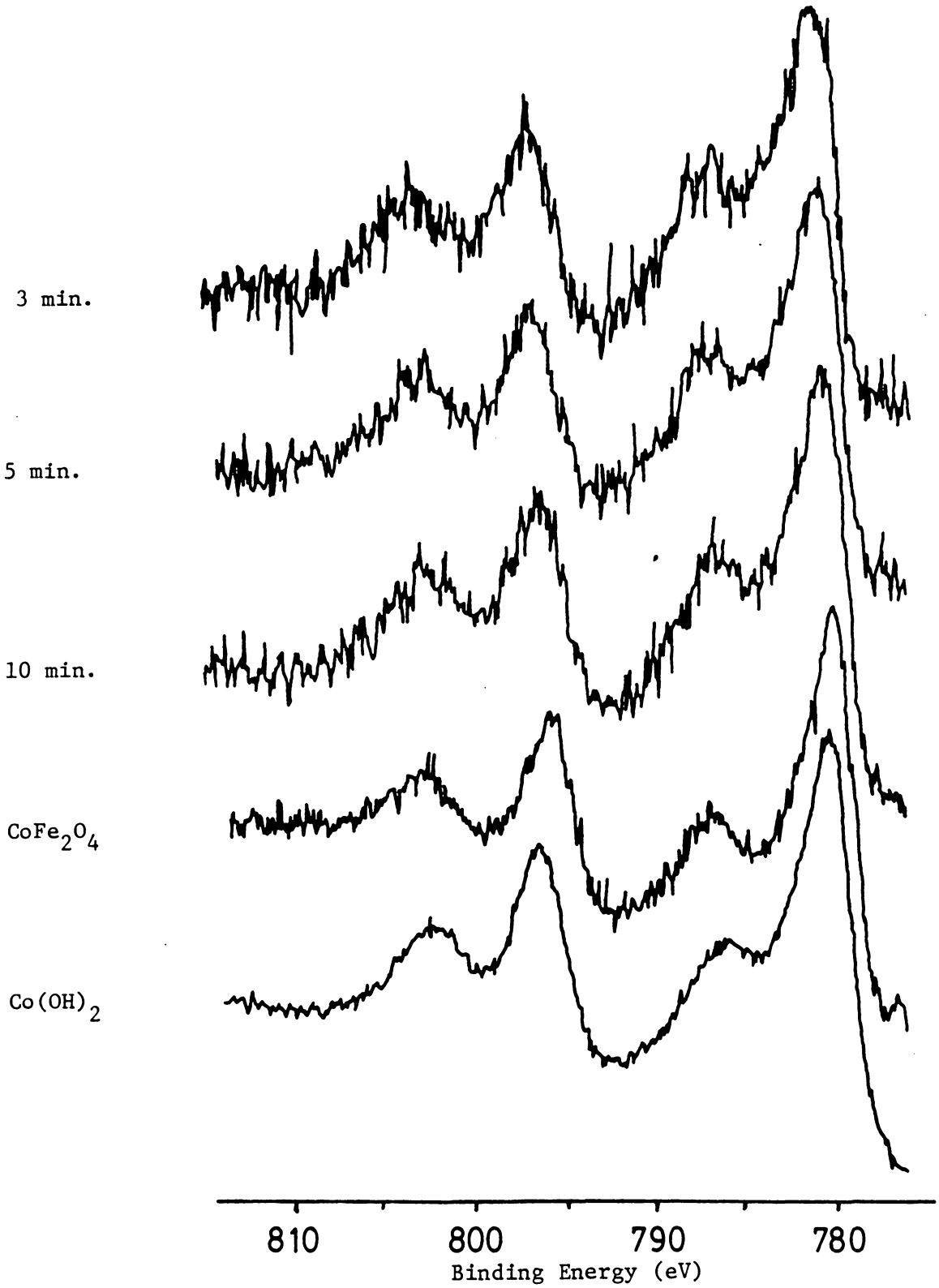

Figure 37. XPS Co 2p Spectra (Early Sampling NH_4OH Kinetic Preparation)

The O 1s spectra for these samples are shown in Figure 38. The O 1s peaks all have the noticeable hydroxyl component discussed previously. The 5 minute sample appears to have the largest hydroxyl component. The valence band spectra are shown in Figure 39. The spectrum for the 3 minute sample shows a small peak near the low energy onset which could arise from a cobalt(II) hydroxide. The small peak is not sufficiently distinct to confirm the presence of $Co(OH)_2$. The remaining Co-γ-Fe_2O_3 valence band spectra are very similar to the valence band spectrum for $CoFe_2O_4$.

The XPS results for the non-annealed samples suggest that the Co(II) species adsorbed during the pH adjustment are similar to those adsorbed immediately after pH adjustment. The observed changes occur later in the reaction when the temperature is increased. The samples taken at 3, 5 and 10 minutes have reaction suspension pHs of 7.4, 8.7 and 9.6, respectively. The binding energy results for these samples are essentially the same and the spectra (Figures 37, 38, and 39) are also similar. The absence of cobalt in the 1 minute sample indicates that Co(II) adsorption principally occurs between a pH of 5.4 and 7.4

The binding energy results for the annealed samples (Table 15) show a slight trend of decreasing Co $2p_{3/2}$ binding energies early in the reaction. Other than this no other trends are observed. The overall Fe $2p_{3/2}$ and Co $2p_{3/2}$ binding energies values are lower (~710.8 eV, 780.3 eV, respectively) than those observed in the other NH_4OH annealed samples (Fe $2p_{3/2}$, 711.1 eV; Co $2p_{3/2}$, 780.7 eV). The reason for this difference is unclear.

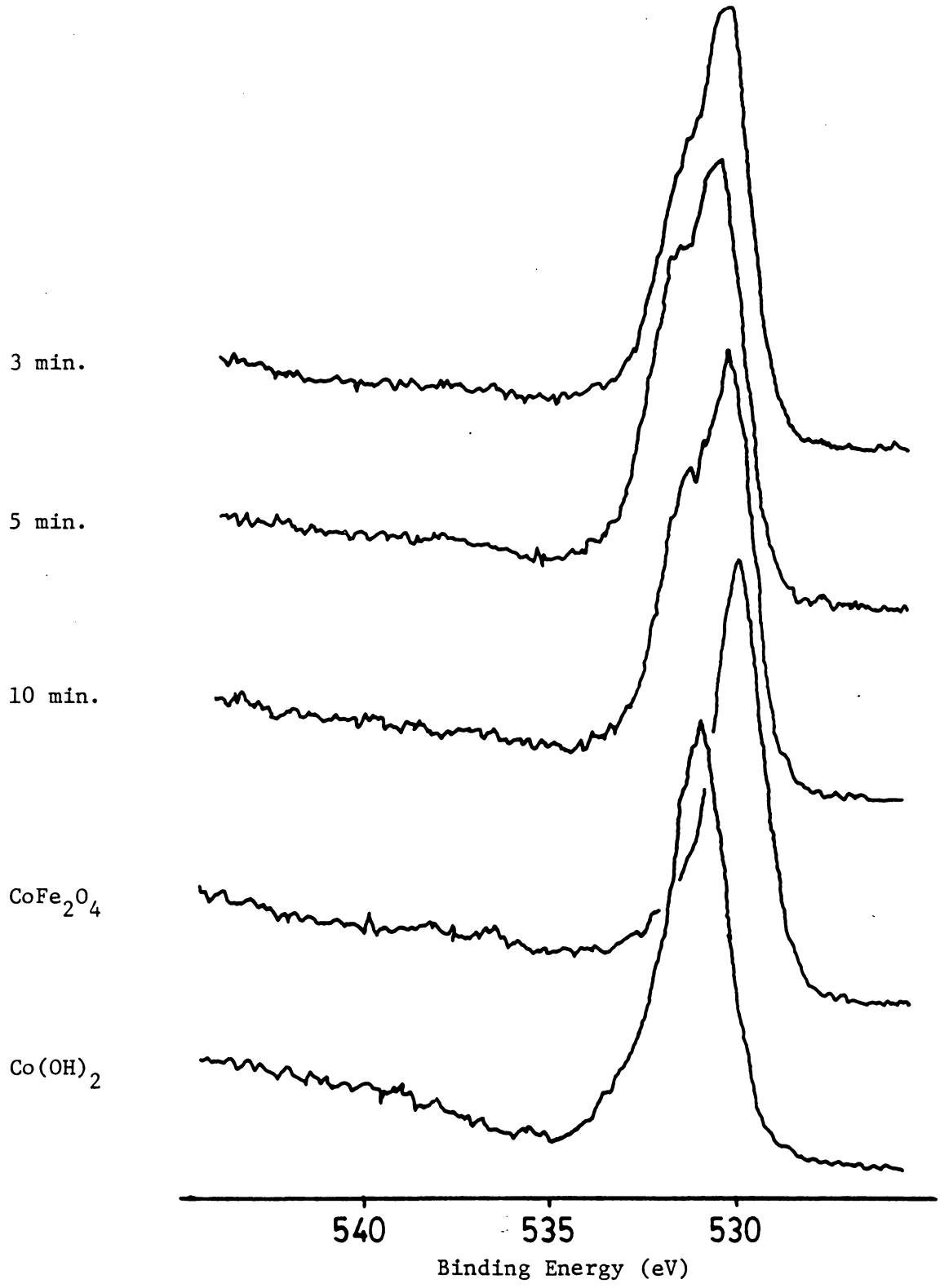

Figure 38. XPS O 1s Spectra (Early Sampling NH_4OH Kinetic Preparation)

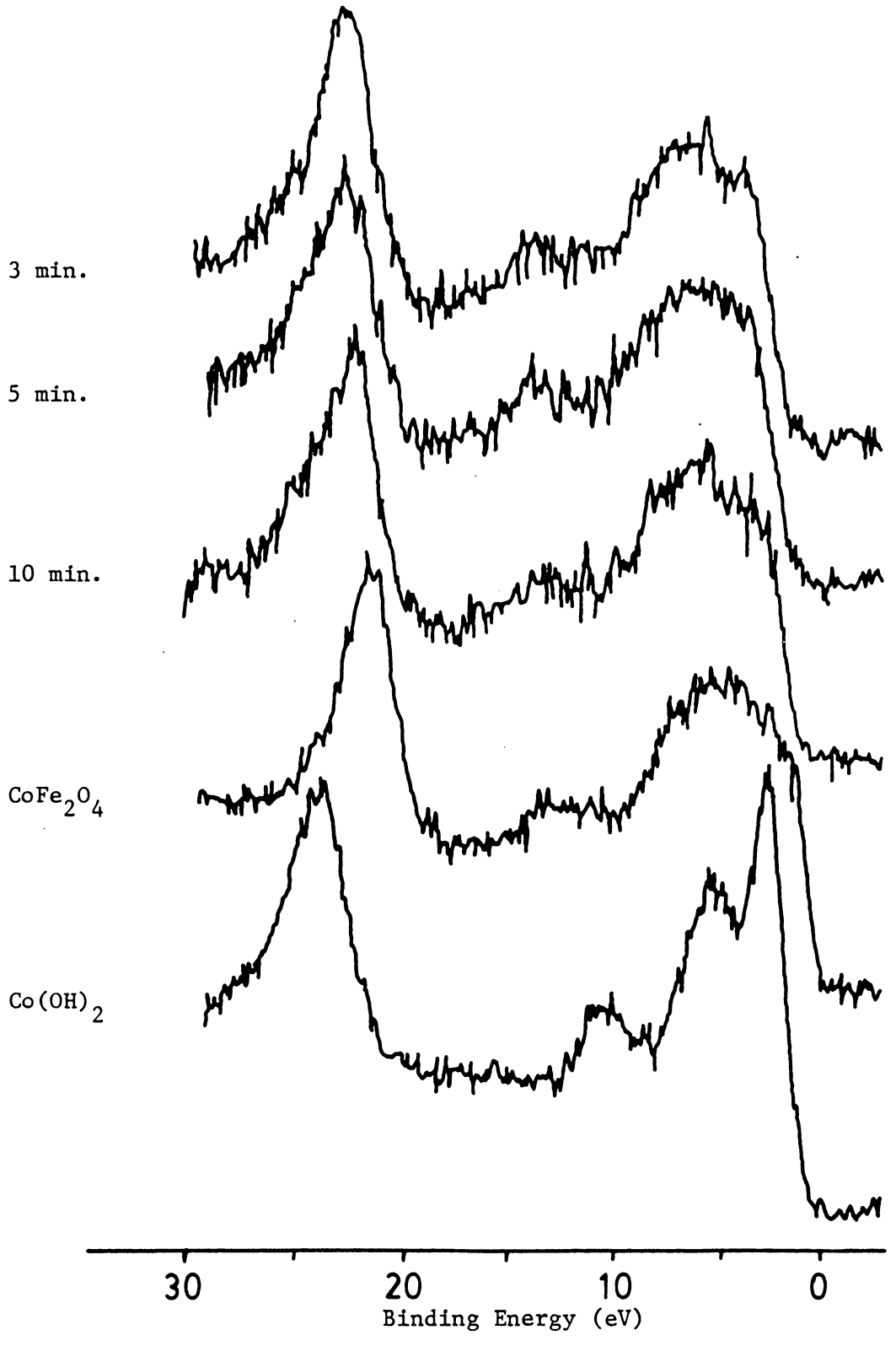

Figure 39. XPS Valence Band Spectra (Early Sampling NH_4OH Kinetic Preparation)

The Co/Fe atomic ratios for the annealed and non-annealed samples are plotted versus reaction time in Figure 40. Both plots show significant increases in the first 5 minutes of reaction. The non-annealed Co/Fe atomic ratio curve shows a small plateau between the 10 and 20 minute samples and then there is a further increase in the Co/Fe atomic ratio. This small plateau occurs when the pH adjustment was stopped and the heating was begun. The second increase in the Co/Fe ratio following the heating of the reaction suspension implies that the suggested ferrite formation during the heating of the reaction suspension causes an increase in the Co/Fe ratio.

The Co/Fe atomic ratio vs. reaction time curves show noticeable similarites with the coercivity reaction time curves (Figure 40). This appears to be an another example of the Co/Fe ratios showing a behavior similar to that for coercivity results.

Fe(II) Content

The percentages of Fe(II) in the non-annealed and annealed samples are given in Table 16. The non-annealed samples show an increase in Fe(II) content with increasing time of reaction. The annealed samples show the same trend and have a higher Fe(II) content compared to the non-annealed samples. This is the same behavior that was found in all of the kinetic preparations. Possible reasons for this behavior have been discussed previously.

Summary of Kinetic Preparations

There were several findings from the kinetic studies of the cobalt interaction reaction with γ-Fe_2O_3. One of these findings was evidence

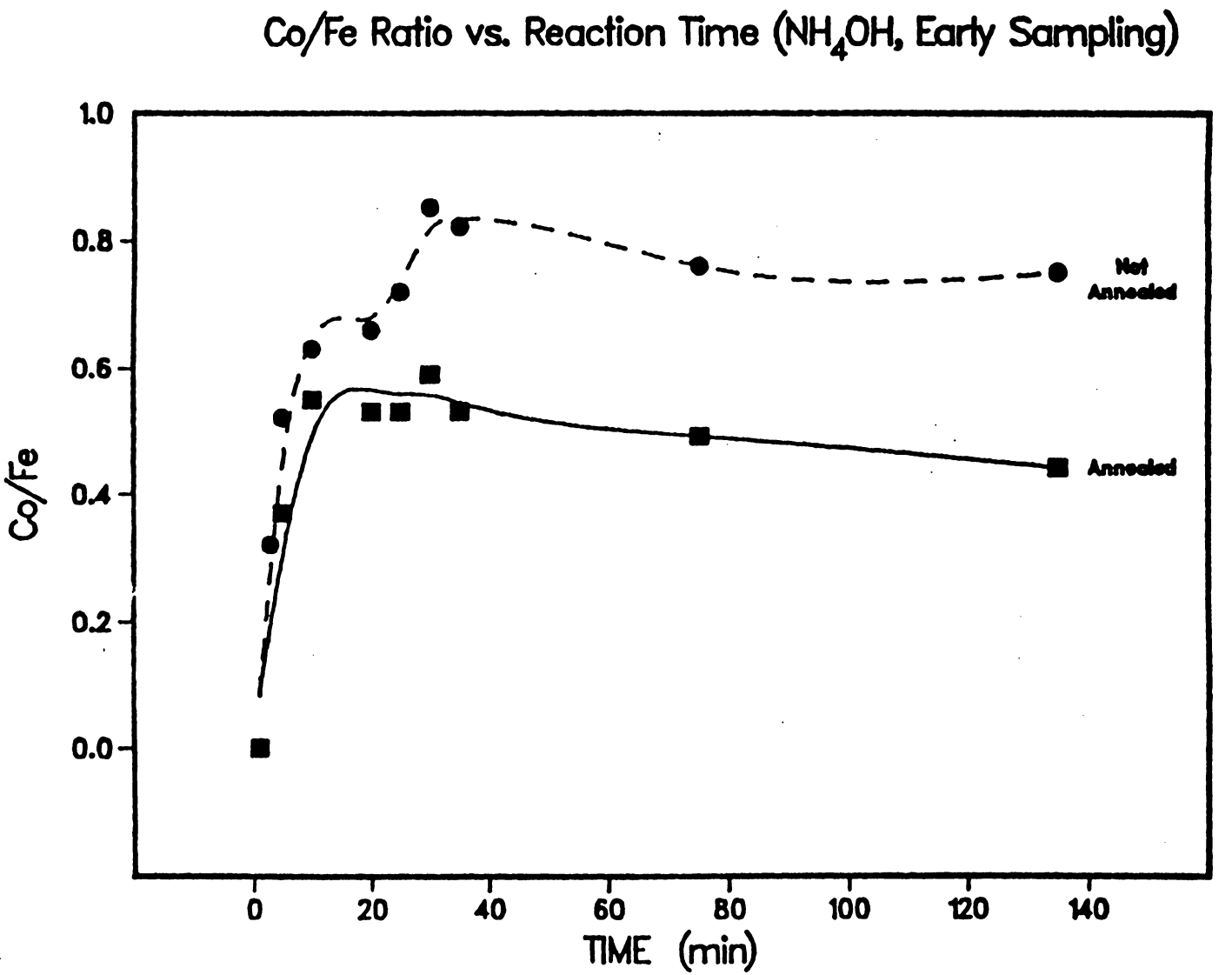

Figure 40. XPS Co/Fe Ratios Versus Reaction Time (Early Sampling NH_4OH Kinetic Preparation)

Table 16

Percent Fe(II) for Early Sampling NH_4OH Kinetic Series

Sample	Non-annealed	Annealed
1 min	0.5%	0.6%
3 min	1.3%	1.5%
5 min	2.1%	4.7%
10 min	2.3%	2.1%
135 min	6.9%	6.9%

from the XPS spectra suggesting that the Co(II)/Fe(II) mixture is initally adsorbed in hydrous forms during the base addition. The XPS spectra also indicated that upon heating the reaction suspension, the surface of the Co-γ-Fe_2O_3 underwent chemical transformation from the original hydrous surface to a surface closer to $CoFe_2O_4$ in composition. These conclusions were obtained primarily from the Co 2p and O 1s spectra for the non-annealed Co-γ-Fe_2O_3 samples, from both NH_4OH and NaOH preparations.

It was also found that the surface chemistry of Co-γ-Fe_2O_3 samples from NH_4OH preparations was different than the surface chemistry of Co-γ-Fe_2O_3 samples prepared with NaOH. Evidence from the XPS spectra suggest that the samples from the NaOH preparations have a surface composition closer to $CoFe_2O_4$ than samples from the NH_4OH preparations. Reasons for the different surface chemistry behavior could be a complexation effect occurring in NH_4OH preparations or the more caustic conditions of the NaOH preparations which facilitate the formation of a more well-defined $CoFe_2O_4$ surface.

The results from the "early sampling" kinetic preparation indicate that the adsorbed Co(II)/Fe(II) species are essentially the same during and after pH adjustment (before heating the suspension). The early samples from the original NH_4OH kinetic preparation show essentially the same XPS results as for samples taken during the pH adjustment in the early sampling preparation.

Chapter V

CONCLUSIONS

Surface XPS analysis of the prepared Co-γ-Fe_2O_3 samples showed that the coercivity enhancement in the thermal treatment corresponds primarily to the diffusion of Co(II) into the bulk. No evidence was obtained suggesting that coercivity enhancement was the result of a chemical transformation.

The XPS results from the kinetic studies indicated that the Co(II)/Fe(II) mixture is initially adsorbed in a hydrous form and as the reaction suspension heats up there is a rapid change to a more $CoFe_2O_4$-like surface. Comparing the XPS results for the kinetic preparations using NaOH and NH_4OH there is evidence suggesting that the surface chemistry of the two preparations is quite different. The surfaces of Co-γ-Fe_2O_3 samples prepared with NaOH appear to have a surface composition closer to stoichiometric $CoFe_2O_4$ than for samples prepared using NH_4OH.

The infrared spectra for the Co-γ-Fe_2O_3 samples showed no evidence of $Co(OH)_2$. The spectra in the 900-400 cm^{-1} IR range exhibited evidence of ferrite formation. The SIMS spectra did not provide much information on the chemistry of the Co-γ-Fe_2O_3 surface. The spectra obtained indicated that the concentration of cobalt was greatest at the surface of Co-γ-Fe_2O_3 samples.

In the kinetic studies an increase in Fe(II) content with reaction time was noted and the annealed samples showed greater Fe(II) content than for the non-annealed samples. The results indicate that Fe(III) is

being reduced; possibly by residual hydrocarbons in the γ-Fe_2O_3.

The overall results support the concept of cobalt ferrite formation on the surface of Co-γ-Fe_2O_3, but there is also evidence that other Co(II) species may be present in varing amounts.

REFERENCES

1. D. J. Craik, in "Magnetic Oxides" Ed. D. J. Craik, Wiley and Sons, London, Part 1, 1975, p.V.

2. D. J. Craik, "Structure and Properties of Magnetic Materials", Pion Limited, London, 1971, p.57.

3. D. J. Craik, in "Magnetic Oxides" Ed. D. J. Craik, Wiley and Sons, London, Part 1, 1975, p. vi.

4. G. Bate, J. Appl. Phys., 52, 2447 (1981).

5. A. R. Corradi, IEEE Trans. Magn., MAG-14, 655 (1978).

6. L. R. Bickford, IEEE Trans. Magn., MAG-21, 2 (1985).

7. G. Bate, in "Magnetic Oxides", D. J. Craik, Ed., Wiley and Sons, London, Part 2, 1975, p. 689.

8. S. Matsumoto, T. Koga, K. Fukai, S. Nakatani, US Patent, 4,202,871 (1980).

9. T. M. Bennetch, H. S. Gremen, K. R. Hancods, M. Hoffman, US Patents 3, 904,540 (1975) and 4,176,172 (1979).

10. G. Bate, in "Magnetic Oxides" Ed. D. J. Craik, Wiley and Sons, London, Part 2, 1975, pp. 720-721.

11. Sir Lawrence Bragg, G. F. Claringbull, "The Crystal Structure of Minerals", Cornell Univ. Press, New York, 1965, p. 102.

12. K. J. Standley, "Oxide Magnetic Materials" Clarendon Press, Oxford, 1972, p.23.

13. R. S. Tebble, D. J. Craik, "Magnetic Materials", Wiley Interscience, New York, 1969, p. 252ff.

14. D. J. Craik, "Structure and Properties of Magnetic Materials", Pion Limited, London, 1971, pp. 28ff, 139ff.

15. G. Bate, Ferrites: Procedings of International Conference, Sept.-Oct. 1980, Japan, p. 509.

16. J. C. Jeschke, E. German Patent 8, 684.

17. F. Krones, Technik der Magnetspreicher, Springer-Verlag: Berlin, 1960, p. 479.

18. J. C. Slonczewski, Phys. Rev., 110, 1341 (1958).

19. Koster, IEEE Trans. Magn., MAG-8, 428 (1972).

20. S. Krupicka, and K. Zaveta, in "Magnetic Oxides", D. J. Craik, ed., Wiley and Sons, London, 1975, p. 235.

21. M. P. Sharrock, private communication (Feb. 1983) 3M, St. Paul.

22. S. Krupicka, and K. Zaveta, in "Magnetic Oxides", D. J. Craik, ed., Wiley and Sons, London, 1975, p. 259.

23. W. D. Haller, R. M. Colline, US Patent 3,573,890 (1971).

24. Y. Imaoka, S. Ameki, Y. Kuboto, Y. Tokuoka, IEEE Trans. Magn., MAG-14, 649 (1978).

25. M. Amemiya, M. Kishimoto, F. Hayama, IEEE Trans. Magn., MAG-16, 17 (1980).

26. F. Hayama, S. Kitaoka, H. Arradoh, M. Amemiya, Ferrites: Procedings of the International Conference, Sept.-Oct., 1981, Japan, p. 521.

27. Y. Tokuoka, H. Sugihara, S. Oka, Y. Imaoka, Chem. Soc. Japan, 10, 1564 (1981).

28. D. Khalafalla, A. H. Morrish, J. Appl. Phys. 43, 643 (1972).

29. A. Ochi, K. Watanabe, M. Kiyama, T. Shinjo, Y. Bando, and T. Takada, Ferrites: Proceedings of the International Conference, Sept.-Oct., 1980, Japan, p. 618.

30. S. Li, P-Q. Zang, G-Q. Ji, H. L. Luo, and S. Ke, Acta Phys. Sinica, 30, 120 (1981).

31. M. P. Sharrock, P. J. Picone, A. H. Morrish, IEEE Trans. Magn., MAG-19, 1466 (1983).

32. K. Sumiya, T. Matsumato, S. Watatain, F. Hayana, J. Phys. Chem. Solid, 40, 1097 (1979).

33. F. E. Witherell, IEEE Trans. Magn. MAG-20, 739 (1984).

34. K. Siegbahn, C. Nordling, A. Fahlman, R. Nordberg, K. Hamrin, J. Hedman, G. Johansson, T. Bergmark, S. Karlsson, I. Lindgren, and B. Lindberg, "ESCA Atomic, Molecular and Solid State Structure Studied by Means of Electron Spectroscopy, "Almqvist and Wiksells, Uppsala, 1967.

35. J. G. Dillard, M. H. Koppelman, J. Colloid Interface Sci., 87, 46, (1982).

36. K. L. Busch, R. G. Cooks, Science, 218, 247, 1982.

37. J. W. Murray, J. G. Dillard, Geochim. Cosmochim. Acta., 43, 781, (1981).

38. K. S. Kim, J. Electron Spectrosc. Relatd. Phenom., 3, 217 (1974).

39. T. A. Carlson, J. C. Carver, L. J. Saethre, F. G. Santibanez, G. A. Vernon, J. Electron Spectrosc. Relatd. Phenom., 5, 247, (1974).

40. D. Briggs, V. A. Gibson, Chem. Phys. Lett., 25, 493, (1974).

41. D. C. Frost, C. A. McDowell, I. S. Woolsey, Chem. Phys. Lett., 17, 320, (1972).

42. T. J. Chuang, C. D. Brundle, D. W. Rice, Surface Sci., 59, 413 (1976).

43. N. S. McIntyre, M. G. Cook, Anal. Chem., 47, 2208 (1975).

44. N. S. McIntyre, D. G. Zetaruk, Anal. Chem., 49, 1521 (1977).

45. D. R. Penn, J. Electron Spectrosc. Relatd. Phenom., 9, 92 (1976).

The vita has been removed from the scanned document

ADSORPTION OF COBALT ON GAMMA Fe_2O_3

by

Martin J. Fay

(ABSTRACT)

The treatment of gamma-Fe_2O_3 with cobalt(II) is an important commercial process since the product is used extensively as a magnetic material for magnetic recording. The preparation of cobalt-doped gamma-Fe_2O_3 consists of interacting Co(II) with particulate gamma-Fe_2O_3 in solution under alkaline conditions.

The surface of cobalt-treated gamma-Fe_2O_3 was characterized using the surface analysis techniques of x-ray photoelectron spectroscopy (XPS) and secondary ion mass spectroscopy (SIMS). Characterization was also accomplished using infrared spectroscopy and quantitative analysis.

Surface analysis results suggest that the Co(II) is initially adsorbed as a hydrous precipitate during base addition (NaOH or NH_4OH). Following base addition, the reaction suspension was heated to 90-95°C. Results from surface analysis indicate that during this warm up period there is a conversion from the hydrous surface to a surface with a composition near $CoFe_2O_4$ (cobalt ferrite). No oxidation of Co(II) to Co(III) was observed. Surface analysis also suggests that cobalt-treated γ-Fe_2O_3 prepared using NaOH has a different surface chemistry than cobalt-treated γ-Fe_2O_3 prepared with NH_4OH.

Following the adsorption of Co(II) on γ-Fe_2O_3 the product underwent a thermal treatment to enhance the coercivity. Surface analysis results indicate that the thermal treatment causes a significant diffusion of Co(II) into the bulk γ-Fe_2O_3. The results also suggest that the coercivity enhancement following thermal treatment is largely due to the inward diffusion of Co(II) and not a change in the surface composition of the cobalt-treated γ-Fe_2O_3.